IDENTIFICATION OF PSGL-1 AND THE SHREK FAMILY OF PROTEINS AS BROAD-SPECTRUM ANTIVIRAL HOST FACTORS

by

Deemah M. Dabbagh

A Dissertation
Submitted to the
Graduate Faculty
of
George Mason University
in Partial Fulfillment of
The Requirements for the Degree
of
Doctor of Philosophy
Biosciences

Committee:

_____	Dr. Yuntao Wu, Committee Chair
_____	Dr. Kylene Kehn-Hall, Committee Member
_____	Dr. Ramin Hakami, Committee Member
_____	Dr. Mikell Paige, Committee Member
_____	Dr. Iosif Vaisman, Director, School of Systems Biology
_____	Dr. Donna M. Fox, Associate Dean, Office of Student Affairs & Special Programs, College of Science
_____	Dr. Fernando Miralles-Wilhem, Dean, College of Science

Date: _____

Summer Semester 2021
George Mason University
Fairfax, VA

Identification of PSGL-1 and the SHREK Family of Proteins as Broad-Spectrum Antiviral Host Factors

A Dissertation submitted in partial fulfillment of the requirements for the degree of Doctor of Philosophy at George Mason University

by

Deemah M. Dabbagh
Master of Science
Georgetown University, 2014
Bachelors of Science
King Saud University, 2009

Director: Yuntao Wu, Professor
George Mason University

Summer Semester 2021
George Mason University
Fairfax, VA

DEDICATION

This work is dedicated to my loving parents, Hanan and Mohammad, who have set up a great example and raised me to be the person I am today. Thank you for everything.

ACKNOWLEDGEMENTS

My journey though graduate school would not have been successful if it weren't for a group of people who have offered me their kind support and help. First and foremost, I must express my deepest appreciation and gratitude to my Ph.D. advisor, mentor of six years and committee chair, Professor Yuntao Wu, who has continually provided me with invaluable knowledge and advice. Without his guidance, this work and dissertation would not have been possible. I am also greatly indebted to my committee members, Dr. Kylene Kehn-Hall, Dr. Ramin Hakami, and Dr. Mikell Paige for their support and for generously providing me with feedback and advice. Additionally, I wish to thank Drs. Eric Freed and David Levy, and their lab members, for their collaborations with us in the PSGL-1 study. I would like to thank Yajing Fu and Sijia He for their tremendous work in the PSGL-1 study, and Sijia He, Brian Hetrick and Linda Chilin for their valuable contributions to the SHREK project. I would also like to thank Zheng Zhou for his contribution to the PSGL-1 study, Janice Yoon for managing the lab and all past and present lab members for their friendship. I would also like to thank Dong Yang Yu, who has been especially helpful whenever I faced technical difficulties during my early years in the program. Finally, I would like to thank the NIH AIDS reagent program, Dr. Akira Ono, Dr. Feng Li, and Drs. Oliver and Caroline Spertini for providing us with HIV-1 reagents, PSGL-1 C-terminal mutant plasmids, the influenza A viral expression vectors and the ΔDR plasmid, respectively. And I also wish to thank all of those at the George Mason University dissertation services who have helped in formatting and publishing this dissertation.

TABLE OF CONTENTS

LIST OF FIGURES

LIST OF ABBREVIATIONS

Acquired Immunodeficiency Syndrome……...AIDS
Amino-Terminus…….....NT
Angiotensin Converting Enzyme 2……...…...ACE2
Beta Lactamase……...BLAM
Capsid……...CA
Carboxy-Terminus……CT
Chemokine Receptor 5……CCR5
Chemokine Receptor Type 4……CXCR4
Cluster of Differentiation 2……CD2
Cluster of Differentiation 34……CD34
Cluster of Differentiation 43……CD43
Cluster of Differentiation 63……CD63
Cluster of Differentiation 164……CD164
Complementary Deoxyribonucleic Acid……cDNA
Deoxyribonucleic Acid……DNA
Decameric Repeats……...DR
Dulbecco's Modified Eagle Medium……DMEM
Enzyme-Linked Immunosorbent Assay……ELISA
Envelope glycoprotein……Env
Endosomal Sorting Complexes Required for Transport……...ESCRT
Endoplasmic Reticulum……ER
Ezrin Radixin Moesin……ERM
Fluorescence-Activated Single Cell Sorting……FACS
Fetal Bovine Serum……FBS
Green Fluorescent Protein……..GFP
Glycoprotein 160……Gp160
Glycoprotein 120……Gp120
Glycoprotein 41……Gp41
Glyceraldehyde 3-Phosphate Dehydrogenase……..GAPDH
Half-Maximal Inhibitory Concentration……IC50
HEK293T Human Embryonic Kidney 293 Large T Antigen……...HEK293T
Henrietta Lacks……HeLa
Highly Active Anti-Retroviral Therapy……...HAART
Highly Basic Region……..HBR
Human Immunodeficiency Virus-1……HIV-1
Hybrid Alphavirus-SARS-CoV-2……HaCoV2

Influenza A Virus……IAV
Intracellular Adhesion Molecule-1……..ICAM-1
Integrase……IN
Integrin Beta 2 Chain……..ITGß2
Interferon Gamma……INF-γ
Long Terminal Repeat……LTR
Luciferase……..…….... Luc
Lymphocyte Function Associated Antigen-1……..……. LFA-1
Madin-Darby Canine Kidney……MDCK
Matrix……..MA
Mucin 1……...MUC1
Mucin 4……...MUC4
Murine Leukemia Virus……MLV
Nucleocapsid……NC
Negative Factor……Nef
Poly-Basic Domain……PBD
Pre-integration Complex……..PIC
P-Selectin Glycoprotein Ligand-1……PSGL-1
Podocalyxin……PODXL1
Podocalyxin-Like Protein 2……PODXL2
Regulator of Expression of Virion Proteins……Rev
Ribonucleic Acid……...RNA
Roswell Park Memorial Institute Medium……...RPMI
Rev Responsive Element……RRE
Reverse Transcriptase……...RT
Surface-Hinged Rigidly Extended Killer……..SHREK
Short Hairpin Ribonucleic Acid……shRNA
Severe Acute Respiratory Syndrome Coronavirus 2……...SARS-CoV-2
T-Cell Receptor……..TCR
Trans-Activator of Transcription……..Tat
Trans-Activation Response Element…….…....TAR
Transmembrane Serine Protease 2……..…….....TMPRSS2
Median Tissue Culture Infectious Dose……...……TCID50
T-cell immunoglobulin and mucin domain-1..... TIM-1
Transmembrane Protein 123.....TMEM123
Uropod-Directed Microdomain..... UDM
Vascular Cell Adhesion Protein-1..... VCAM-1
Viral Infectivity Factor..... Vif
Viral Protein R..... Vpr
Viral Protein U..... Vpu
Vesicular Stomatitis Virus Glycoprotein..... VSV-G
Wild Type..... WT

ABSTRACT

IDENTIFICATION OF PSGL-1 AND THE SHREK FAMILY OF PROTEINS AS BROAD-SPECTRUM ANTIVIRAL HOST FACTORS

Deemah M. Dabbagh, Ph.D.

George Mason University, 2021

Dissertation Director: Dr. Yuntao Wu

PSGL-1 (P-selectin glycoprotein ligand-1) is a dimeric, mucin-like glycoprotein with a molecular weight of 120 kDa and functions as a ligand for P-, E-, and L-selectins. PSGL-1 is predominantly expressed on the surface of myeloid cells and lymphoid cells and is up-regulated during inflammation to mediate leukocyte tethering and rolling on the endothelium's surface for migration into inflamed tissues. Previous work has reported that PSGL-1 expression restricts HIV-1 infectivity. However, the mechanism by which PSGL-1 inactivates HIV-1 infectivity remained elusive. Here, we demonstrated that PSGL-1 inhibits HIV-1 particle infectivity by incorporating into assembling virion particles and subsequently preventing virus particle binding to target cells through steric hindrance. The anti-HIV effect of PSGL-1 occurred irrespectively of receptor usage; particles bearing either the HIV-1 envelope glycoprotein, the vesicular stomatitis virus G (VSV-G) glycoprotein, or completely lacking viral glycoproteins were all impaired in

their ability to bind target cells. Mutational mapping revealed that the extracellular domain of PSGL-1 is required for its anti–HIV-1 activity, while the cytoplasmic domain slightly contributed to virus inhibition. Additionally, we found that PSGL-1 inhibits the infectivity of other enveloped viruses including murine leukemia virus and influenza A virus, indicating that PSGL-1 is a host factor with broad-spectrum antiviral activity. We also tested a panel of mucins and mucin-like molecules that share structural features with PSGL-1(CD43, TIM-1, CD34, PODXL1, PODXL2, CD164, MUC1, MUC4, and TMEM123). We found these proteins also inactivated HIV-1 infectivity. We demonstrated that, like PSGL-1, these mucin domain-containing proteins block HIV-1 infectivity by inhibiting virus particle attachment to target cells. Based on their shared structural characteristics and antiviral activity, we have named these proteins the Surface-Hinged, Rigidly Extended Killer (SHREK) family of virion inactivators. Besides inhibiting HIV-1, the proteins tested blocked infection by the influenza A virus and a subset of them inhibited the infectivity of a hybrid alphavirus-SARS-CoV-2 (HaCoV2) pseudovirus, demonstrating that SHREK proteins are broad-spectrum host antiviral factors. Collectively, these results suggest that SHREK proteins may be a part of host innate immunity against enveloped viruses.

CHAPTER ONE: INTRODUCTION

Overview of HIV Disease

HIV-1, the causative agent of AIDS (acquired immunodeficiency syndrome), has caused one of the world's most devastating pandemics in history (1-4). Despite the availability of treatments that suppress viral replication, HIV-1 remains a serious public health challenge (4-6), with approximately 38 million people living with HIV/AIDS as of 2020 (7). CD4 T cells, the central mediators of the immune response, are the primary targets of HIV infection (8, 9). Following transmission through mucosal membranes, HIV quickly spreads to lymphoid tissues where the virus replicates (10-12). Subsequently, the viral load (HIV RNA concentration in the plasma) rises and becomes detectable in the blood at about two weeks post-exposure due to rapid replication. During this period of acute infection, HIV patients may experience short-lasting symptoms including fever, lymphadenopathy, rashes and malaise. Other patients may show more-severe complications, such as meningitis, while a good number of people remain asymptomatic (12). Within a few months after infection, innate and adaptive immune responses can partially mitigate viral replication (11, 13, 14). As a result, the viral load declines to a stable point called the "setpoint" (14, 15). Nevertheless, the immune system is unable to clear the infection and the patient enters a long period of clinical latency, characterized by a progressive reduction in CD4 T cell numbers along with low level viral replication

and chronic inflammation (12, 16, 17). Early during the acute phase of infection, HIV viral reservoirs are established primarily within memory CD4 T cells. Reservoirs may also be established in naive CD4 T cells, monocytes, tissue macrophages, brain microglial cells, and hematopoietic stem cells (HSCs) (18). Integration of HIV DNA into the host chromatin allows the virus to persist and to undergo numerous replication cycles, for as long as the host cell remains alive (19). Highly active antiretroviral therapy (HAART) suppresses viral replication and prevents new cells from getting infected. However, HAART cannot purge the virus from the cells in which HIV DNA has already been integrated (19). Moreover, even though HAART can reduce the viral load to undetectable levels, low levels of replication continue to take place, often leading to the evolution of viral quasispecies (16, 17). The erroneous nature of reverse transcriptase, recombination events and short generation times are all contributors to quasispecies development, which ultimately increases the incidence of drug resistance (20). Thus, the establishment of latent reservoirs in long-lasting cell populations combined with the continuous low level viral replication is the primary obstacle standing in the way of completely eradicating the infection (19).

If left untreated, HIV infection leads to a significant loss of CD4 T cells, which is the hallmark feature of HIV infection (21, 22). This drastic decline in CD4 T cells is believed to be multifactorial (22, 23). One of the oldest hypotheses on the underlying mechanisms of CD4 T cell depletion is that the virus destroys CD4 T cells by direct viral attack (24, 25). According to this hypothesis, also called the “tap and drain” theory, the CD4 T cells (analogous to water in a sink) are continually being eliminated out by HIV

(the drain), while the body is constantly replacing them with new cells (the tap). However, this balance is eventually disrupted when efforts to produce CD4 T cells for restoring homeostasis are exhausted (26). This theory has been validated by quantitative image analysis on HIV-1 infected patients revealing a reduction in the numbers of CD4 T cells and an increase in cellular proliferation and apoptosis (27, 28). Early in the infection, the accelerated production and destruction of CD4 T cells is accompanied by continuous replacement of dead CD4 T cells with native CD4 T cells that originate from the thymus (27). Reports have shown that during HIV infection, approximately 1 billion HIV particles are produced daily. This increases the number of infected CD4 T cells (27), causing the infection to spread to memory T cells in the thymus where the virus further replicates. HIV infection of memory CD4 T cells triggers their elimination through a process believed to be mediated by HIV integration. It has been found that HIV integration induces cell death by activation of DNA-dependent protein kinase (DNA-PK) and by phosphorylation of p53 (28). However, this direct attack model does not explain how un-infected CD4 T cells die. Therefore, the pathogenesis of AIDS cannot be entirely explained by this hypothesis (23).

Another well-accepted model for explaining CD4 T cell depletion is the hyperimmune activation hypothesis. This model suggests that during HIV infection, there is a high rate of cell division among CD4 T- and CD8 T-, NK-, and B cells, accompanied with an upregulation of cell activation markers, which collectively leads to immune dysfunction (29). It was suggested that the constant activation of CD4 T cells causes their premature loss by activation-induced cell death or apoptosis (26). Studies on HIV-1

infection have demonstrated that the immune system of HIV-infected individuals remains in a hyperactive state characterized by high T cell turnover, non-specific T cell activation and proliferation, polyclonal activation of B cells, and increased proinflammatory cytokines (30). HIV has been found to activate the immune system via induction of inflammatory cytokines (23), and through mechanisms mediated by viral gene products (23, 26). Nef and Vpr have been found to stimulate monocytes and macrophage cells (23), while HIV RNA has been shown to activate plasmacystoid dendritic cells through toll-like receptor-mediated recognition, which induces the production of interferon (31). Further, the mere presence of HIV DNA in the cytoplasm has been shown to cause caspase-1 activation and release of proinflammatory cytokines including interleukin (IL)-1β (31), suggesting that even abortive HIV infection could induce immune activation if there is viral DNA in the cell.

Apoptosis is also a well-recognized mechanism known to contribute to CD4 T cell loss in HIV infection. In T cell types that are permissive to HIV infection, apoptosis was found to be mediated by caspase-3 (32). However, in non-permissive T cell subsets that do not support HIV replication, cell death is believed to occur through pyroptosis, a highly inflammatory form of programmed cell death, driven by caspase-1 (32). During pyroptosis, the dying cell releases all its cytoplasmic contents, including inflammatory cytokines, which then trigger pyroptosis in other T cells in a continuous cycle of abortive "bystander" T cell depletion (33). Studies have demonstrated that only 5% of CD4 T cell depletion is attributed to apoptosis, while the 95% remaining quiescent lymphoid CD4 T cells die from caspase-1-mediated pyroptosis triggered by abortive viral infection (32,

33). Pyroptosis can therefore be regarded as a contributor to both CD4 T cell depletion and chronic inflammation, creating a recurring pathologic cycle in which dying CD4 T cells release inflammatory signals that stimulate other cells to die (34).

A patient is considered to have clinical AIDS when the CD4 T cell blood count drops below 200 cells/ml (35). At this stage, individuals become prone to various opportunistic bacterial, viral, and fungal infections, and many oncological complications (36). Most of the HIV-related deaths result from these AIDS-associated infections and/or cancers, rather than being a direct effect of HIV (36, 37). The currently administered HAART regimen typically comprises a combination of three drugs: dual nucleoside reverse transcriptase (RT) inhibitors (NRTIs) plus a non-nucleoside RT inhibitor or integrase inhibitor (38, 39). HAART is highly effective and can completely or nearly completely suppress HIV replication (39). However, these drugs do not offer a cure, necessitating lifelong treatment, which is associated with drug toxicity and an increased risk of viral resistance (19, 40). Thus, there is a vital need for research geared towards exploring novel therapeutic strategies, including those that target steps in the viral replication cycle not addressed by currently available drugs.

HIV-1 Biology and Replication Cycle

HIV-1 is an enveloped virus belonging to the family Retrovirdae and the Lentivirus genus (41). Its genome comprises two identical copies of single-stranded, positive-sense RNA encoding nine open reading frames that produce 15 proteins with structural and regulatory functions (41, 42). HIV-1's replication cycle can be divided into an early and a late phase. The early phase events include: (a) virus attachment to cell

surface receptors; (b) viral entry; (c) reverse transcription of the viral RNA to cDNA; (d) uncoating of the viral capsid; nuclear import of viral DNA, and (e) DNA integration. The late phase events comprise: (a) transcription of viral genes; (b) export of viral RNAs from the nucleus to the cytoplasm; (c) translation of viral RNAs to produce the polyprotein precursors Gag and GagPol, the viral envelope glycoproteins (Env glycoproteins), and the regulatory and accessory viral proteins; (d) trafficking of Gag and GagPol precursors and Env glycoproteins to the plasma membrane; (e) assembly of the Gag and GagPol polyproteins at the plasma membrane; (f) encapsidation of the viral RNA genome; (g) incorporation of the viral Env glycoproteins; (h) budding of the new virions from the infected cell; and (i) particle maturation (43).

HIV-1 infection begins with the adhesion of an infectious virion to its target cell. This binding is mainly mediated by the HIV-1 envelope (Env) proteins (44). Sometimes, the initial attachment of the virus to the cell membrane can be relatively non-specific, mediated by the interaction of Env with the various target cell receptors (e.g., negatively charged cell-surface heparan sulfate proteoglycans (45) and a4β7 integrin (46, 47), or by interactions between virion-incorporated host proteins and surface proteins on the target cell (44). Although non-essential, such non-specific interactions are believed to bring Env closer to the primary receptor (44), CD4 (48), and to the coreceptor, CXCR4 or CCR5, depending upon the tropism of the viral Env protein, and on the cell being infected (49). HIV strains are generally classified based on their coreceptor usage. Viruses utilizing CCR5 are termed R5 HIV, those that use CXCR4 are termed X4 HIV, and viruses that can use both coreceptors are called R5X4 HIV (50). HIV-1 Env comprises two subunits,

gp120 and gp41, arranged in a trimer. The gp120 subunit contains five conserved domains (C1-C5) and five variable loops (V1-V5) and mediates binding to CD4 (51). This binding event results in conformational rearrangements in the variable regions of Env, ultimately facilitating coreceptor interaction (44, 51). Once Env has engaged its primary and secondary receptors, another conformational change occurs that exposes the hydrophobic fusion peptide of gp41. This fusion peptide inserts into the host cell membrane, and tethers the viral and host membranes, leading to fusion (52).

After the fusion of HIV-1 particles with the host cell, the viral capsid cone is released into the cytoplasm and starts its migration toward the nucleus. During this journey, the viral RNA is reverse transcribed into double-stranded viral DNA, which then forms a complex with cellular and viral proteins, termed the preintegration complex (PIC) (53). The enzyme reverse transcriptase (RT) first synthesizes a negative-sense DNA strand from the viral RNA template, using virus-incorporated host tRNALys3, as a primer for DNA extension (54). This is followed by positive sense DNA strand synthesis to generate a complementary double-stranded DNA molecule (cDNA) encoding the complete viral genome (55). Contents of PIC complex include the cDNA, the viral enzymes reverse transcriptase and integrase (IN), the viral capsid (CA) and nucleocapsid proteins (NC), and other cellular and viral proteins. The PIC enters the nucleus through interaction with the nuclear pore complex. In the nucleus, the viral enzyme integrase catalyzes the integration of the viral cDNA into the host genome (56). The integrated provirus can then serve as a template for the transcription of viral genes by the host RNA polymerase II (57).

HIV gene expression involves a synergy of complex interactions between chromatin-associated proviral DNA, cell transcription factors, and the virally encoded Tat (trans-activator of transcription) protein. Viral transcription is first mediated by direct interaction between cellular transcription factors and cis-acting elements located in the viral long terminal repeat (LTR) promoter (58). Following this initial phase of transcription, viral gene expression becomes highly reliant on the accumulation of sufficient amounts of Tat from the earlier transcription events (58). The Tat protein interacts with host transcription factors and the trans-activation response element (TAR), located at the 5’ end of viral mRNAs, to actively upregulate viral gene transcription (59). Successful transcription of proviral DNA yields multiple viral mRNA species, which are generated from a single full-length transcript by alternative splicing and contain common 5' and 3' ends. The spliced transcripts include the multiply spliced mRNA encoding early regulatory proteins such as Tat, negative regulatory factor (Nef) and regulator of expression of virion proteins (Rev), and the partially spliced mRNA encoding viral protein P (Vpu), viral infectivity factor (Vif), viral protein R (Vpr) and viral envelope protein (Env) (60). The un-spliced, full-length mRNA encodes the Gag and Gag-Pol polyprotein precursors. In eukaryotic cells, intron-containing transcripts are usually retained in the nucleus until they are completely spliced or degraded. Nuclear export of un-spliced and partially spliced viral RNAs is mediated by a cis-acting RNA element called the Rev Responsive Element (RRE) (58, 60). The virus-encoded Rev, which shuttles between the nucleus and cytoplasm, specifically interacts with RRE to permit nuclear export of these intron-containing viral transcripts (60).

Once the full-length viral RNA transcript is in the cytoplasm, the Gag and GagPol polyproteins are synthesized. Gag is produced as a 55kDa precursor protein that forms the virus particle, and it has its own initiation and termination codons (61). Synthesis of the 160 kDa Gag-Pol polyprotein precursor- which contains the viral enzymes protease, reverse transcriptase and integrase, results from a frameshifting event at the Sp2 region of the Gag coding sequence (62). The Gag precursor is comprises 4 major structural domains, Matrix (MA), Capsid (CA), Nucleocapsid (NC), and the viral late domain (p6). Formation of viral particles is achieved by the coordinated process of membrane binding and multimerization of Gag. The exact mechanism of how Gag is trafficked to the plasma membrane is still unclear (61). However, it is known that the modification of Gag by removal of the initiator methionine residue, followed by N-terminal myristoylation, allows Gag to stably interact with the host cell membrane (63). Gag can specifically interact with phosphatidylinositol-(4,5) bisphosphate 2 (PI4,5P2), a phospholipid highly abundant in the inner leaflet of the cell membrane, through the highly basic region (HBR) of the MA domain. This interaction is believed to promote both binding and targeting of Gag to the plasma membrane (64, 65).

The CA domain of Gag contains two helical domains connected by a flexible linker: the C-terminal domain (CA-CTD) and the N-terminal domain (CA-NTD) (61). The CA-CTD contains a dimer interface, which plays a crucial role in Gag multimerization (61, 66). The NC domain of Gag is primarily responsible for driving viral RNA packaging. Being a nucleic acid chaperone, NC is also involved in incorporating the tRNA primer and in reverse transcription (67). NC contains two zinc-

finger domains that interact with a structural motif on the viral RNA called the packaging signal, or the ψ-element, located near the 5′ end of the genomic RNA in the 5′ untranslated region (UTR). This interaction directs the encapsidation of viral genomic RNA into the assembling Gag lattice (67, 68).

The viral envelope glycoprotein (Env) is translated as a precursor protein (gp160), after which it is extensively glycosylated by host cell machinery in the endoplasmic reticulum and Golgi. Following these modifications, Env is trafficked through the secretory pathway to the plasma membrane, where it is incorporated into assembling virus particles (69). Although the mechanism by which Env is incorporated into virions is incompletely understood (61), it is believed to depend on specific interactions between the cytoplasmic tail of Env and certain residues in the MA domain of Gag (70, 71). Several theories have been suggested for the mechanism of Env incorporation. These include incorporation by a passive process, by co-targeting of Gag and Env to a common lipid raft on the plasma membrane, by direct recruitment of Env by Gag, or by indirect recruitment of Env by Gag via a host cell cross-linking protein (61, 69). Once the immature Gag lattice assembles at the plasma membrane, the nascent particle must undergo membrane fission to be released from the infected cell (61). This scission step is mediated by the cellular endosomal sorting complexes required for transport (ESCRT) pathway, which is hijacked by HIV-1 Gag (72). The p6 domain of Gag is essential for the recruitment of ESCRT complexes to facilitate virus budding (61, 73). Host ESCRT machinery comprises a multi-subunit assembly that catalyzes a membrane bending and scission reaction in a direction away from the cytoplasm, usually involved in processes

like the multivesicular body (MVB) pathway, cytokinesis and cell division (74). All these ESCRT-mediated processes are characterized by budding away from the cytoplasm. Retroviruses have therefore evolved to strategically exploit the ESCRT machinery for their egress (73).

For the virion particle to be infectious, the immature Gag polyprotein lattice must be converted to the mature lattice by the enzyme viral protease, which is packaged into virions as part of the GagPol precursor (61). Concurrent with viral release, virus maturation is triggered by protease-mediated cleavage at multiple cut sites within the Gag and GagPol polyproteins. The HIV-1 protease is a dimeric aspartic protease with an active site located in a cleft at the dimer juncture (61, 72). This protease enzyme cleaves each of its target sites with considerably varying efficiencies, setting off a highly organized, stepwise processing cascade (61, 75). Mutations that alter the processing of protease cleavage sites within Gag can be detrimental to maturation and particle infectivity, as they can lead to the formation of aberrant, non-functional cores (75, 76). Successful maturation causes a change in the virion morphology from a radial conformation to the typical cone shaped of the HIV-1 core. Once the maturation process is complete, the virus particle becomes infectious and can start a second round of infection (61).

Restriction Factors and their Viral Antagonists

Mammalian cells express several host proteins that can inhibit HIV-1 replication at various stages of its life cycle. These proteins are rereferred to as restriction factors (77) and often possess commonly shared features. They are germline encoded, expressed

in different cell types and their expression is often upregulated by interferon, which is a hallmark of restriction factors. These host factors usually can limit viral replication and confer a restrictive phenotype when expressed in an otherwise permissive cell. They are also usually encoded by genes that have undergone positive selection as a result of host adaptation to viral infection. Many restriction factors are counteracted by viruses through downmodulation or cellular protein degradation pathways (77, 78). The inhibitory effects of restriction factors may be a product of a direct interference exerted by these intrinsic proteins or may result indirectly from a cell-regulatory function (78). Virus-host co-evolution has caused restriction factors to be less effective against viruses in their natural hosts but more potent against cross-species transmission (77-79).

To date, several types of restriction factors have been identified that target different steps in the HIV-1 replication cycle (77-80). The well-characterized restriction factor apolipoprotein B mRNA editing enzyme, catalytic polypeptide-like (APOBEC3G) or A3G, a member of the family of cytidine deaminases, restricts a wide range of viruses including endogenous and pathogenic retroviruses and HBV. A3G inhibits HIV-1 cDNA synthesis by causing detrimental G-to-A hypermutations in the proviral genome during reverse transcription (81-84). Other members of the APOBEC3 family have also been reported to inhibit HIV-1 replication (85, 86). Upon HIV-1 infection, A3G and other APOBEC family members, such as A3F, are incorporated into budding virions, thus exerting their antiviral activity in newly infected cells (81-84). The HIV-1 Vif protein has evolved mechanisms to antagonize the antiviral activity of A3G and other HIV-restricting APOBEC family members (87, 88). It has been shown that Vif binds to A3G promoting

the recruitment of the ElonginB/C-Cullin-5 E3 ubiquitin ligase complex leading to A3G poly-ubiquitination and proteasomal degradation, which ultimately reduces the rate of A3G incorporation into the newly produced virions (81, 88, 89).

Another well-studied restriction factor is tetherin or bone marrow stromal antigen 2 (BST-2), which strongly anchors budding viral particles on the infected cell's membrane, preventing the release of HIV-1 and other enveloped viruses (90, 91). This function is achieved by tetherin's unique structure that contains an N-terminal transmembrane domain and a C-terminal glycosyl-phosphatidylinositol group, which allows one end of the protein to be attached to the plasma membrane and the other to the viral envelope. The retained virions are then internalized and degraded via the endosomal/lysosomal pathway (90-92). Human HIV and non-human primate SIV viruses have evolved countermeasures for protection against tetherin. The HIV-1 Vpu protein overcomes human tetherin restriction by promoting poly-ubiquitination of its transmembrane domain inducing its proteasomal degradation. HIV-1 Vpu also downregulates tetherin from the cell surface and sequesters it in endosomal compartments leading to its lysosomal degradation (93-95).

TRIM5a is another interferon-inducible restriction factor belonging to the family of tripartite motif (TRIM)-containing proteins. This large family of cellular proteins participates in various cellular processes, including proliferation, differentiation, development, apoptosis, oncogenesis, and innate immunity (96-98). Several members of the TRIM family exhibit anti-retroviral activity, among which TRIM5a is the most extensively studied. TRIM5a-mediated restriction occurs upon retroviral entry into the

target cell cytoplasm. The virion core is targeted by TRIM5a through capsid recognition (96, 97, 99, 100). This is generally accompanied by a failure to synthesize viral cDNA (96), although the exact mechanisms by which TRIM5 proteins block retroviral infection have not been completely elucidated. It has been demonstrated that TRIM5a can directly bind to HIV-1 capsids, and incoming retroviral capsids that encounter TRIM5a lose their structural integrity on entry into the cytoplasm (101). These findings suggest that TRIM5a, and other members of the TRIM family, accelerate capsid fragmentation soon after viral entry, thereby disrupting reverse transcription complex (RTC) architecture and blocking reverse transcription (101-103). The countermeasures that HIV-1 uses to resist the effects of TRIM proteins are poorly understood, it has been reported, however, that the accessory protein Vpr can regulate the levels of TRIM11 in the cell, and this regulation depends on the expression levels of Vpr (104).

SAMHD1 (Sterile Alpha Motif and Histidine Aspartate domain-containing protein 1) is a deoxynucleotide triphosphohydrolase that restricts HIV-1 by interfering with reverse transcription by reducing the availability of cellular dNTPs (105-107). Following HIV-1 entry into CD4 T cells and delivery of the HIV-1 capsid into the cytoplasm, the HIV-1 RNA is reverse transcribed into DNA, a process strongly affected by the repertoire of dNTPs in the cell. SAMHD1 possesses a dNTPase activity and controls the pool of cytosolic dNTPs by hydrolyzing all four dNTPs to yield deoxynucleosides and inorganic triphosphate, thus preventing proviral DNA formation and subsequent HIV-1 replication (105, 108). Recent reports have suggested that SAMHD1's ribonuclease activity contributes to SAMHD1-mediated viral restriction by

targeting viral RNA for degradation before reverse transcription (109, 110). However, the relevance of this RNase activity to HIV-1 restriction is still questionable (109, 111, 112). To counteract the inhibitory effect of SAMHD1, HIV-2 and some simian immunodeficiency virus strains (SIVsm/SIVmac) encode the accessory protein Vpx (113, 114), which interacts with the C-terminal domain of SAMHD1 to recruit the Cullin-4 E3 ubiquitin ligase, which targets SAMHD1 for poly-ubiquitination and proteasomal degradation, alleviating SAMHD1-mediated retroviral restriction (108, 113, 115). HIV-1 lacks Vpx and therefore cannot antagonize SAMHD1, which makes the virus susceptible to its effects (108).

SERINC3 and SERINC5 are multi-pass transmembrane proteins belonging to the serine incorporator (SERINC) gene family. These proteins function to incorporate the amino acid serine into the lipids of cell membranes (116). SERINC3 and SERINC5 restrict Nef-deficient HIV-1 mutants (117, 118); in the absence of Nef, SERINC5 gets incorporated into assembling virion particles in producer cells and results in reduced viral infectivity (117-119). Fluorescent microscopy and super-resolution imaging of single viral particles have revealed that SERINC5 packaging into viral particles leads to reduced viral fusion with the target cell membrane (120, 121). The Nef proteins of HIV-1, HIV-2 and SIV have all been shown to counteract the restrictive activity of SERINC3/5 (117, 118). It has been shown that the Nef-mediated antagonism of SERINC5 may involve vesicular trafficking, endolysosomal degradation, and targeting of SERINC5 to endolysosomal vesicular bodies (117, 118, 122-125). The susceptibility of SERINC5 to

downmodulation by Nef was shown to be dependent on the terminal cytoplasmic loops of SERINC5 (126, 127).

Interferon-induced transmembrane proteins (IFITMs) are a family of small transmembrane proteins that are evolutionarily conserved and are upregulated in response to interferon viral infection (128). IFITM3, the most extensively studied member of this family, restricts multiple viruses including HIV-1, influenza virus and flaviviruses (129-131). Although the mechanism of IFITM3-mediated restriction is not completely understood, this restriction factor is known to target two distinct stages of the viral life cycle. When expressed in target cells, IFITM3 has been found to block entry, while its expression in producer cells reduces virion infectivity (129, 130, 132-135). At the entry stage, IFITM3 impedes fusion pore formation between the viral and host membranes by altering membrane lipid components and fluidity. As a result, the viral genome does not enter the cytosol, preventing virus replication (131, 136-139). If expressed in virus-producing cells, IFITM3 is incorporated into nascent retroviral particles which substantially abolishes their infectivity (130, 133, 134, 140). IFITM3 interferes with the processivity of the HIV-1 Env protein gp160, leading to a reduced amount of mature Env in viral particles (135, 140, 141). IFITM3 was also observed to affect the incorporation of the murine leukemia virus (MLV) Env, and its effects were shown to be counteracted by the glyco-Gag protein of Moloney MLV (135). It is unknown, however, whether any HIV-1 proteins possess the ability to antagonize IFTIM3.

Myxovirus resistance protein 2 (MX2) belongs to the dynamin superfamily of guanosine triphosphatases (GTPases) (142). Humans encode two closely related MX

genes; MX1 and MX2, both having antiviral properties (142). The MX genes are inducible by type 1 and type 3 interferons (IFNs). MX2 has been identified as an interferon-induced protein with potent antiviral activity against HIV-1 and other primate lentiviruses (143-147). While the precise mechanism of MX2-mediated inhibition of HIV-1 infection has not been fully elucidated, MX2's anti-viral effect is known to take place after reverse transcription but preceding nuclear import and integration of viral DNA in the host chromatin (143-145, 148). It was shown that MX2 expression did not affect late reverse transcription products but caused a decrease in the levels of HIV-1 2-LTR circles and integrated proviral DNA (143-146). Moreover, the HIV-1 capsid protein is an important determinant for MX2-mediated restriction, as demonstrated by capsid protein mutations, which allow the virus to escape the antiviral effects of MX2 (143, 144, 146, 149). Further, studies have shown that multiple nuclear pore complex components interact with MX2 to block nuclear import of HIV-1 (147, 150). Whether there are any viral antagonists to counteract MX2 restriction remains unknown (151).

Membrane-associated RING-CH 8 (MARCH8) is a protein in the RING finger E3 ubiquitin ligase family (152, 153) that downregulates HIV-1 Env glycoproteins from the cell surface, resulting in reduced incorporation of Env into viral particles (153, 154). This results in a substantial decrease in virus fusion efficiency (153). A tyrosine motif in the cytosolic tail of HIV-1 Env was shown to be a determinant for its MARCH8-mediated downregulation (153, 154). Besides its anti-HIV activity, MARCH8 has recently been found to have broad-spectrum effects. Other envelope glycoproteins, including those of the Vesicular Stomatitis Virus (VSV) and Ebolavirus were also shown to be

downregulated from the cell surface in the presence of MARCH8 (153, 155). Although MARCH8 is not inducible by interferon, two members of the MARCH family, MARCH1 and MARCH2, have been reported to inhibit HIV-1 and VSV envelope incorporation, and their expression was inducible by interferon (156, 157).

Guanylate-binding protein-5 (GBP5) is a small GTPase that responds to induction by interferon-γ (158). It was discovered as a potential HIV-1 restriction factor in an evolutionary screen of human genes that have undergone positive selection (159). GBP5 was shown to restrict HIV-1 infectivity by interfering with the activity of the cellular protease furin, leading to defective envelope processing and incorporation (160, 161). Mutations in the GTPase domain of GBP5 did not affect its ability to restrict HIV-1 (160). Other viruses, including MLV, influenza virus, and measles virus, were also found to be susceptible to the GBP5-mediated inhibition of furin cleavage (161, 162). There is currently no evidence of viral antagonisms against GBP5; however, mutations in the Vpu initiation codon were suggested to confer resistance to the antiviral action of GBP5 (160, 163).

HIV-1 Rev-Dependent Indicator CD4 T Cell Line (A3R5-Rev-GFP)

Most of the infectivity experiments in the upcoming chapters have been performed utilizing an HIV-1 Rev-dependent indicator cell line, called A3R5-Rev-GFP (Fig. 1.1). This cell line, constructed by Wu et al. (164), is a T cell line derived from A3.01 cells that have been genetically modified to express the green fluorescent protein (GFP) in response to HIV-1 infection. A3R5-Rev-GFP cells exhibit natural CD4, CXCR4 and α4β7 expression and constitutive expression of CCR5. These cells offer a major

advantage over the commonly used HIV indicator cells in terms of specificity and sensitivity (164); the reporter system of A3R5-Rev-GFP cells is considerably different from the other LTR-based reporter cells, which rely only on the HIV long terminal repeat (LTR) promoter, to drive reporter expression. The issue with depending solely on the LTR promoter for driving reporter gene expression lies in the susceptibility of the LTR to non-HIV stimuli (164). In addition to responding to the early HIV protein, tat, the LTR also responds to cell culture conditions and a variety of factors including cytokines, mitogens, HDAC inhibitors, lipopolysaccharide, certain anti-tumor drugs, free viral proteins, and other unknown factors (164-166). The presence of such non-HIV-dependent reporter expression greatly diminishes reporter specificity and sensitivity. To solve these issues, the rev-dependent expression vector was made to contain numerous HIV DNA sequences, including the Rev-response element and HIV splicing sites efficiently used by human cells (Fig. 1.1) (164). Additionally, the construct also contains a reading frame that, in the absence of HIV Rev, becomes eliminated by cellular splicing activity. In the absence of HIV infection, the transcription of the reporter provirus generates a single transcript that is rapidly spliced, which removes the GFP- coding reading frame. However, in the presence of HIV-1 Rev, incompletely spliced and non-spliced transcripts are delivered to the cytosol through interactions with the Rev responsive element, resulting in the expression of GFP (164) (Fig.1.1).

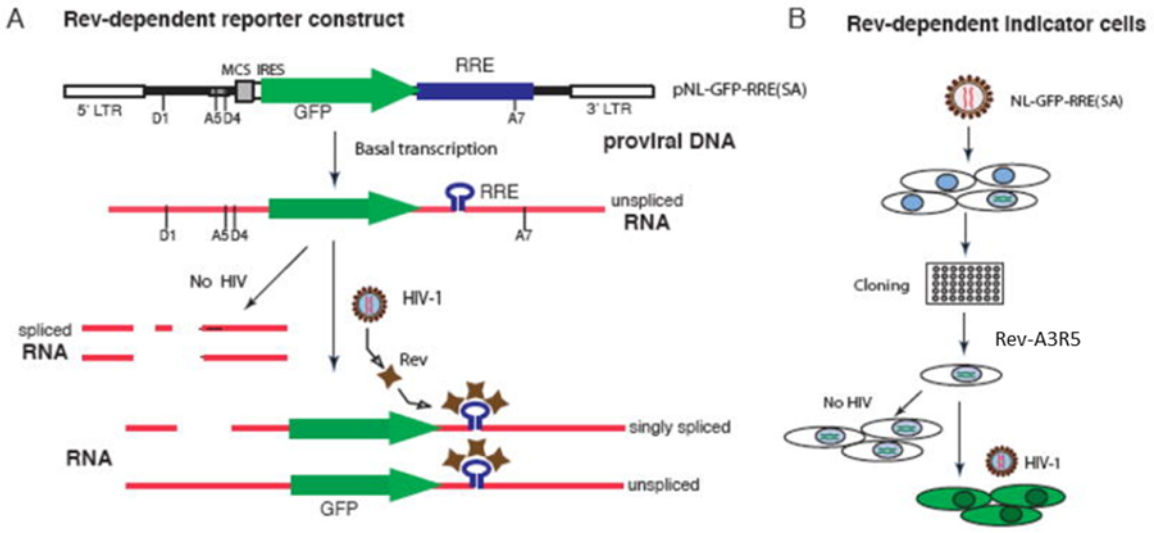

Figure 1.1 Rev-dependent reporter vector and indicator cells.
A) The construct has four segments of the HIV genome and no intact HIV genes. The first segment (the 5′ end of the vector) contains the HIV 5′ LTR, splice donor site 1 (D1), and a segment of the gag open reading frame that includes the packaging signal. The second HIV segment is derived from the tat1/rev1 exon that contains splice acceptor site 5 (A5), and splice donor site 4 (D4). The third segment is from the HIV DNA env exon and encompasses the RRE, and splice acceptor site 7 (A7). The last segment includes the entire 3′ LTR and a small portion of the nef reading frame, 5′ to the LTR. In the absence of HIV infection, the reporter provirus undergoes basal transcription tielding a single transcript that is rapidly spliced, resulting in the removal of the GFP reading frame. In the presence of HIV Rev, partially spliced and non-spliced transcripts are delivered to the cytosol by Rev, and the reporter gene is expressed. B) A3R5 cells were infected with a lentiviral vector encoding the Rev-dependent green fluorescent protein (GFP) reporter construct. A clone was isolated and infection by HIV resulted in generation of GFP. This figure was modified from (164).

References

1. Barré-Sinoussi F, Chermann JC, Rey F, Nugeyre MT, Chamaret S, Gruest J, et al. Isolation of a T-lymphotropic retrovirus from a patient at risk for acquired immune deficiency syndrome (AIDS). Science. 1983;220(4599):868-71.
2. Quinn TC. Global burden of the HIV pandemic. Lancet. 1996;348(9020):99-106.
3. Sharp PM, Hahn BH. Origins of HIV and the AIDS pandemic. Cold Spring Harb Perspect Med. 2011;1(1):a006841.
4. Becerra JC, Bildstein LS, Gach JS. Recent Insights into the HIV/AIDS Pandemic. Microb Cell. 2016;3(9):451-75.
5. Ndung'u T, McCune JM, Deeks SG. Why and where an HIV cure is needed and how it might be achieved. Nature. 2019;576(7787):397-405.
6. Fitzpatrick MC, Gray GE, Galvani AP. The Challenge of Vanquishing HIV for the Next Generation-Facing the Future. JAMA Pediatr. 2018;172(7):609-10.
7. WHO. HIV/AIDS [updated Nov 30, 2020. Available from: https://www.who.int/news-room/fact-sheets/detail/hiv-aids.
8. Okoye AA, Picker LJ. CD4(+) T-cell depletion in HIV infection: mechanisms of immunological failure. Immunol Rev. 2013;254(1):54-64.
9. Phetsouphanh C, Xu Y, Zaunders J. CD4 T Cells Mediate Both Positive and Negative Regulation of the Immune Response to HIV Infection: Complex Role of T Follicular Helper Cells and Regulatory T Cells in Pathogenesis. Front Immunol. 2014;5:681.
10. Levy JA. Pathogenesis of human immunodeficiency virus infection. Microbiol Rev. 1993;57(1):183-289.
11. Naif HM. Pathogenesis of HIV Infection. Infect Dis Rep. 2013;5(Suppl 1):e6.
12. Maartens G, Celum C, Lewin SR. HIV infection: epidemiology, pathogenesis, treatment, and prevention. Lancet. 2014;384(9939):258-71.
13. Simon V, Ho DD, Abdool Karim Q. HIV/AIDS epidemiology, pathogenesis, prevention, and treatment. Lancet. 2006;368(9534):489-504.
14. Robb ML, Ananworanich J. Lessons from acute HIV infection. Curr Opin HIV AIDS. 2016;11(6):555-60.
15. Mackelprang RD, Carrington M, Thomas KK, Hughes JP, Baeten JM, Wald A, et al. Host genetic and viral determinants of HIV-1 RNA set point among HIV-1 seroconverters from sub-saharan Africa. J Virol. 2015;89(4):2104-11.
16. Lassen K, Han Y, Zhou Y, Siliciano J, Siliciano RF. The multifactorial nature of HIV-1 latency. Trends Mol Med. 2004;10(11):525-31.
17. Sarmati L, D'Ettorre G, Parisi SG, Andreoni M. HIV Replication at Low Copy Number and its Correlation with the HIV Reservoir: A Clinical Perspective. Curr HIV Res. 2015;13(3):250-7.
18. Khanal S, Schank M, El Gazzar M, Moorman JP, Yao ZQ. HIV-1 Latency and Viral Reservoirs: Existing Reversal Approaches and Potential Technologies, Targets, and Pathways Involved in HIV Latency Studies. Cells. 2021;10(2):475.
19. Deeks SG, Overbaugh J, Phillips A, Buchbinder S. HIV infection. Nat Rev Dis Primers. 2015;1:15035.

20. Andrews SM, Rowland-Jones S. Recent advances in understanding HIV evolution. F1000Res. 2017;6:597.
21. Moir S, Chun TW, Fauci AS. Pathogenic mechanisms of HIV disease. Annu Rev Pathol. 2011;6:223-48.
22. McCune JM. The dynamics of CD4+ T-cell depletion in HIV disease. Nature. 2001;410(6831):974-9.
23. Vidya Vijayan KK, Karthigeyan KP, Tripathi SP, Hanna LE. Pathophysiology of CD4+ T-Cell Depletion in HIV-1 and HIV-2 Infections. Front Immunol. 2017;8:580.
24. De Boer RJ. Time scales of CD4+ T cell depletion in HIV infection. PLoS Med. 2007;4(5):e193.
25. Ho DD, Neumann AU, Perelson AS, Chen W, Leonard JM, Markowitz M. Rapid turnover of plasma virions and CD4 lymphocytes in HIV-1 infection. Nature. 1995;373(6510):123-6.
26. Yates A, Stark J, Klein N, Antia R, Callard R. Understanding the slow depletion of memory CD4+ T cells in HIV infection. PLoS Med. 2007;4(5):e177.
27. Hazenberg MD, Hamann D, Schuitemaker H, Miedema F. T cell depletion in HIV-1 infection: how CD4+ T cells go out of stock. Nat Immunol. 2000;1(4):285-9.
28. Cooper A, Garcia M, Petrovas C, Yamamoto T, Koup RA, Nabel GJ. HIV-1 causes CD4 cell death through DNA-dependent protein kinase during viral integration. Nature. 2013;498(7454):376-9.
29. Février M, Dorgham K, Rebollo A. CD4+ T cell depletion in human immunodeficiency virus (HIV) infection: role of apoptosis. Viruses. 2011;3(5):586-612.
30. Sodora DL, Silvestri G. Immune activation and AIDS pathogenesis. AIDS. 2008;22(4):439-46.
31. O'Brien M, Manches O, Bhardwaj N. Plasmacytoid dendritic cells in HIV infection. Adv Exp Med Biol. 2013;762:71-107.
32. Doitsh G, Cavrois M, Lassen KG, Zepeda O, Yang Z, Santiago ML, et al. Abortive HIV infection mediates CD4 T cell depletion and inflammation in human lymphoid tissue. Cell. 2010;143(5):789-801.
33. Doitsh G, Galloway NL, Geng X, Yang Z, Monroe KM, Zepeda O, et al. Cell death by pyroptosis drives CD4 T-cell depletion in HIV-1 infection. Nature. 2014;505(7484):509-14.
34. Doitsh G, Greene WC. Dissecting How CD4 T Cells Are Lost During HIV Infection. Cell Host Microbe. 2016;19(3):280-91.
35. Mayoclinic. HIV/AIDS - Diagnosis and treatment 2021 [Available from: https://www.mayoclinic.org/diseases-conditions/hiv-aids/diagnosis-treatment/drc-20373531
36. Chu C, Pollock LC, Selwyn PA. HIV-Associated Complications: A Systems-Based Approach. Am Fam Physician. 2017;96(3):161-9.
37. Chu C, Selwyn PA. Complications of HIV infection: a systems-based approach. Am Fam Physician. 2011;83(4):395-406.
38. Gunthard HF, Saag MS, Benson CA, del Rio C, Eron JJ, Gallant JE, et al. Antiretroviral Drugs for Treatment and Prevention of HIV Infection in Adults: 2016

Recommendations of the International Antiviral Society-USA Panel. JAMA. 2016;316(2):191-210.
39. Ford N, Migone C, Calmy A, Kerschberger B, Kanters S, Nsanzimana S, et al. Benefits and risks of rapid initiation of antiretroviral therapy. AIDS. 2018;32(1):17-23.
40. Pitman MC, Lewin SR. Towards a cure for human immunodeficiency virus. Intern Med J. 2018;48(1):12-5.
41. Engelman A, Cherepanov P. The structural biology of HIV-1: mechanistic and therapeutic insights. Nat Rev Microbiol. 2012;10(4):279-90.
42. Frankel AD, Young JA. HIV-1: fifteen proteins and an RNA. Annu Rev Biochem. 1998;67:1-25.
43. Adamson CS, Freed EO. Novel approaches to inhibiting HIV-1 replication. Antiviral Res. 2010;85(1):119-41.
44. Wilen CB, Tilton JC, Doms RW. HIV: cell binding and entry. Cold Spring Harb Perspect Med. 2012;2(8):a006866.
45. Saphire AC, Bobardt MD, Zhang Z, David G, Gallay PA. Syndecans serve as attachment receptors for human immunodeficiency virus type 1 on macrophages. J Virol. 2001;75(19):9187-200.
46. Arthos J, Cicala C, Martinelli E, Macleod K, Van Ryk D, Wei D, et al. HIV-1 envelope protein binds to and signals through integrin alpha4beta7, the gut mucosal homing receptor for peripheral T cells. Nat Immunol. 2008;9(3):301-9.
47. Cicala C, Martinelli E, McNally JP, Goode DJ, Gopaul R, Hiatt J, et al. The integrin alpha4beta7 forms a complex with cell-surface CD4 and defines a T-cell subset that is highly susceptible to infection by HIV-1. Proc Natl Acad Sci U S A. 2009;106(49):20877-82.
48. Bour S, Geleziunas R, Wainberg MA. The human immunodeficiency virus type 1 (HIV-1) CD4 receptor and its central role in promotion of HIV-1 infection. Microbiol Rev. 1995;59(1):63-93.
49. Shen HS, Yin J, Leng F, Teng RF, Xu C, Xia XY, et al. HIV coreceptor tropism determination and mutational pattern identification. Sci Rep. 2016;6:21280.
50. Arif MS, Hunter J, Leda AR, Zukurov JPL, Samer S, Camargo M, et al. Pace of Coreceptor Tropism Switch in HIV-1-Infected Individuals after Recent Infection. J Virol. 2017;91(19):e00793-17.
51. Chen B, Vogan EM, Gong H, Skehel JJ, Wiley DC, Harrison SC. Structure of an unliganded simian immunodeficiency virus gp120 core. Nature. 2005;433(7028):834-41.
52. Blumenthal R, Durell S, Viard M. HIV entry and envelope glycoprotein-mediated fusion. J Biol Chem. 2012;287(49):40841-9.
53. Suzuki Y, Craigie R. The road to chromatin - nuclear entry of retroviruses. Nat Rev Microbiol. 2007;5(3):187-96.
54. Isel C, Ehresmann C, Marquet R. Initiation of HIV Reverse Transcription. Viruses. 2010;2(1):213-43.
55. Hu WS, Hughes SH. HIV-1 reverse transcription. Cold Spring Harb Perspect Med. 2012;2(10).
56. Krishnan L, Engelman A. Retroviral integrase proteins and HIV-1 DNA integration. J Biol Chem. 2012;287(49):40858-66.

57. Craigie R, Bushman FD. HIV DNA integration. Cold Spring Harb Perspect Med. 2012;2(7):a006890.
58. Wu Y. HIV-1 gene expression: lessons from provirus and non-integrated DNA. Retrovirology. 2004;1:13.
59. Debaisieux S, Rayne F, Yezid H, Beaumelle B. The ins and outs of HIV-1 Tat. Traffic. 2012;13(3):355-63.
60. Wu Y, Marsh JW. Gene transcription in HIV infection. Microbes Infect. 2003;5(11):1023-7.
61. Freed EO. HIV-1 assembly, release and maturation. Nat Rev Microbiol. 2015;13(8):484-96.
62. Jacks T, Power MD, Masiarz FR, Luciw PA, Barr PJ, Varmus HE. Characterization of ribosomal frameshifting in HIV-1 gag-pol expression. Nature. 1988;331(6153):280-3.
63. Gottlinger HG, Sodroski JG, Haseltine WA. Role of capsid precursor processing and myristoylation in morphogenesis and infectivity of human immunodeficiency virus type 1. Proc Natl Acad Sci U S A. 1989;86(15):5781-5.
64. Ono A, Ablan SD, Lockett SJ, Nagashima K, Freed EO. Phosphatidylinositol (4,5) bisphosphate regulates HIV-1 Gag targeting to the plasma membrane. Proc Natl Acad Sci U S A. 2004;101(41):14889-94.
65. Chukkapalli V, Ono A. Molecular determinants that regulate plasma membrane association of HIV-1 Gag. J Mol Biol. 2011;410(4):512-24.
66. Bharat TA, Davey NE, Ulbrich P, Riches JD, de Marco A, Rumlova M, et al. Structure of the immature retroviral capsid at 8 A resolution by cryo-electron microscopy. Nature. 2012;487(7407):385-9.
67. Olson ED, Musier-Forsyth K. Retroviral Gag protein-RNA interactions: Implications for specific genomic RNA packaging and virion assembly. Semin Cell Dev Biol. 2019;86:129-39.
68. Lu K, Heng X, Summers MF. Structural determinants and mechanism of HIV-1 genome packaging. J Mol Biol. 2011;410(4):609-33.
69. Kirschman J, Qi M, Ding L, Hammonds J, Dienger-Stambaugh K, Wang JJ, et al. HIV-1 Envelope Glycoprotein Trafficking through the Endosomal Recycling Compartment Is Required for Particle Incorporation. J Virol. 2018;92(5):e01893-17.
70. Postler TS, Desrosiers RC. The tale of the long tail: the cytoplasmic domain of HIV-1 gp41. J Virol. 2013;87(1):2-15.
71. Pezeshkian N, Groves NS, van Engelenburg SB. Single-molecule imaging of HIV-1 envelope glycoprotein dynamics and Gag lattice association exposes determinants responsible for virus incorporation. Proc Natl Acad Sci U S A. 2019;116(50):25269-77.
72. Sundquist WI, Krausslich HG. HIV-1 assembly, budding, and maturation. Cold Spring Harb Perspect Med. 2012;2(7):a006924.
73. Ramdas P, Sahu AK, Mishra T, Bhardwaj V, Chande A. From Entry to Egress: Strategic Exploitation of the Cellular Processes by HIV-1. Front Microbiol. 2020;11:559792.
74. McCullough J, Colf LA, Sundquist WI. Membrane fission reactions of the mammalian ESCRT pathway. Annu Rev Biochem. 2013;82:663-92.

75. Adamson CS. Protease-Mediated Maturation of HIV: Inhibitors of Protease and the Maturation Process. Mol Biol Int. 2012;2012:604261.
76. Kaplan AH, Zack JA, Knigge M, Paul DA, Kempf DJ, Norbeck DW, et al. Partial inhibition of the human immunodeficiency virus type 1 protease results in aberrant virus assembly and the formation of noninfectious particles. J Virol. 1993;67(7):4050-5.
77. Ghimire D, Rai M, Gaur R. Novel host restriction factors implicated in HIV-1 replication. J Gen Virol. 2018;99(4):435-46.
78. Kluge SF, Sauter D, Kirchhoff F. SnapShot: antiviral restriction factors. Cell. 2015;163(3):774- e1.
79. Colomer-Lluch M, Ruiz A, Moris A, Prado JG. Restriction Factors: From Intrinsic Viral Restriction to Shaping Cellular Immunity Against HIV-1. Front Immunol. 2018;9:2876.
80. Zotova AA, Atemasova AA, Filatov AV, Mazurov DV. [HIV Restriction Factors and Their Ambiguous Role during Infection]. Mol Biol (Mosk). 2019;53(2):240-55.
81. Sheehy AM, Gaddis NC, Malim MH. The antiretroviral enzyme APOBEC3G is degraded by the proteasome in response to HIV-1 Vif. Nat Med. 2003;9(11):1404-7.
82. Salter JD, Bennett RP, Smith HC. The APOBEC Protein Family: United by Structure, Divergent in Function. Trends Biochem Sci. 2016;41(7):578-94.
83. Okada A, Iwatani Y. APOBEC3G-Mediated G-to-A Hypermutation of the HIV-1 Genome: The Missing Link in Antiviral Molecular Mechanisms. Front Microbiol. 2016;7:2027.
84. Yang H, Ito F, Wolfe AD, Li S, Mohammadzadeh N, Love RP, et al. Understanding the structural basis of HIV-1 restriction by the full length double-domain APOBEC3G. Nat Commun. 2020;11(1):632.
85. Smith HC, Bennett RP, Kizilyer A, McDougall WM, Prohaska KM. Functions and regulation of the APOBEC family of proteins. Semin Cell Dev Biol. 2012;23(3):258-68.
86. Kitamura S, Ode H, Iwatani Y. Structural Features of Antiviral APOBEC3 Proteins are Linked to Their Functional Activities. Front Microbiol. 2011;2:258.
87. Henriet S, Mercenne G, Bernacchi S, Paillart JC, Marquet R. Tumultuous relationship between the human immunodeficiency virus type 1 viral infectivity factor (Vif) and the human APOBEC-3G and APOBEC-3F restriction factors. Microbiol Mol Biol Rev. 2009;73(2):211-32.
88. Marin M, Rose KM, Kozak SL, Kabat D. HIV-1 Vif protein binds the editing enzyme APOBEC3G and induces its degradation. Nat Med. 2003;9(11):1398-403.
89. Yu X, Yu Y, Liu B, Luo K, Kong W, Mao P, et al. Induction of APOBEC3G ubiquitination and degradation by an HIV-1 Vif-Cul5-SCF complex. Science. 2003;302(5647):1056-60.
90. Neil SJ, Zang T, Bieniasz PD. Tetherin inhibits retrovirus release and is antagonized by HIV-1 Vpu. Nature. 2008;451(7177):425-30.
91. Van Damme N, Goff D, Katsura C, Jorgenson RL, Mitchell R, Johnson MC, et al. The interferon-induced protein BST-2 restricts HIV-1 release and is downregulated from the cell surface by the viral Vpu protein. Cell Host Microbe. 2008;3(4):245-52.

92. Perez-Caballero D, Zang T, Ebrahimi A, McNatt MW, Gregory DA, Johnson MC, et al. Tetherin inhibits HIV-1 release by directly tethering virions to cells. Cell. 2009;139(3):499-511.
93. Iwabu Y, Fujita H, Kinomoto M, Kaneko K, Ishizaka Y, Tanaka Y, et al. HIV-1 accessory protein Vpu internalizes cell-surface BST-2/tetherin through transmembrane interactions leading to lysosomes. J Biol Chem. 2009;284(50):35060-72.
94. Douglas JL, Viswanathan K, McCarroll MN, Gustin JK, Fruh K, Moses AV. Vpu directs the degradation of the human immunodeficiency virus restriction factor BST-2/Tetherin via a {beta}TrCP-dependent mechanism. J Virol. 2009;83(16):7931-47.
95. Blanchet FP, Mitchell JP, Piguet V. Beta-TrCP dependency of HIV-1 Vpu-induced downregulation of CD4 and BST-2/tetherin. Curr HIV Res. 2012;10(4):307-14.
96. Stremlau M, Owens CM, Perron MJ, Kiessling M, Autissier P, Sodroski J. The cytoplasmic body component TRIM5alpha restricts HIV-1 infection in Old World monkeys. Nature. 2004;427(6977):848-53.
97. Nisole S, Stoye JP, Saib A. TRIM family proteins: retroviral restriction and antiviral defence. Nat Rev Microbiol. 2005;3(10):799-808.
98. Yu A, Skorupka KA, Pak AJ, Ganser-Pornillos BK, Pornillos O, Voth GA. TRIM5alpha self-assembly and compartmentalization of the HIV-1 viral capsid. Nat Commun. 2020;11(1):1307.
99. Perez-Caballero D, Hatziioannou T, Yang A, Cowan S, Bieniasz PD. Human tripartite motif 5alpha domains responsible for retrovirus restriction activity and specificity. J Virol. 2005;79(14):8969-78.
100. Uchil PD, Quinlan BD, Chan WT, Luna JM, Mothes W. TRIM E3 ligases interfere with early and late stages of the retroviral life cycle. PLoS Pathog. 2008;4(2):e16.
101. Stremlau M, Perron M, Lee M, Li Y, Song B, Javanbakht H, et al. Specific recognition and accelerated uncoating of retroviral capsids by the TRIM5alpha restriction factor. Proc Natl Acad Sci U S A. 2006;103(14):5514-9.
102. Grutter MG, Luban J. TRIM5 structure, HIV-1 capsid recognition, and innate immune signaling. Curr Opin Virol. 2012;2(2):142-50.
103. Yang H, Ji X, Zhao G, Ning J, Zhao Q, Aiken C, et al. Structural insight into HIV-1 capsid recognition by rhesus TRIM5alpha. Proc Natl Acad Sci U S A. 2012;109(45):18372-7.
104. Yuan T, Yao W, Huang F, Sun B, Yang R. The human antiviral factor TRIM11 is under the regulation of HIV-1 Vpr. PLoS One. 2014;9(8):e104269.
105. Lahouassa H, Daddacha W, Hofmann H, Ayinde D, Logue EC, Dragin L, et al. SAMHD1 restricts the replication of human immunodeficiency virus type 1 by depleting the intracellular pool of deoxynucleoside triphosphates. Nat Immunol. 2012;13(3):223-8.
106. Goldstone DC, Ennis-Adeniran V, Hedden JJ, Groom HC, Rice GI, Christodoulou E, et al. HIV-1 restriction factor SAMHD1 is a deoxynucleoside triphosphate triphosphohydrolase. Nature. 2011;480(7377):379-82.
107. Powell RD, Holland PJ, Hollis T, Perrino FW. Aicardi-Goutieres syndrome gene and HIV-1 restriction factor SAMHD1 is a dGTP-regulated deoxynucleotide triphosphohydrolase. J Biol Chem. 2011;286(51):43596-600.

108. Laguette N, Sobhian B, Casartelli N, Ringeard M, Chable-Bessia C, Segeral E, et al. SAMHD1 is the dendritic- and myeloid-cell-specific HIV-1 restriction factor counteracted by Vpx. Nature. 2011;474(7353):654-7.
109. Ryoo J, Choi J, Oh C, Kim S, Seo M, Kim SY, et al. The ribonuclease activity of SAMHD1 is required for HIV-1 restriction. Nat Med. 2014;20(8):936-41.
110. Choi J, Ryoo J, Oh C, Hwang S, Ahn K. SAMHD1 specifically restricts retroviruses through its RNase activity. Retrovirology. 2015;12:46.
111. Antonucci JM, St Gelais C, de Silva S, Yount JS, Tang C, Ji X, et al. SAMHD1-mediated HIV-1 restriction in cells does not involve ribonuclease activity. Nat Med. 2016;22(10):1072-4.
112. Ballana E, Este JA. SAMHD1: at the crossroads of cell proliferation, immune responses, and virus restriction. Trends Microbiol. 2015;23(11):680-92.
113. Hrecka K, Hao C, Gierszewska M, Swanson SK, Kesik-Brodacka M, Srivastava S, et al. Vpx relieves inhibition of HIV-1 infection of macrophages mediated by the SAMHD1 protein. Nature. 2011;474(7353):658-61.
114. Goujon C, Arfi V, Pertel T, Luban J, Lienard J, Rigal D, et al. Characterization of simian immunodeficiency virus SIVSM/human immunodeficiency virus type 2 Vpx function in human myeloid cells. J Virol. 2008;82(24):12335-45.
115. Ahn J, Hao C, Yan J, DeLucia M, Mehrens J, Wang C, et al. HIV/simian immunodeficiency virus (SIV) accessory virulence factor Vpx loads the host cell restriction factor SAMHD1 onto the E3 ubiquitin ligase complex CRL4DCAF1. J Biol Chem. 2012;287(15):12550-8.
116. Inuzuka M, Hayakawa M, Ingi T. Serinc, an activity-regulated protein family, incorporates serine into membrane lipid synthesis. J Biol Chem. 2005;280(42):35776-83.
117. Rosa A, Chande A, Ziglio S, De Sanctis V, Bertorelli R, Goh SL, et al. HIV-1 Nef promotes infection by excluding SERINC5 from virion incorporation. Nature. 2015;526(7572):212-7.
118. Usami Y, Wu Y, Gottlinger HG. SERINC3 and SERINC5 restrict HIV-1 infectivity and are counteracted by Nef. Nature. 2015;526(7572):218-23.
119. Sharma S, Lewinski MK, Guatelli J. An N-Glycosylated Form of SERINC5 Is Specifically Incorporated into HIV-1 Virions. J Virol. 2018;92(22):e00753-18.
120. Sood C, Marin M, Chande A, Pizzato M, Melikyan GB. SERINC5 protein inhibits HIV-1 fusion pore formation by promoting functional inactivation of envelope glycoproteins. J Biol Chem. 2017;292(14):6014-26.
121. Chen YC, Sood C, Marin M, Aaron J, Gratton E, Salaita K, et al. Super-Resolution Fluorescence Imaging Reveals That Serine Incorporator Protein 5 Inhibits Human Immunodeficiency Virus Fusion by Disrupting Envelope Glycoprotein Clusters. ACS Nano. 2020;14(9):10929-43.
122. Shi J, Xiong R, Zhou T, Su P, Zhang X, Qiu X, et al. HIV-1 Nef Antagonizes SERINC5 Restriction by Downregulation of SERINC5 via the Endosome/Lysosome System. J Virol. 2018;92(11):e00196-18.
123. Ahmad I, Li S, Li R, Chai Q, Zhang L, Wang B, et al. The retroviral accessory proteins S2, Nef, and glycoMA use similar mechanisms for antagonizing the host restriction factor SERINC5. J Biol Chem. 2019;294(17):7013-24.

124. Kmiec D, Akbil B, Ananth S, Hotter D, Sparrer KMJ, Sturzel CM, et al. SIVcol Nef counteracts SERINC5 by promoting its proteasomal degradation but does not efficiently enhance HIV-1 replication in human CD4+ T cells and lymphoid tissue. PLoS Pathog. 2018;14(8):e1007269.
125. Staudt RP, Smithgall TE. Nef homodimers down-regulate SERINC5 by AP-2-mediated endocytosis to promote HIV-1 infectivity. J Biol Chem. 2020;295(46):15540-52.
126. Dai W, Usami Y, Wu Y, Gottlinger H. A Long Cytoplasmic Loop Governs the Sensitivity of the Anti-viral Host Protein SERINC5 to HIV-1 Nef. Cell Rep. 2018;22(4):869-75.
127. Stoneham CA, Ramirez PW, Singh R, Suarez M, Debray A, Lim C, et al. A Conserved Acidic-Cluster Motif in SERINC5 Confers Partial Resistance to Antagonism by HIV-1 Nef. J Virol. 2020;94(7):e01554-19.
128. Zhao X, Li J, Winkler CA, An P, Guo JT. IFITM Genes, Variants, and Their Roles in the Control and Pathogenesis of Viral Infections. Front Microbiol. 2019;9:3228.
129. Perreira JM, Chin CR, Feeley EM, Brass AL. IFITMs restrict the replication of multiple pathogenic viruses. J Mol Biol. 2013;425(24):4937-55.
130. Compton AA, Bruel T, Porrot F, Mallet A, Sachse M, Euvrard M, et al. IFITM proteins incorporated into HIV-1 virions impair viral fusion and spread. Cell Host Microbe. 2014;16(6):736-47.
131. Brass AL, Huang IC, Benita Y, John SP, Krishnan MN, Feeley EM, et al. The IFITM proteins mediate cellular resistance to influenza A H1N1 virus, West Nile virus, and dengue virus. Cell. 2009;139(7):1243-54.
132. Lu J, Pan Q, Rong L, He W, Liu SL, Liang C. The IFITM proteins inhibit HIV-1 infection. J Virol. 2011;85(5):2126-37.
133. Tartour K, Appourchaux R, Gaillard J, Nguyen XN, Durand S, Turpin J, et al. IFITM proteins are incorporated onto HIV-1 virion particles and negatively imprint their infectivity. Retrovirology. 2014;11:103.
134. Appourchaux R, Delpeuch M, Zhong L, Burlaud-Gaillard J, Tartour K, Savidis G, et al. Functional Mapping of Regions Involved in the Negative Imprinting of Virion Particle Infectivity and in Target Cell Protection by Interferon-Induced Transmembrane Protein 3 against HIV-1. J Virol. 2019;93(2):e01716-18.
135. Ahi YS, Yimer D, Shi G, Majdoul S, Rahman K, Rein A, et al. IFITM3 Reduces Retroviral Envelope Abundance and Function and Is Counteracted by glycoGag. mBio. 2020;11(1).
136. Londrigan SL, Wakim LM, Smith J, Haverkate AJ, Brooks AG, Reading PC. IFITM3 and type I interferons are important for the control of influenza A virus replication in murine macrophages. Virology. 2020;540:17-22.
137. Spence JS, He R, Hoffmann HH, Das T, Thinon E, Rice CM, et al. IFITM3 directly engages and shuttles incoming virus particles to lysosomes. Nat Chem Biol. 2019;15(3):259-68.
138. McMichael TM, Zhang L, Chemudupati M, Hach JC, Kenney AD, Hang HC, et al. The palmitoyltransferase ZDHHC20 enhances interferon-induced transmembrane

protein 3 (IFITM3) palmitoylation and antiviral activity. J Biol Chem. 2017;292(52):21517-26.
139. Desai TM, Marin M, Chin CR, Savidis G, Brass AL, Melikyan GB. IFITM3 restricts influenza A virus entry by blocking the formation of fusion pores following virus-endosome hemifusion. PLoS Pathog. 2014;10(4):e1004048.
140. Yu J, Li M, Wilkins J, Ding S, Swartz TH, Esposito AM, et al. IFITM Proteins Restrict HIV-1 Infection by Antagonizing the Envelope Glycoprotein. Cell Rep. 2015;13(1):145-56.
141. Wang Y, Pan Q, Ding S, Wang Z, Yu J, Finzi A, et al. The V3 Loop of HIV-1 Env Determines Viral Susceptibility to IFITM3 Impairment of Viral Infectivity. J Virol. 2017;91(7):e02441-16.
142. Mitchell PS, Young JM, Emerman M, Malik HS. Evolutionary Analyses Suggest a Function of MxB Immunity Proteins Beyond Lentivirus Restriction. PLoS Pathog. 2015;11(12):e1005304.
143. Goujon C, Moncorgé O, Bauby H, Doyle T, Ward CC, Schaller T, et al. Human MX2 is an interferon-induced post-entry inhibitor of HIV-1 infection. Nature. 2013;502(7472):559-62.
144. Kane M, Yadav SS, Bitzegeio J, Kutluay SB, Zang T, Wilson SJ, et al. MX2 is an interferon-induced inhibitor of HIV-1 infection. Nature. 2013;502(7472):563-6.
145. Liu Z, Pan Q, Ding S, Qian J, Xu F, Zhou J, et al. The interferon-inducible MxB protein inhibits HIV-1 infection. Cell Host Microbe. 2013;14(4):398-410.
146. Bulli L, Apolonia L, Kutzner J, Pollpeter D, Goujon C, Herold N, et al. Complex Interplay between HIV-1 Capsid and MX2-Independent Alpha Interferon-Induced Antiviral Factors. J Virol. 2016;90(16):7469-80.
147. Dicks MDJ, Betancor G, Jimenez-Guardeno JM, Pessel-Vivares L, Apolonia L, Goujon C, et al. Multiple components of the nuclear pore complex interact with the amino-terminus of MX2 to facilitate HIV-1 restriction. PLoS Pathog. 2018;14(11):e1007408.
148. Matreyek KA, Wang W, Serrao E, Singh PK, Levin HL, Engelman A. Host and viral determinants for MxB restriction of HIV-1 infection. Retrovirology. 2014;11:90.
149. Xu F, Zhao F, Zhao X, Zhang D, Liu X, Hu S, et al. Pro-515 of the dynamin-like GTPase MxB contributes to HIV-1 inhibition by regulating MxB oligomerization and binding to HIV-1 capsid. J Biol Chem. 2020;295(19):6447-56.
150. Kane M, Rebensburg SV, Takata MA, Zang TM, Yamashita M, Kvaratskhelia M, et al. Nuclear pore heterogeneity influences HIV-1 infection and the antiviral activity of MX2. Elife. 2018;7:e35738.
151. Staeheli P, Haller O. Human MX2/MxB: a Potent Interferon-Induced Postentry Inhibitor of Herpesviruses and HIV-1. J Virol. 2018;92(24):e00709-18.
152. Ohmura-Hoshino M, Goto E, Matsuki Y, Aoki M, Mito M, Uematsu M, et al. A novel family of membrane-bound E3 ubiquitin ligases. J Biochem. 2006;140(2):147-54.
153. Tada T, Zhang Y, Koyama T, Tobiume M, Tsunetsugu-Yokota Y, Yamaoka S, et al. MARCH8 inhibits HIV-1 infection by reducing virion incorporation of envelope glycoproteins. Nat Med. 2015;21(12):1502-7.

154. Zhang Y, Tada T, Ozono S, Kishigami S, Fujita H, Tokunaga K. MARCH8 inhibits viral infection by two different mechanisms. Elife. 2020;9:e57763.
155. Yu C, Li S, Zhang X, Khan I, Ahmad I, Zhou Y, et al. MARCH8 Inhibits Ebola Virus Glycoprotein, Human Immunodeficiency Virus Type 1 Envelope Glycoprotein, and Avian Influenza Virus H5N1 Hemagglutinin Maturation. mBio. 2020;11(5):e01882-20.
156. Zhang Y, Lu J, Liu X. MARCH2 is upregulated in HIV-1 infection and inhibits HIV-1 production through envelope protein translocation or degradation. Virology. 2018;518:293-300.
157. Zhang Y, Tada T, Ozono S, Yao W, Tanaka M, Yamaoka S, et al. Membrane-associated RING-CH (MARCH) 1 and 2 are MARCH family members that inhibit HIV-1 infection. J Biol Chem. 2019;294(10):3397-405.
158. Olszewski MA, Gray J, Vestal DJ. In silico genomic analysis of the human and murine guanylate-binding protein (GBP) gene clusters. J Interferon Cytokine Res. 2006;26(5):328-52.
159. McLaren PJ, Gawanbacht A, Pyndiah N, Krapp C, Hotter D, Kluge SF, et al. Identification of potential HIV restriction factors by combining evolutionary genomic signatures with functional analyses. Retrovirology. 2015;12:41.
160. Krapp C, Hotter D, Gawanbacht A, McLaren PJ, Kluge SF, Sturzel CM, et al. Guanylate Binding Protein (GBP) 5 Is an Interferon-Inducible Inhibitor of HIV-1 Infectivity. Cell Host Microbe. 2016;19(4):504-14.
161. Braun E, Hotter D, Koepke L, Zech F, Gross R, Sparrer KMJ, et al. Guanylate-Binding Proteins 2 and 5 Exert Broad Antiviral Activity by Inhibiting Furin-Mediated Processing of Viral Envelope Proteins. Cell Rep. 2019;27(7):2092-104 e10.
162. Li Z, Qu X, Liu X, Huan C, Wang H, Zhao Z, et al. GBP5 Is an Interferon-Induced Inhibitor of Respiratory Syncytial Virus. J Virol. 2020;94(21):e01407-20.
163. Hotter D, Sauter D, Kirchhoff F. Guanylate binding protein 5: Impairing virion infectivity by targeting retroviral envelope glycoproteins. Small GTPases. 2017;8(1):31-7.
164. Wu Y, Beddall MH, Marsh JW. Rev-dependent indicator T cell line. Curr HIV Res. 2007;5(4):394-402.
165. Siekevitz M, Josephs SF, Dukovich M, Peffer N, Wong-Staal F, Greene WC. Activation of the HIV-1 LTR by T cell mitogens and the trans-activator protein of HTLV-I. Science. 1987;238(4833):1575-8.
166. Sweet MJ, Hume DA. RAW264 macrophages stably transfected with an HIV-1 LTR reporter gene provide a sensitive bioassay for analysis of signalling pathways in macrophages stimulated with lipopolysaccharide, TNF-alpha or taxol. J Inflamm. 1995;45(2):126-35.

CHAPTER TWO: PSGL-1 IS A BROAD-SPECTRUM ANTIVIRAL HOST FACTOR AGAINST ENVELOPED VIRUSES

Abstract

PSGL-1 (P-selectin glycoprotein ligand-1) is a dimeric, mucin-like glycoprotein with a molecular weight of 120 kDa and functions as a ligand for P-, E-, and L-selectins. PSGL-1 is predominantly expressed on the surface of myeloid and lymphoid cells and is up-regulated during inflammation to mediate leukocyte tethering and rolling on the endothelium's surface for migration into inflamed tissues. Previous work has reported that PSGL-1 expression restricts HIV-1 infection. However, the mechanism by which PSGL-1 elicits its anti-HIV activity remained elusive. Here, we demonstrate that PSGL-1 inhibits HIV-1 particle infectivity by preventing virus particle binding to target cells. The anti-HIV effect of PSGL-1 occurred irrespectively of the viral envelope glycoprotein expressed on the particle. The adhesion of particles bearing either the HIV-1 envelope glycoprotein or vesicular stomatitis virus G glycoprotein, or those completely lacking a viral glycoprotein was impaired by PSGL-1. Mutational mapping revealed that the extracellular domain of PSGL-1 is required for its anti–HIV-1 activity, while the cytoplasmic domain contributed, to a lesser extent, to virus inhibition. Furthermore, our data shows that CD43, a PSGL-1-related monomeric glycoprotein, effectively suppresses HIV-1 infectivity. Finally, we found that PSGL-1 inhibits the infectivity of other

enveloped viruses including murine leukemia virus and influenza A virus, demonstrating that PSGL-1 is a host factor with broad-spectrum antiviral activity.

Introduction to PSGL-1 and its Role in Leukocyte Trafficking

P-selectin glycoprotein ligand-1 (PSGL-1), also known as SELPLG or CD162, is a 120-Kda transmembrane mucin-like glycoprotein that acts as a ligand for selectin proteins (1-3). PSGL-1 is constitutively expressed on platelets (4) and most leukocytes (1, 5, 6). During the inflammatory response, PSGL-1 is upregulated to promote leukocyte tethering and rolling on activated endothelium for recruitment to inflamed tissues (7-9). These events involve interactions between PSGL-1 on leukocytes and selectins on the vascular endothelium (5, 7). PSGL-1 can bind P- E- and L-selectins through interactions mediated by its N-terminal glycosylated domain, with the highest affinity for P-selectin (5). PSGL-1's role in cell recruitment has been widely demonstrated by its requirement for neutrophil migration into the inflamed peritoneum (10), for recruiting CD8+ T cells into the inflamed colon (11), and CD4+ T cells into the intestinal lamina propria (12), and reactive lymph nodes (13), emphasizing PSGL-1's fundamental role in the inflammatory response.

The migration of leukocytes from the bloodstream is a highly coordinated process of adhesive and signaling events that regulate inflammatory responses to infection or injury (14-16). In the absence of inflammation, leukocytes are continuously moving passively within the bloodstream (17). Exposure to microbial or inflammatory stimuli triggers the capture of leukocytes and their extravasation to the inflamed interstitial tissues (15, 17, 18). Under resting conditions, leukocytes make short-lived, reversible

contacts with the endothelium in a rolling phenomenon known as steady-state rolling (17, 19). This steady rolling is largely mediated by the interaction of endothelial P-selectins with their leukocyte glycoprotein counterreceptors, primarily PSGL-1 (19, 20). In an inflammatory environment, the leukocyte rolling speed significantly slows down (17, 21). This dramatic decrease in rolling velocity coincides with the expression of E-selectins on the inflamed endothelium, which presents more binding sites for PSGL-1 to facilitate leukocyte capture (17, 22, 23). Additionally, a conformational change is triggered in the leukocyte function associated antigen 1 (LFA-1), leading to further leukocyte–endothelial cell interactions through binding of LFA-1 to its endothelial ligand ICAM-1 during the slow rolling state (17, 22, 24-26). The inflamed endothelium also expresses additional cell surface molecules including membrane-bound chemokines and cytokines that further enhance leukocyte activation (17, 20, 22, 23). This causes LFA-1, and other integrins on the leukocyte, to form stronger bonds with endothelial integrin ligands, such ICAM-1 and VCAM-1 (17, 21-23). This high affinity binding prompts full arrest of the rolling leukocyte at the endothelial surface. Arrested leukocytes then spread over the endothelium to strengthen their adhesion, where they begin a crawling motion mediated by leukocyte-bound Mac-1 and endothelial-expressed ICAM-1. Once they find their destination, leukocytes infiltrate the endothelial layer to enter the underlying inflamed tissues (22, 23). In addition to binding to endothelial P-and/or E-selectins, PSGL-1 also binds L-selectin (on other leukocytes), which amplifies the recruitment of leukocytes to the vascular wall. Additionally, activated platelets may also collect more leukocytes to

sites of inflammation via interactions between P-selectin (on platelets) and PSGL-1 on leukocytes (17, 27, 28).

The PSGL-1 molecule is typically expressed as a homodimer of two monomers linked via a disulfide bridge. Each subunit of the PSGL-1 dimer constitutes an extended, heavily glycosylated N-terminal domain, a transmembrane domain, and a cytosolic C-terminal domain (27, 29, 30). A large part of the PSGL-1 extracellular comprises a mucin–like domain, which contains 14-16 tandem repeats of 10 amino acids with the consensus sequence (-A-T/M-E-A-Q-T-T-X-P/L-A/T-). These repeat domains are known as decameric repeats (DRs). Each repeat also contains numerous O-glycosylated threonines (30%) and prolines (10%), which function to elongate and strengthen the protein backbone and separate the N-terminal selectin- binding sites from the cell membrane (29, 30). The PSGL-1 DRs are necessary for selectin-binding, as their deletion has been shown to impair PSGL-1 interaction with L- and P-selectins (31). Post-translational O-glycosylation and sulfation are required for PSGL-1 to bind its selectin ligands. Optimal binding to all three selectins requires the presence of fucosylated core-2 O-glycans, which contain sialyl Lewis-x (sLex) and/or Lex determinants, attached to Thr-57 (32). While sulfation of Tyr-46, -48 and -51 is necessary for efficient binding of L- and P- but not E-selectin to PSGL-1 (32). The transmembrane and intracellular domains of PSGL-1 are highly conserved among mammalian species (32). In the transmembrane domain, there is a conserved cysteine residue at the junction of the extracellular and transmembrane region, C310, which forms the disulfide bond for PSGL-1 dimerization, a requirement for optimal recognition by P-selectin (33).

It is uncertain whether the intracellular domain of PSGL-1 has any intrinsic signaling capabilities. However, the cytoplasmic tail of PSGL-1 has been shown to interact with scaffolding and signaling molecules and can therefore mediate signal transduction (34, 35). The binding of leukocyte-expressed PSGL-1 to selectins on platelets and/or endothelium generates signals that act synergistically with those from other activators to elicit effector responses (14, 21). Conserved residues in the intracellular region of PSGL-1 can bind and form complexes with ezrin and moesin, members of the ezrin/radixin/moesin (ERM) family of actin-adapter proteins. These complexes link PSGL-1 to the actin cytoskeleton and to molecules that transmit downstream signaling (32, 36-38). Cells expressing a truncated PSGL-1 intracellular tail, or which are treated with agents disrupting the actin cytoskeleton have exhibited a significant loss of their rolling efficiency (39), demonstrating that PSGL-1's cytoplasmic domain is required for this function. Moreover, the cytoplasmic domain of PSGL-1 can also interact with the immunoreceptor tyrosine-based activation motif (ITAM) adapter proteins DAP12 and FcRg (40). PSGL-1 ligation to P- and E-selectin has been reported to result in the phosphorylation of the src family kinases (SFKs), spleen tyrosine kinase (Syk), and phospholipase C (PLC) γ2 (40-42). This signaling cascade results in LFA-1 activation and its interaction with ICAM-1, leading to slow rolling in neutrophils. Specifically, it was shown that following PSGL-1 and E-selectin engagement, the cytoplasmic domain of PSGL-1 induces signaling through the src-family kinase Fgr and the ITAM adapters DAP12 and FcRg (40). These events lead to the recruitment of Syk, whose downstream effects involve the activation of SH2 domain-containing leukocyte

phosphoprotein of 76 kD (SLP-76), which activates Bruton tyrosine kinase (Btk) (43-45). Btk then promotes the phosphorylation of Akt, PLC γ 2, and the p38 mitogen-activated protein kinase (p38 MAPK), which finally culminates in LFA-1-dependent slow rolling of neutrophils on ICAM-1 (26, 42). While the interactions of PSGL-1 with SFKs and ITAM adaptor proteins signal were shown to cause slow rolling, the interactions of PSGL-1 with ezrin and moesin were found to promote leukocyte transcriptional changes that increase cell activation (34, 36). Specifically, PSGL-1 was shown to indirectly associate with Syk through moesin and ezrin, whose ITAM motif can directly interact with Syk, eventually inducing SRE-dependent transcriptional activity (46). Moreover, upon ligation with selectins, PSGL-1 is redistributed to membrane microdomains at the rear end of migrating leukocytes (37). Several signal transduction molecules including tyrosine kinases, lipid kinases and members of Rho GTPase family are thought to regulate the cytoskeletal rearrangements that drive PSGL-1/selectin-dependent leukocyte polarization (47).

Migration-Independent Roles for PSGL-1 in Immunity and Infection

Various studies have revealed roles for PSGL-1 in modulating immune responses, and in infectious diseases. PSGL-1 has been found to be involved in regulating of Th1-mediated immune responses (48). A mouse model of uveoretinitis demonstrated that during T cell activation, stimulating T cells with the Th1 cytokines INF-γ and IL-12 leads to PSGL-1 expression preferentially in the INF-γ-producing T cell population, suggesting that PSGL-1 could be an INF-γ- regulated factor involved in Th1-mediated immune responses (48). PSGL-1 was also shown to be an immune factor regulating T-cell

checkpoints (49). In mouse models of tumors and chronic viral infection, PSGL-1 deficient mice were shown to have enhanced T cell survival, viral control and anti-tumor immunity to melanoma. On the other hand, normal PSGL-1 expression in wild type mice was found to dampen TCR signals, limit the survival of effector T cells, and promote immune inhibitory receptor expression, indicating a role for PSGL-1 in regulating viral control and immunopathology (50). Moreover, PSGL-1 has been identified as a receptor for Enterovirus 71 (EV71) on leukocytes (51). It was shown that the N-terminus of PSGL-1 binds specifically to EV71, with five out of eight EV71 strains utilizing PSGL-1 as the primary receptor for infection of Jurkat T cells, while three other EV71 strains did not use PSGL1, suggesting the presence of alternative receptors for EV71 (52). It was also demonstrated that O-glycosylation on the amino acid T57 of PSGL-1, which is critical for PSGL-1-selectin interaction, is unnecessary for PSGL-1 binding to EV71. On the other hand, the tyrosine sulfation sites in the N-terminal region of PSGL-1 were shown to be important for PSGL-1 binding to EV71 (53).

In the context of HIV-1 infection, Conner et al. observed that PSGL-1 was up-regulated on monocytes derived from HIV-infected individuals. Additionally, soluble CD40 ligand (sCD40L) and glutamate, which are factors reported to be increased with HIV infection, were shown to induce PSGL-1 transcription in HIV-negative human monocytes ex vivo (54). These results were validated in an EcoHIV mouse model where expression of PSGL-1 in monocytes was increased in a CD40L-dependent manner (54). Further mapping of the signaling cascades induced by CD40L and glutamate revealed that the MAPK pathway and oxidative stress were critical mediators of PSGL-1 up-

regulation (54). Studies by Ono et al. have shown that PSGL-1 co-localizes with HIV Gag in T-cell uropods (55, 56), and at plasma membrane sites where HIV-1 assembles (56). Gag localization to uropods was shown to require Gag multimerization and selective association with specific uropod-directed microdomains (UDMs) containing the adhesion molecules PSGL-1, CD43, and CD44 but not ICAM-1, ICAM-3, or CD59 (56). The study revealed that Gag reorganizes UDMs via its multimerization activity, and that the association of Gag with these UDMs depends on the highly basic region (HBR) in the Gag matrix (MA) domain. The HBR of Gag was determined to be required for Gag-PSGL-1 co-clustering, and a polybasic domain (PBD) in the PSGL-1 cytoplasmic tail was found to be an important determinant for this colocalization (55, 56). However, the biological relevance of PSGL-1 and Gag colocalization during viral assembly has not been investigated in these previous works. In a proteomic profiling analysis of HIV-1-infected CD4+ T cells (57), PSGL-1 was identified as a factor that is downregulated specifically in HIV+ cells. PSGL-1 was also upregulated in response to interferon induction and inhibited HIV-1 infection early in the post entry stages (57). The study also demonstrated that PSGL-1 expression in HIV-1-producing cells causes progeny virions to drastically lose their infectivity (57). However, how PSGL-1 inhibited HIV-1 infectivity remained elusive.

In this chapter, we investigated the mechanisms by which PSGL-1 restricts HIV-1. We demonstrated that when expressed in virus producer cells, PSGL-1 is incorporated into HIV-1 particles and blocks virion infectivity by sterically blocking virus interaction with target cells. Additionally, mutational analysis of PSGL-1 structural domains was

used to determine the molecular components required for PSGL-1 to exert its anti-HIV-1 activity. Finally, we also explored the broad-spectrum anti-viral effects of PSGL-1. The results of this chapter have been published in the Proceedings of the National Academy of Sciences in April 2020.

Materials and Methods

Cells and cell lines

Peripheral blood buffy coats from HIV-1-negative adults were purchased from the New York Blood Center or received from the NIH Blood Bank. CD4+ T cells were isolated by negative selection using the Dynabeads Untouched magnetic separation kit (Invitrogen) or as previously described (58). CD4+ T cells were cultured in RPMI 1640 plus 10% fetal bovine serum (FBS) and 1x penicillin-streptomycin (Invitrogen). Resting CD4 T cells were activated by culturing in PHA (2 μg/ml) plus IL-2 (2 ng/mL) (PepTech). HEK293T cells (ATCC) and HeLaJC.53 cells (kindly provided by Dr. David Kabat) were maintained in Dulbecco-modified Eagle's medium (DMEM) (Invitrogen) containing 10% FBS and 1x penicillin-streptomycin (Invitrogen). To construct PSGL-1-HeLaJC53 cells, HeLaJC.53 cells were seeded into a 6-well plate and cultured in DMEM with 10% FBS. Cells were transfected with 2 μg pCMV3-PSGL-1 or pCMV3-Empty DNA using Jetprime transfection reagent (Polyplus) as recommended by the manufacturer. Transfected cells were cultured, selected in DMEM containing 10% FBS and 550 μg/ml of hygromycin B (Invitrogen) to generate stably transfected cells. Stable transfectants were maintained in DMEM containing 10% FBS and 550 μg/ml of hygromycin B (Invitrogen) plus 1x penicillin-streptomycin (Invitrogen).

Plasmids, vectors, transfection, and virion production and purification

The infectious HIV-1 molecular clone pNL4-3, codon-optimized Vpu expression vector (pcDNA-Vphu), and NL4-3 ΔVpu infectious molecular clone (pNL-U35) were obtained from the NIH AIDS Re- agent Program. pCMV3-PSGL-1, pCMV3-CD43, and pCMV3-empty vectors were obtained from Sinobiological. pRetroPSGL-1-NT, pRetroPSGL-1-CT, and pRetroPSGL-1 were synthesized and cloned into pMSCVneo vector by GeneScript. pPSGL-1- 3A, pPSGL-1-6A, pPSGL-1-C310A, pPSGL-1-ΔCT, and pPSGL-1(Wt) were kindly provided by Akira Ono (56). pPSGL-1ΔDR was kindly provided by Caroline Spertini and Olivier Spertini (31). pCMV3-CD43 was obtained from Sinobiological. pSV-ψ-MLV-env− was obtained from the NIH AIDS Reagent Program. pNLΔΨEnv (gp160) and pHCMV-G expressing the HIV-1 Env and the vesicular stomatitis virus G glycoprotein, respectively, were previously described (59). The GFP-expressing retroviral vector pRetroQ-AcGFP1-N1 was obtained from Clontech. The env-defective pNL4-3 derivative pNL4-3/KFS was described previously (60).

The procedure for HIV-1 particle production in HEK293T cells was described previously (58). For GFP reporter MLV particle assembly, pRetroQ-AcGFP1-N1 (0.5 μg), pSV-ψ- MLV-env- (0.375 μg), and pHCMV-G (0.125 μg) were cotransfected with either pCMV3-PSGL-1 or pCMV3-Empty vector (at indicated dosages) in a 6-well plate. Virus supernatants were collected 48 hours post-transfection. For transient transfection of HeLaJC.53 cells, 0.5 million cells were transfected with 2 μg of either pCMV3-Empty or pCMV-PSGL-1 using the transfection reagent Jetprime (Polyplus) as recommended by the manufacturer. Following transfection, cells were cultured for the indicated times until

analysis. For the p24 release assay in HEK293T cells, cells were co-transfected with 1 μg of HIV-1 NL4-3 and indicated doses of pCMV3-PSGL-1 or pCMV3-Empty DNA using Lipofectamine 2000 (Invitrogen). The supernatant was collected 48 hours post-transfection. To purify virions by ultracentrifugation, supernatants harvested from transfected HEK293T cells first filtered through a 0.45um filter, then concentrated by Vivaspin20 concentrator. Concentrated viruses were purified by ultra-speed centrifugation through a gradient of 6-18% OptiPrep solution (Sigma-Aldrich) (40,000 rpm for 2 hours, SW41Ti rotor from Beckman) followed by a second round of ultracentrifugation to pellet the virus (20,000 rpm for 1.5 hours, SW41Ti).

Infectivity assays

For flow cytometry-based infectivity assay, virus particles were produced in HEK293T cells by co-transfection with pNL4-3, pNL4-3ΔVpu, or pNL4-3ΔNef with pCMV3-PSGL- 1, pCMVCD43, or pCMV3-Empty, or by co-transfection with pNL4-3/KFS, pHCMV-G, and pCMV3- PSGL-1 or pCMV3-Empty vector (using the indicated plasmid inputs) in a 6-well plate with Lipofectamine 2000 (Invitrogen). Viral particles were also produced in CEM-SS cells by electroporation. Briefly, CEM-SS cells (2 million) were electroporated with pNL4-3 (2 μg) plus 400 ng of pCMV3-PSGL-1 or pCMV3-Empty using a T cell electroporation kit (Lonza). Viral particles were harvested at 3 days post electroporation. Rev-A3R5-GFP cells were infected with each of the indicated viruses (0.2-0.5 million cells/infection). The cells were then washed and cultured in fresh media. Flow cytometry analysis of GFP expression was performed on the indicated days. The percentage of GFP+ cells was quantified. For infectivity assays in

HeLa JC53-PSGL-1 and HeLa-JC53-empty cell lines, the cells were seeded in 6-well plates at a density of 0.2 x 10^6/well 24 hours before infection. Cells were infected with the indicated p24 equivalents of either WT NL4-3 or NL43ΔVpu. Viral replication was quantified by virion p24 released into the medium by p24 ELISA. For MLV (murine leukemia virus) virion infectivity, MLV-GFP reporter virus was assembled by co-transfecting HEK293T cells (in 6-well plate) with pSV-Ψ-MLV-env- (0.375 μg), pRetroQ-AcGFP1-N1 (0.5 μg), pHCMV-G (0.125 μg), and pCMV3-PSGL1 or an empty vector at the indicated dosages. An equal amount of DNA was used across all transfections. Viral supernatants were harvested 48h post transfection and used to infect HEK293T cells for 6 hours in the presence of Infectin (Virongy, Manassas, VA). Cells were washed to remove virus and Infectin and cultured for 48 hours for flowcytometry analyses.

To determine the effect of PSGL-1 on influenza A virus replication, HEK293T and MDCK cells were co-cultured at approximately 70 % confluence in 6-well plates and transfected with either empty vector or pCMV3-PSGL-1 (both vectors at 1.0 or 3.0 μg), together with an eight-plasmid influenza A/WSN/33 reverse genetics system (RGS) (1.0μg of each plasmid). Transfection reaction was prepared with PEI (polyethyleneimine). Culture supernatants were collected at 16 and 24 h post-transfection and titrated in MDCK cells to determine end-point titers (TCID50 per ml). For SARS-CoV2-S-pesudotyped lentivirus infectivity assay, Calu-3 cells (0.5 million cells/infection) were pre-treated with Infectin II (Virongy) for 1 hour at 37°C and then infected with equal p24 inocula of SARS-CoV-2 S-pseudotyped luciferase reporter lentiviruses

produced in the presence of PSGL-1, MUC1, MUC4 or empty vector. Cells were lysed at 72 hours post-infection using Luciferase Assay Lysis Buffer (Promega). Luminescence was measured by using GloMax® Discover Microplate Reader (Promega).

shRNA knockdown of PSGL-1

Lentiviral vectors carrying shRNAs against PSGL-1 or non- target control (NTC) (Sigma MISSION shRNA, PSGL-1 TRCN0000436811 or shRNA NTC) were purchased from Sigma. Virion particles were assembled by cotransfecting HEK293T cells with 0.5 μg of pHCMV-G, 1.5 μg pCMV-ΔR8.2, and 2 μg of lentiviral vectors using Lipofectamine 3000 (Invitrogen). The supernatant was collected at 48 hours post co-transfection, and then filtered through a 0.45um filter. Virion particles were used to transduce Jurkat T cells for 6 hours. Cells were then washed twice and cultured in fresh media for 3 days, and then selected in puromycin (4 μg /ml) for one to two weeks. PSGL-1 knockdown was confirmed by surface staining with an anti-PSGL-1 antibody (KPL-1) (BD Pharmingen) followed by staining with Alexa Fluor 488- conjugated goat anti-mouse secondary antibody (Invitrogen). PSGPL-1 knockdown or NTC control cells (2 x 106) were also transfected with 2 μg of HIV-1(NL4-3) DNA by electroporation using a T cell electroporation kit (Lonza). Viruses were harvested and used for the infection of Rev-A3R5-GFP cells (20 ng p24 per infection). Flow cytometry analysis of GFP expression was performed on the indicated days. Lentiviral vector-mediated ShRNA knockdown of PSGL-1 in primary CD4 T cells was performed as described previously (58). Briefly, blood resting CD4 T cells were purified by negative depletion, transiently stimulated with anti-CD3/CD28 beads (1 -2 beads per cell) for 12 hours, and then

transduced with the lentiviral vectors carrying shRNAs against PSGL-1 or non-target control (NTC) (Sigma MISSION shRNA, PSGL-1 TRCN0000436811 or shRNA NTC). Following transduction, the beads were removed at 12 hours, and cells were cultured for 3 days, and then analyzed from surface PSGL-1 expression. Cells were also subsequently transfected with HIV-1(NL4-3) DNA by electroporation using a T cell electroporation kit (Lonza). HIV-1 viral replication was monitored by harvesting cell culture supernatant, and HIV p24 was detected by an in-house p24 ELISA kit.

Viral attachment assay

Virion particles produced in the presence of PSGL-1, or the empty vector were incubated with HelaJC.53 cells (prechilled at 4 °C for 1 h) at 4 °C for 2 h. The cells were then washed extensively (five times) with cold PBS buffer and then lysed with LDS lysis buffer (Invitrogen) for analysis by Western blot.

Western blots

These antibodies were from the NIH AIDS Reagent Program: anti-HIV-1 p24 monoclonal antibody (183-H12-5C), anti-HIV Env (16H3) antibody, anti-HIV-1 gp41 monoclonal antibody (2F5), anti-HIV-1 gp41 monoclonal antibody (10E8). Cells or virus pellets were solubilized in lysis buffer containing 50 mM Tris-HCl (pH 7.4), 150 mM NaCl, 1 mM EDTA, 0.5% Triton X-100, and protease inhibitor cocktail (Roche Life Science, Basel, Switzerland) or LDS lysis buffer (Invitrogen). Proteins were denatured by boiling in sample buffer and subjected to SDS-PAGE, transferred to PVDF or nitrocellulose membrane, and incubated overnight at 4°C with one of these primary antibodies: anti-PSGL-1 monoclonal antibody (clone KPL-1, BD Pharmingen) (1:1000

dilution); anti-PSGL-1 TC-2 monoclonal antibody (Abcam) (1:1000 dilution); anti-PSGL-1 polyclonal antibody (Abcam) (1:1000 dilution); anti-PSGL-1-C terminal polyclonal antibody (anti-PSGL-1 amino acid 350 to the C-terminus) (Abcam) (1 μg/ml); anti-GAPDH goat polyclonal antibody (Abcam) (1:1000 dilution); anti-HIV envelope antibodies (183-H12-5C, 16H3, 2F5), and anti-CD63 polyclonal antibody (System Biosciences) (1:1000 dilution). Membranes were then incubated with HRP-labeled goat anti-mouse IgG (KPL) (1:2500 dilution) or anti-rabbit IgG (Cell Signaling) (1:2000 dilution) for 60 min at room temperature. Chemiluminescence signal was detected by using West Pico or West Femto chemiluminescence reagent (Thermo Fisher Scientific). Images were captured with a CCD camera (FluorChem 9900 Imaging Systems) (Alpha Innotech). Protein bands were also quantified using Image lab-Chemidoc (Bio-Rad Laboratories, France). On occasion, western blot was also performed using infrared imaging (Odyssey infrared imager, Licor Biosciences) with IR Dye goat anti-mouse or rabbit 680 or 800 cw labeled antibodies (Licor Biosciences) (1:5000 diluted in blocking buffer) for 1h at 4°C. The blots were washed three times for 15 minutes and scanned with Odyssey Infrared Imager (Licor Biosciences).

Viral entry assay (BLAM assay)

The viral entry assay was performed as previously described (61). Briefly, viruses were generated by cotransfection of HEK293T cells with three plasmids: pNL4-3, pAdvantage (Promega) and pCMV4-3BlaM-Vpr (kindly provided by Dr. Warner C. Greene) (at a ratio of 6:1:2). The supernatant was harvested at 48 hours post-transfection, concentrated, and then used for infection as suggested (61). Flow cytometry was

performed using a Becton Dickinson LSR II (Becton Dickinson). β-lactamase and CCF2 measurements were performed using a 407-nm violet laser with emission filters of 525/50 nm (green fluorescence) and 440/40 nm (blue fluorescence), respectively. Green and blue emission spectra were separated using a 505LP dichroic mirror. The UV laser was turned off during the analysis. Data analysis was performed using FlowJo software (FlowJo).

FACS analysis

For PSGL-1 surface staining, 0.5–1 million cells were stained with anti-PSGL1 antibody (KPL-1) (BD Pharmingen) followed by staining with Alexa Fluor 488-conjugated goat anti-mouse secondary antibody (Invitrogen). For surface staining of infected blood resting CD4 T cells, HIV-1 infection was done using 125 ng to 320 ng p24 gag equivalents of NLENG1-ES-IRES GPF reporter virus (64) (pseudotyped with HIV-1 NL4-3 envelope) per million cells. Cells were washed and cultured in 10% FBS RPMI with IL-7 (2 ng/mL) (64). On the indicated days, cells were harvested and stained at 4°C for 30 min with AF687 anti-PSGL-1 antibody (KPL-1, BD Pharmingen) and analyzed by flow cytometry. For surface PSGL-1 staining of Jurkat, CEM-SS, and A3R5.7 cells, 0.5 million cells were stained with FITC-conjugated anti-PSGL-1 antibody (Abcam) and analyzed by flow cytometry. For HIV-1-infected Jurkat T-cell surface staining, 0.5 million cells were infected with different volumes of HIV-1 NL4-3. At 3 days post-infection, cells were stained with anti-PSGL-1 antibody [KPL-1] (BD Pharmingen), followed by staining with Alexa Fluor 488-conjugated goat anti-mouse secondary antibody (Invitrogen) and flow cytometry analysis. For HEK293T cells, 0.5 million cells were cotransfected with different dosages (1 μg to 4 μg) of HIV NL4-3 Vpu and 100 ng

of pCMV3-PSGL-1 or pCMV3-CD43 using Lipofectamine 2000 (Invitrogen). Cells were stained at 48 hours post-transfection with anti-PSGL-1 antibody [KPL-1] (BD Pharmingen), followed by staining with Alexa Fluor 488-conjugated goat anti-mouse secondary antibody (Invitrogen).

P24 ELISA

HIV-1 p24 released into the cell culture supernatant was detected by an in-house p24 ELISA kit. Briefly, microtiter plates (Sigma-Aldrich) were coated with anti-HIV-1 p24 monoclonal antibody (183-H12-5C) (NIH AIDS Reagent Program). Samples were incubated for 2 hours at 37oC, followed by washing and incubating with biotinylated anti-HIV immune globulin (HIVIG) (NIH AIDS Reagent Program) for 1 hour at 37oC. Plates were then washed and incubated with avidin-peroxidase conjugate (R &D Systems) for 1 hour at 37° C, followed by washing and incubating with tetramethylbenzidine (TMB) substrate. Plates were kinetically read using an ELx808 automatic microplate reader (Bio-Tek Instruments) at 630 nm.

Results

PSGL-1 is downregulated in HIV-1 infected cells

A recent study by Liu et al. has identified PSGL-1 as a host restriction factor inducible by interferon-y in activated CD4+ T cells leading to the inhibition of HIV-1 infection (57). We, therefore, sought to study the potential effects of HIV-1 on PSGL-1 expression. First, we measured the basil levels of PSGL-1 in CD4 T cells and transformed Jurkat T- and CEM-SS T-cells by surface staining. We found that un-infected resting CD4+ T cells express high levels of PSGL-1 (Fig.2.1A), and their

activation with IL-2 and PHA led to PSGL-1 downmodulation (Fig. 1A), a finding that correlates with increased susceptibility of activated CD4+ T cells to HIV-1 infection (62). Jurkat cells showed lower levels of PSGL-1 expression while CEM-SS cells and the non-lymphoid cell lines, HeLa and 293T, had no detectable levels of PSGL-1 (Fig. 2.1B-D). Next, we quantified PSGL-1 expression in HIV-1-infected primary resting CD4 T cells, which were treated with IL-7 to allow low-level HIV replication (63, 64). As shown in figure 2.2A, we found that PSGL-1 was downregulated in resting CD4 T cells exclusively in the HIV+ cell population. We also infected Jurkat T cells with multiple doses of HIV-1 (Fig. 2.2A), and we observed an HIV-dosage-dependent downmodulation of PSGL-1 (Fig. 2.2C-D). These results are consistent with other studies showing PSGL-1 downregulation during HIV infection of transformed T cell lines (57, 65). Thus, the finding that PSGL-1 is targeted for downmodulation by HIV-1 supports the previous notion implicating PSGL-1 as an antiviral host protein (57).

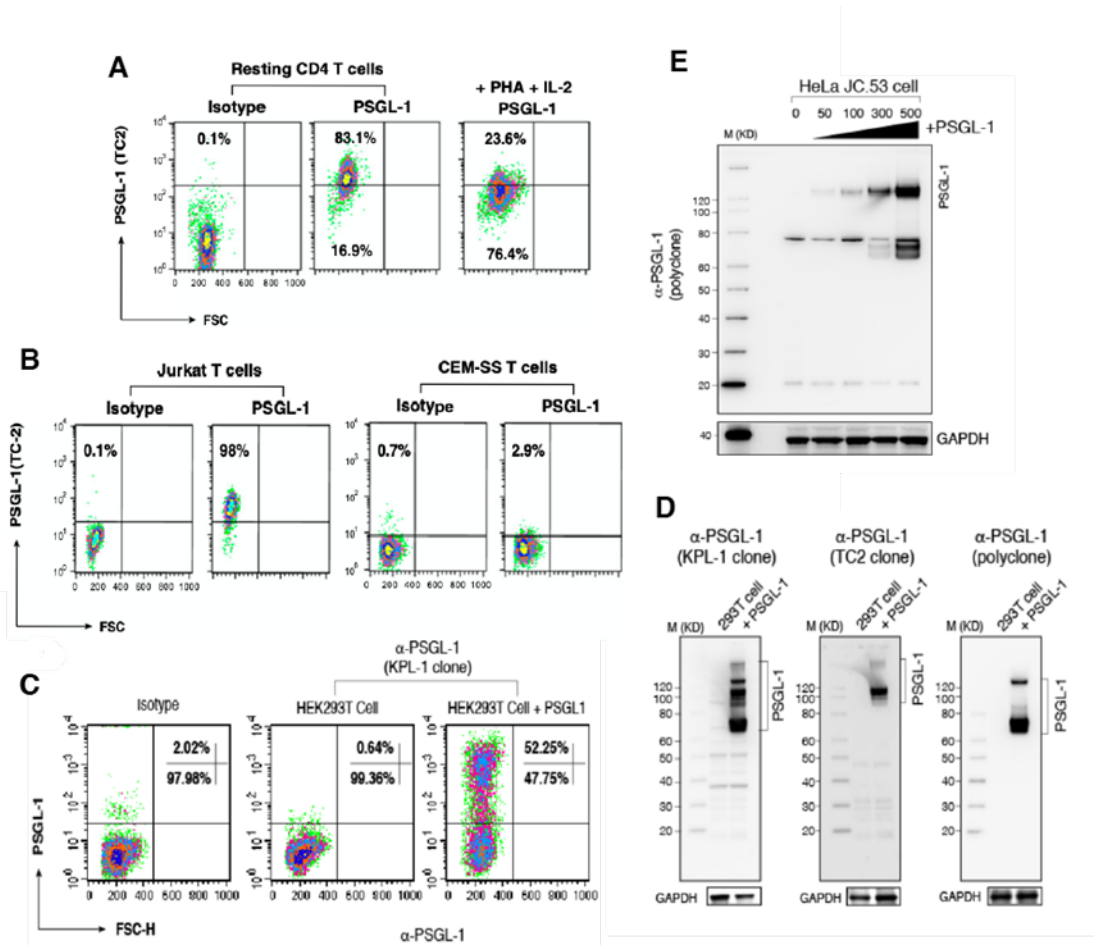

Figure 2.1 PSGL-1 expression in CD4+ T cells, T cell lines, and non-lymphoid cell lines.
A) Peripheral blood resting CD4 T cells were purified by negative selection, activated with PHA+IL-2, or left unstimulated. Cell surface PSGL-1 expression was analyzed by flow cytometry. B) Jurkat and CEM-SS cells were similarly stained for surface PSGL-1. C) Un-transfected HEK293T cells and PSGL-1-transfected HEK293T cells were analyzed by surface staining and flow cytometry. D) PSGL-1-transfected and un-transfected HEK293T cells were also analyzed by western blot using 3 different commercial antibodies. E) HeLa JC.53 cells were transfected with pCMV3-PSGL-1 using the indicated concentrations (ng of DNA). PSGL-1 expression was analyzed in transfected and un-transfected cells by western blot at 48 hours post-transfection with an anti-PSGL-1 polyclonal antibody. For all the shown western blots, GAPDH expression was analyzed as the loading control.

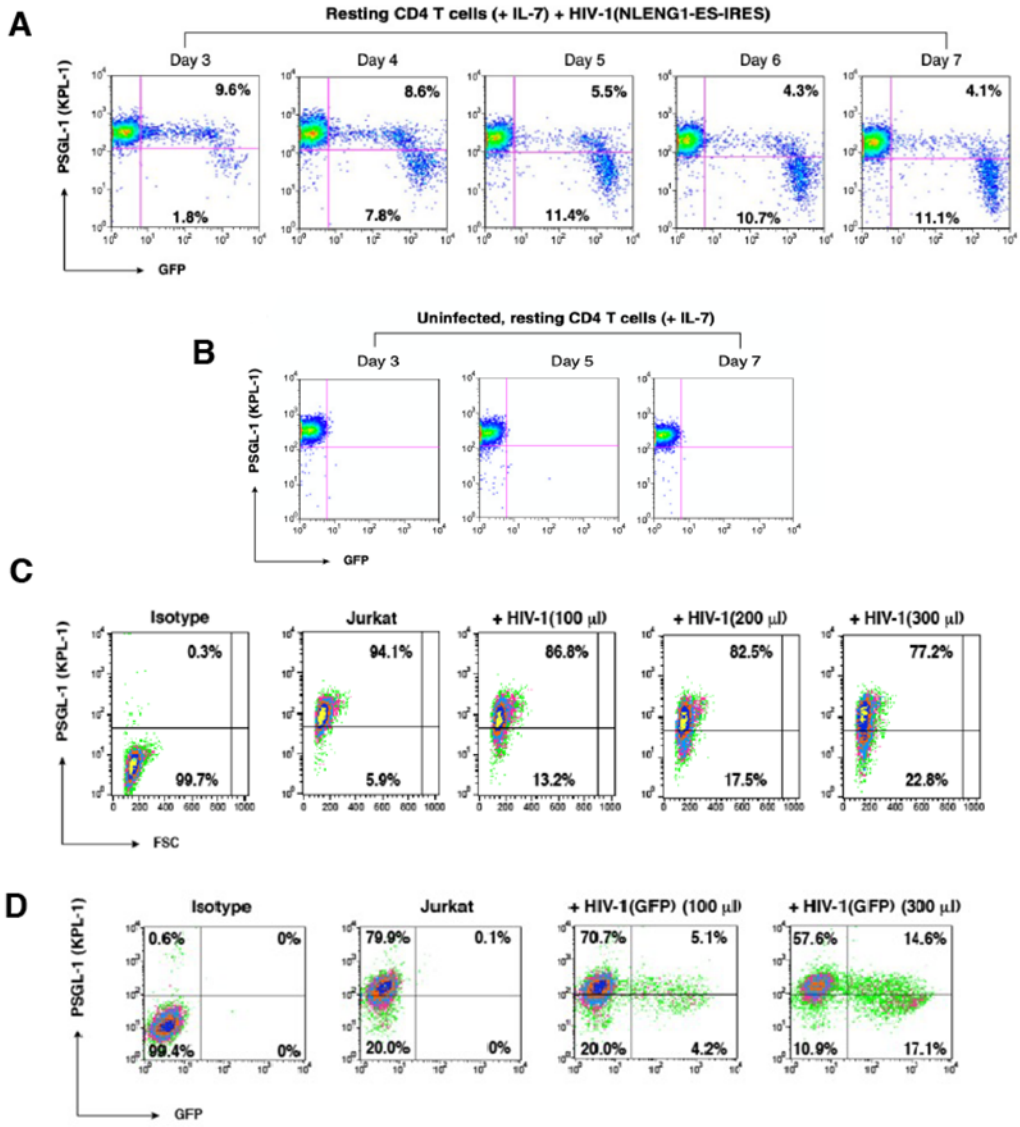

Figure 2.2 PSGL-1 is downregulated following HIV-1 infection.
A) Down-regulation of PSGL-1 by HIV-1 in primary CD4 T cells. Primary resting CD4 T cells were infected with NLENG1-ES-IRES, a GFP reporter virus. Following infection, cells were washed and cultured in complete medium plus IL-7 (2 ng/mL) to permit low-level viral replication. Surface PSGL-1 expression was analyzed at the indicated time-points. Shown are percentages of the GFP+ or GFP− cells with low or high PSGL-1 staining in each panel. PSGL-1 down- regulation was observed only in the HIV-infected (GFP+) cell population. B) As a control, uninfected cells were similarly cultured in IL-7, and surface PSGL-1 expression was analyzed at the indicated days. Culturing of resting CD4 T cells in IL-7 did not affect PSGL-1 expression. C-D) Dose-dependent down regulation of PSGL-1 in HIV-1-infected Jurkat cells. C) Jurkat T cells were infected with different inputs of HIV-1, washed and cultured for 3 days, and then stained for surface PSGL-1 expression, and analyzed by flow cytometry. Shown are the percentages of cells with high or low PSGL-1 staining in each panel. D) Cells were similarly infected with different inputs of an HIV-1 reporter virus, HIV-1(GFP), and then stained for surface PSGL-1 expression. Shown are the percentages of the GFP+ or GFP- cells with low or high PSGL-1 staining in each panel.

Inhibition of HIV-1 infection in a PSGL-1-expressing cell line

Given the observed down-modulation of PSGL-1 by HIV-1 in infected CD4 T cells (Fig. 2.2), we investigated the role of PSGL-1 in HIV-1 infection. We constructed a HeLa JC53 cell-line that stably expresses PSGL-1 (HeLa JC53-PSGL-1) (Fig.2.3A) and infected them with different inocula of HIV-1, ranging from 0.32 ng to 32 ng P24. As a control, a cell line stably expressing an empty vector (HeLaJC53-Empty) was similarly infected. Viral replication was measured by quantifying the levels of p24 in the supernatant of infected cells. Over a 14-day time course, we observed inhibition of HIV-1 replication and spread in the PSGL-1-expressing cells, with all inputs of HIV-1. Previous studies by Liu et al. have demonstrated that the HIV-1 accessory protein Vpu can counteract the antiviral activity of PSGL-1 by mediating its intracellular proteasomal degradation (57). Thus, we also infected the HeLa JC53-PSGL-1 and HeLa JC53-Empty cell lines with a Vpu-deficient HIV-1 mutant (HIVΔVpu), using virus inocula equal to those applied in the WT infection. Consistent with previous findings, the Vpu-deficient derivative was more susceptible to PSGL-1 restriction than its WT counterpart, as it showed a complete lack of ability to establish a spreading infection (Fig. 2.3B).

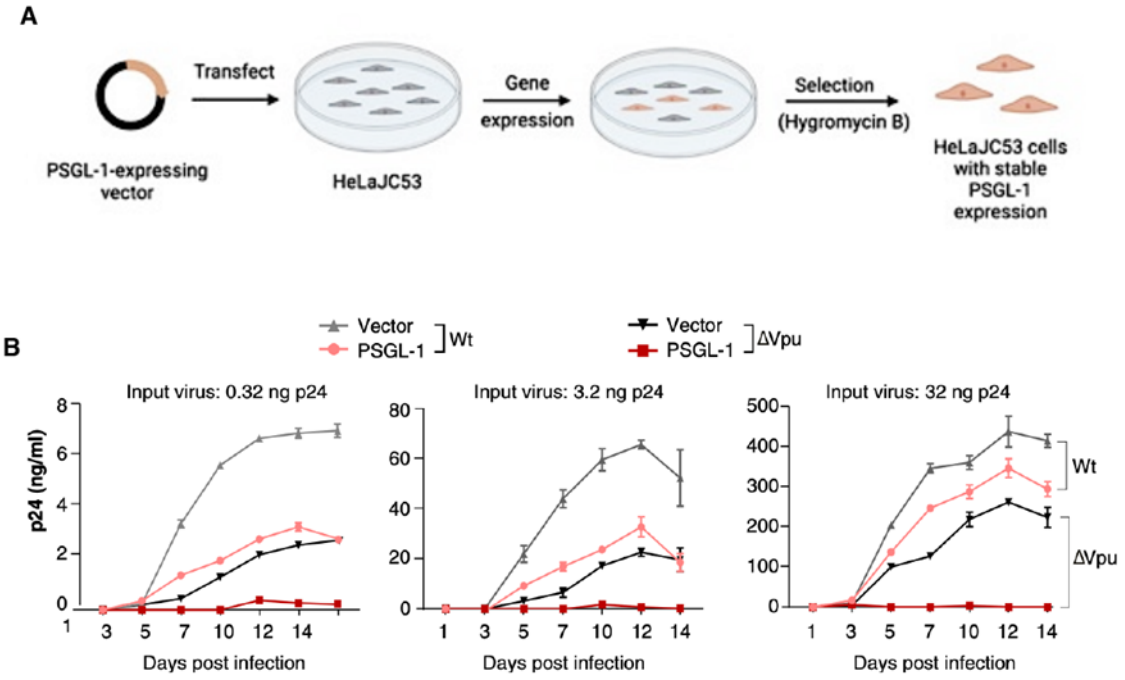

Figure 2.3 PSGL-1 inhibits HIV-1 infection and spread.
A) Schematic of the construction of a HeLaJC53 cell line stably expressing PSGL-1. HeLaJC53 cells were transfected with either a PSGL1-expressing vector (pCMV3-PSGL-1) or an empty vector (pCMV3-Empty). The transfected cells were cultured under selection by hygromycin B to obtain cells stably expressing PSGL-1 or empty vector. B) HeLa JC.53-PSGL-1 or HelaJC53-empty vector were infected with the indicated inputs of HIV-1(NL4-3) WT or HIV-1(ΔVpu). Viral replication was quantified by p24 release.

PSGL-1 has minimal effects on viral release

A previous study has reported that PSGL-1 blocks reverse transcription in the early stages of HIV infection and impairs virion infectivity later in the virus life cycle (57). To determine the step/s in the replication cycle targeted by PSGL-1, we examined its effects in a single round of HIV-1 infection. We used the HeLaJC53-PSGL-1 and HeLaJC53-vector cells described above as target cells for infection with an HIV-1 Env-pseudotyped, single-cycle virus, HIV (gp160) (66) (Fig. 2.4A). The amount of produced

virus was quantified by the levels of p24 in the supernatant, which showed that PSGL-1 did not inhibit particle release in a single round of infection.

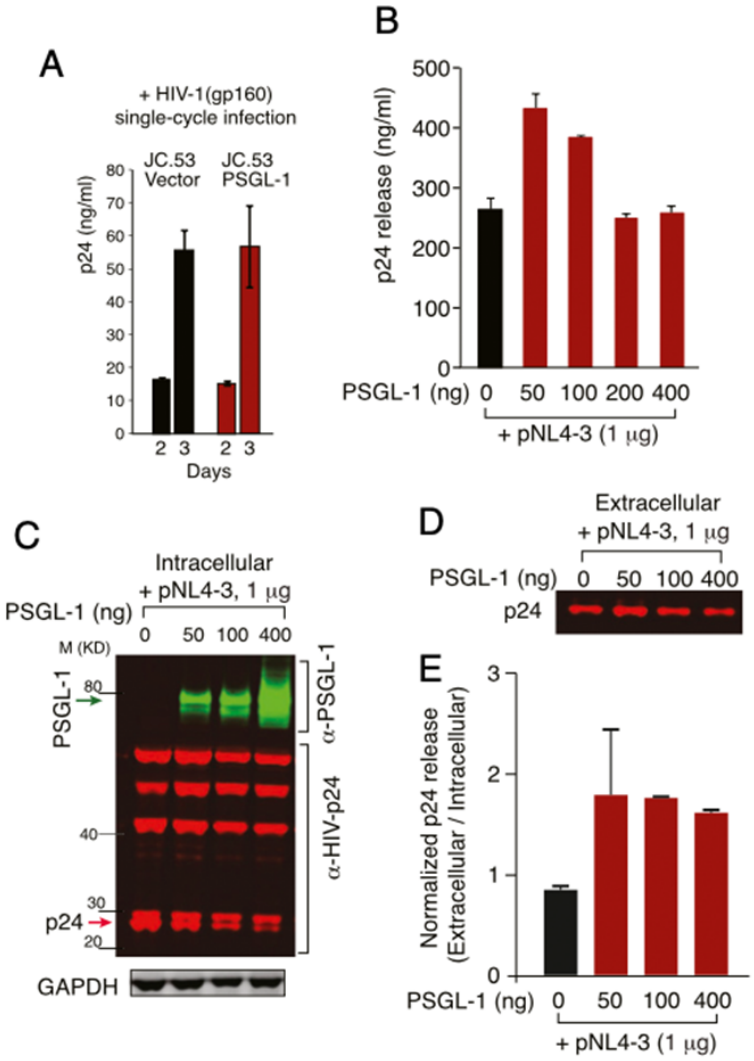

Figure 2.4 The effects of PSGL-1 on HIV-1 virion release.
A) HeLa JC.53 cells stably expressing PSGL-1 or an empty vector were infected with the single-round vector HIV-1 (gp160) for single-round infection. Viral replication was quantified by p24 release. The black and red bars represent empty vector and PSGL-1 vector-transfected cells, respectively. B–E) HEK293T cells were co-transfected with HIV(NL4-3) DNA (1 μg) plus different amounts of PSGL-1 expression vector. B) Viral p24 release was quantified at 48 h. C) Cells were also lysed and analyzed by Western blot for intracellular PSGL-1 and HIV-1 proteins. D) Extracellular virion p24 was also analyzed by Western blot D), and the relative ratio of extracellular and intracellular p24 was plotted E). The black and red bars represent empty vector and PSGL-1 vector co-transfected cells, respectively.

This result suggests PSGL-1 did not block any steps in the viral replication cycle up to the release of virion particles. The observed inhibition of HIV-1 in a multi-round spreading infection (Fig. 2.3B), but not in a single-cycle infection (Fig. 2.4A), indicates that the inhibitory effect of PSGL-1, seen in our experimental conditions, likely occurred after the first round of replication.

To further verify that PSGL-1 did not affect viral release, we looked at its impact on the production of HIV-1 particles from virus-producing cells, a method previously employed for other anti-HIV host proteins (67-69). We utilized a co-transfection system in which we co-transfected HEK293T cells with a plasmid containing HIV-1 proviral DNA (1 μg of NL43) with multiple doses of an expression vector encoding human PSGL-1 (50 to 400 ng). A plasmid expressing an empty backbone was used as a co-transfection control. The quantity of virus produced was then analyzed by supernatant p24 ELISA. We observed some enhancement in particle release at PSGL-1 doses lower than 100 ng, while the higher doses (200 and 400 ng) had no notable effect (Fig. 2.4B). However, upon extracellular to intracellular p24 normalization, we found that PSGL-1 did not impact the release of HIV virions at any of the co-transfected doses (Fig. 2.4 C–E).

PSGL-1 expression in virus-producing cells diminishes progeny virion infectivity

Considering that reducing virion infectivity is a common mechanism of restriction factors (70), we tested the effect of PSGL-1 on the infectivity of HIV-1 virions, using the same co-transfection scheme described above. Virus particles were assembled by co-expressing HIV-1 proviral- and PSGL-1 DNA in virus producer cells (HEK293T). We

then quantified the infectivity of the released particles in a Rev-dependent, HIV indicator CD4 T cell line, Rev-A3R5-GFP, which expresses GFP upon HIV-1 infection. In contrast to reporter cell lines driven solely by the LTR promoter, this cell line exhibits high sensitivity and specificity to HIV-1 and is not susceptible to noninfectious HIV stimuli (71, 72). As shown in Fig. 2.5A, PSGL-1 expression in virus-producer cells drastically reduced the infectivity of the released virions at the PSGL-1 DNA doses of 50-400 ng (Fig. 2.5A). The lower doses of PSGL-1 also blocked HIV-1 infectivity in a dosage-dependent manner, with visible inhibitory effects at DNA inputs as low as 1-5 ng (Fig. 2.5B).

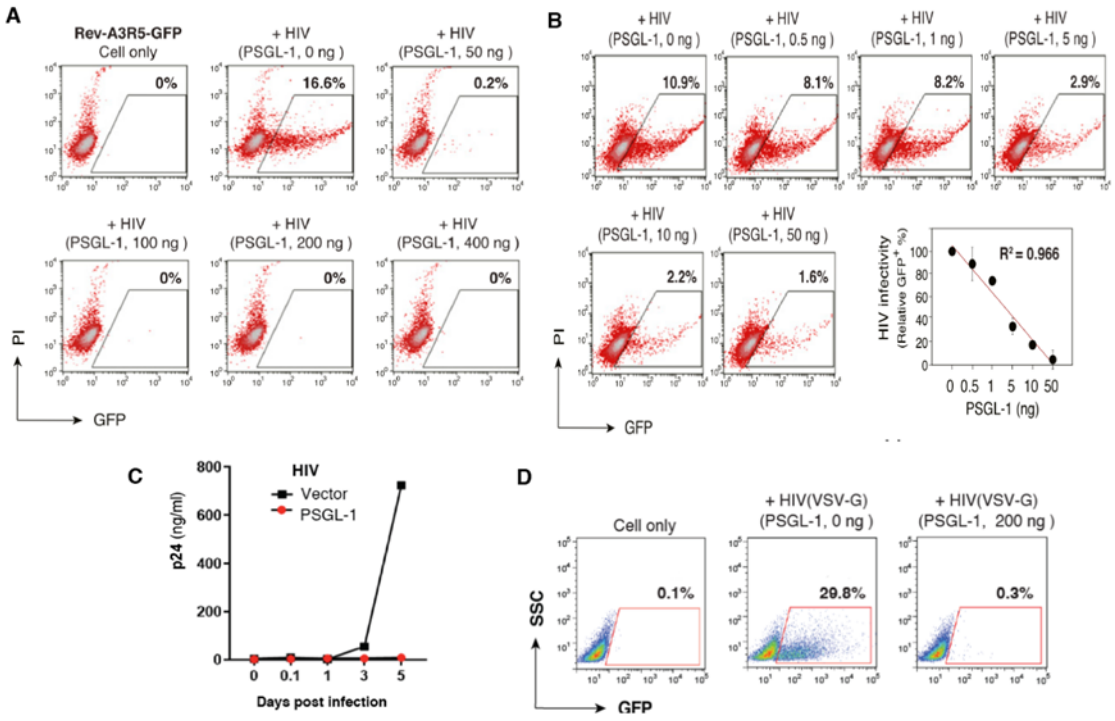

Figure 2.5 PSGL-1 inactivates HIV-1 infectivity.
A-B) HIV-1 virions were assembled in HEK293T cells by co-transfection with HIV(NL4-3) DNA (1 µg) plus PSGL-1 DNA (0.5 to 400 ng). Virus particles were harvested at 48 h and normalized for p24, and viral infectivity was quantified by infecting the T cell line-derived Rev-A3R5-GFP indicator cell line. HIV-1 replication was quantified by GFP expression. Shown are the percentages of GFP+ cells at 2dpi. B) The PSGL-1 dose-dependent inhibition curve was plotted using results from three independent experiments. C) HEK293T cells (3 x 106) were co-transfected with 12 µg of HIV(NL4-3) plus 2.4 µg pCMV-PSGL-1 or an empty vector. Viruses were harvested at 48 hours post-transfection and equal p24 equivalents were used to infect A3R5.7 CD4 T cells for 4 hours. Cells were then washed and cultured for 5 days. HIV replication was analyzed by p24 release. D) PSGL-1 blocks the infectivity of VSV-G-pseudotyped HIV-1. Virus particles produced in the presence of PSGL-1 or the empty vector were assayed for infectivity using Rev-A3R5-GFP indicator cells.

We also monitored HIV-1 infection over the course of 5 days in A3R5.7 CD4 T cells after infecting them with virus particles assembled in the presence or absence of PSGL-1 expression. The particles derived from PSGL-1-expressing- producer cells showed diminished viral infectivity and failed to establish a spreading infection (Fig. 2.5C). The infectivity of VSVG-pseudotyped HIV-1 virions was also significantly inhibited by PSGL-1 expression in the virus-producer cells (Fig. 2.5D). Collectively,

these results indicate that PSGL-1 expression in producer cells inactivates progeny virion infectivity, and that the impairment in infectivity occurs independently of the type of viral glycoprotein expressed on the virus.

To further validate that PSGL-1 in producer cells leads to the formation of defective HIV-1 particles, we additionally used a CD4 T cell line, CEM-SS, for viral production. We assembled virion particles by co-electroporating HIV-1- and PSGL-1 DNA into CEM-SS cells. Consistent with the results observed with virions produced in HEK29T cells, we found that the presence of PSGL-1 in CEM-SS cells also abolished HIV-1 progeny virion infectivity (Fig. 2.6).

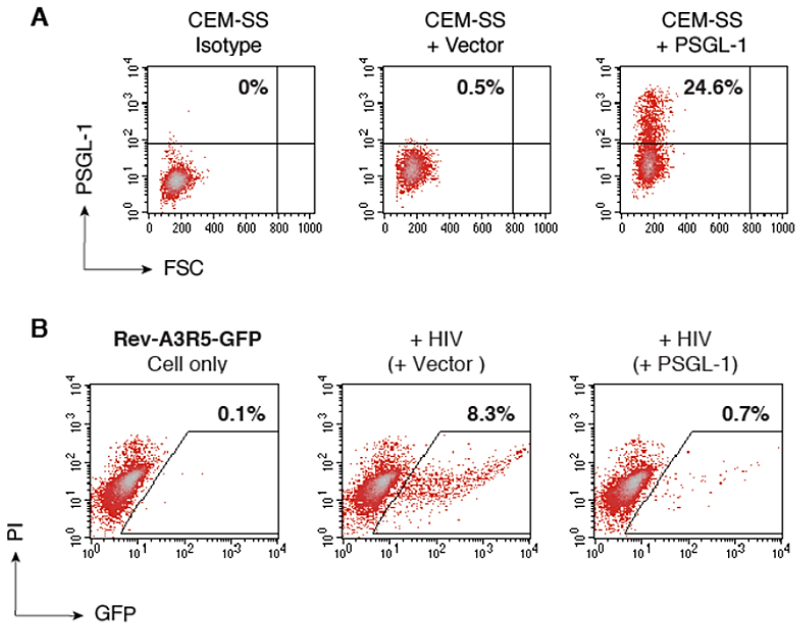

Figure 2.6 PSGL-1 inactivates the infectivity of HIV-1 virions produced from CEM-SS cells.
A) CEM-SS cells were electroporated with HIV-1(NL4-3) DNA plus PSGL-1 DNA or an empty vector. PSGL-1 surface expression was quantified at 3 days post-electroporation. B) To quantify HIV infectivity, virions were

harvested at 3 days post-electroporation, and used to infect Rev-A3R5- GFP cells, using an equal amount of p24 for infection. GFP expression was quantified at 3 days post-infection.

We next asked whether endogenous PSGL-1 levels could affect viral replication. To answer this question, we performed an shRNA knockdown of PSGL-1 in Jurkat T cells, which express inherently low levels of PSGL-1 (Fig. 2.1B). Jurkat cells were infected with a lentiviral vector encoding an shRNA targeting PSGL-1, followed by verification of PSGL-1 downmodulation by cell surface staining (Fig. 2.7A). The knockdown cells were then grown in selection media to obtain a stable pool of Jurkat cells with reduced PSGL-1 expression (shRNA PSGL-1) (Fig. 2.7A). To examine the effects of PSGL-1 knockdown on progeny virion infectivity, both the PSGL-1 knockdown cells and shRNA non-targeting control cells (shRNA NTC) were used for virion production. These cells were transfected with HIV-1 DNA by nucleofection to assemble virus particles. Viral replication in the shRNA PSGL-1 cells was assessed by quantifying p24 in the supernatant. Upon measuring extracellular p24 levels at days 3 and 4 post-transfection, we found a four-fold increase in HIV-1 replication when PSGL-1 was knocked down. (Fig. 2.7B). We speculated this increase resulted from enhanced virion infectivity. When we used p24-normalized particles derived from either shRNA PSGL-1 or shRNA NTC to infect the Rev-A3R5-GFP indicator cells, we observed higher infectivity for particles released from the PSGL-1 knockdown cells (Fig. 2.7C). These results corroborate our data from the PSGL-1 co-expression experiments in HEK293T cells (Fig. 2.5), demonstrating that the presence of PSGL-1 in virus-producing cells, even at low levels like those found naturally in Jurkat cells, can reduce virion infectivity.

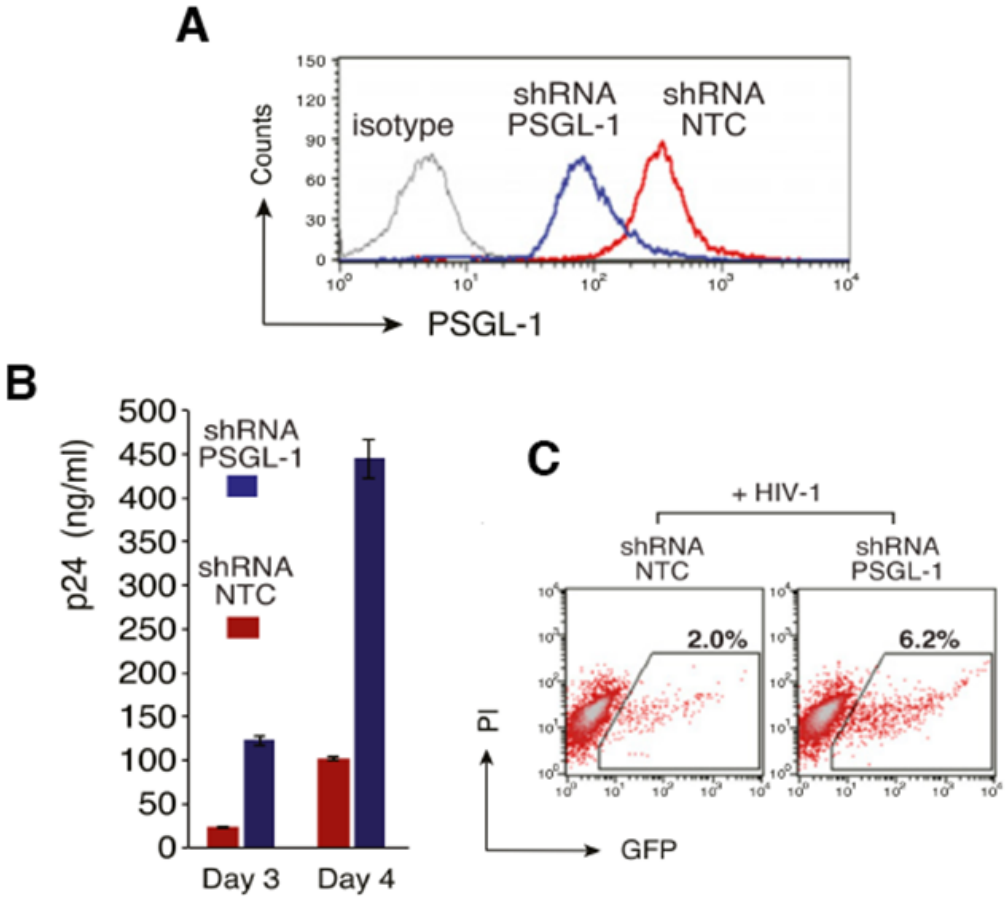

Figure 2.7 PSGL-1 depletion from Jurkat cells leads to enhanced HIV-1 replication and infectivity.
A) Jurkat cells were transduced with a lentiviral vector expressing shRNA against PSGL-1 (shRNA PSGL-1) or a non-target sequence (shRNA NTC). PSGL-1 surface expression was quantified at 12 days following transduction and puromycin selection. B) Cells were also electroporated with HIV-1(NL4-3) DNA, and viral replication in knockdown Jurkat cells was quantified by measuring p24 in the supernatant at the indicated days. C) To quantify HIV infectivity, virions were harvested at 48 h post-electroporation and used to infect Rev-A3R5-GFP cells, using an equal amount of p24 for infection.

Additionally, we confirmed these findings by examining the effect of PSGL-1 depletion in CD4 T cells. We used the same PSGL-1 shRNA-expressing lentiviral vector described above to knock down PSGL-1 in preactivated primary CD4 T cells, and we

observed a notable enhancement in HIV-1 replication in the shRNA PSGL-1 CD4 T cells (Fig. 2.8).

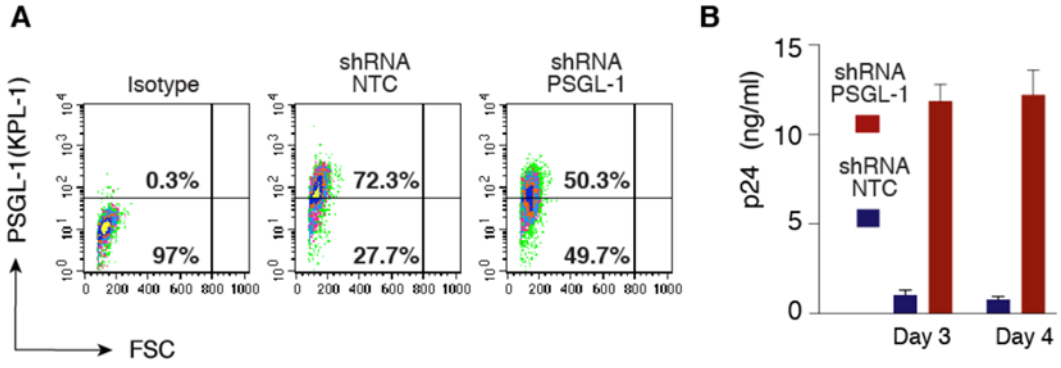

Figure 2.8 shRNA knockdown of PSGL-1 in primary CD4 T cells enhances HIV-1 replication.
A) Blood resting CD4 T cells were purified by negative depletion, activated with anti-CD3 and CD28 magnetic beads, and then transduced with a lentiviral vector expressing shRNA against PSGL-1 (shRNA PSGL-1) or a non-target sequence (shRNA NTC). PSGL-1 surface expression was quantified at day 3 post-transduction. B) Cells were also electroporated with HIV-1(NL4-3) DNA, and viral replication in the PSGL-1 knockdown or the control NTC CD4 T cells was quantified by measuring p24 in the supernatant.

PSGL-1 is incorporated into HIV-1 particles and inhibits virion attachment and entry

PSGL-1 has been found to co-localize with HIV-1 Gag at sites of particle assembly in uropod microdomains following Gag multimerization (55, 56). However, the biological role of PSGL-1/Gag co-localization during HIV virion assembly remains unclear. Given the reported colocalization of Gag and PSGL-1 in virus-producing cells, we asked whether PSGL-1 is incorporated into HIV-1 particles. We co-transfected HIV(NL4-3) DNA with the PSGL-1 expression vector, purified the virion particles by two rounds of ultracentrifugation through an OptiPrep gradient, and analyzed the virion

content by western blot. As shown in Figure 2.9, we detected PSGL-1 in virions. We also verified that the virus-containing gradient fractions were not contaminated with extracellular vesicles containing PSGL-1 (Fig. 2.9B).

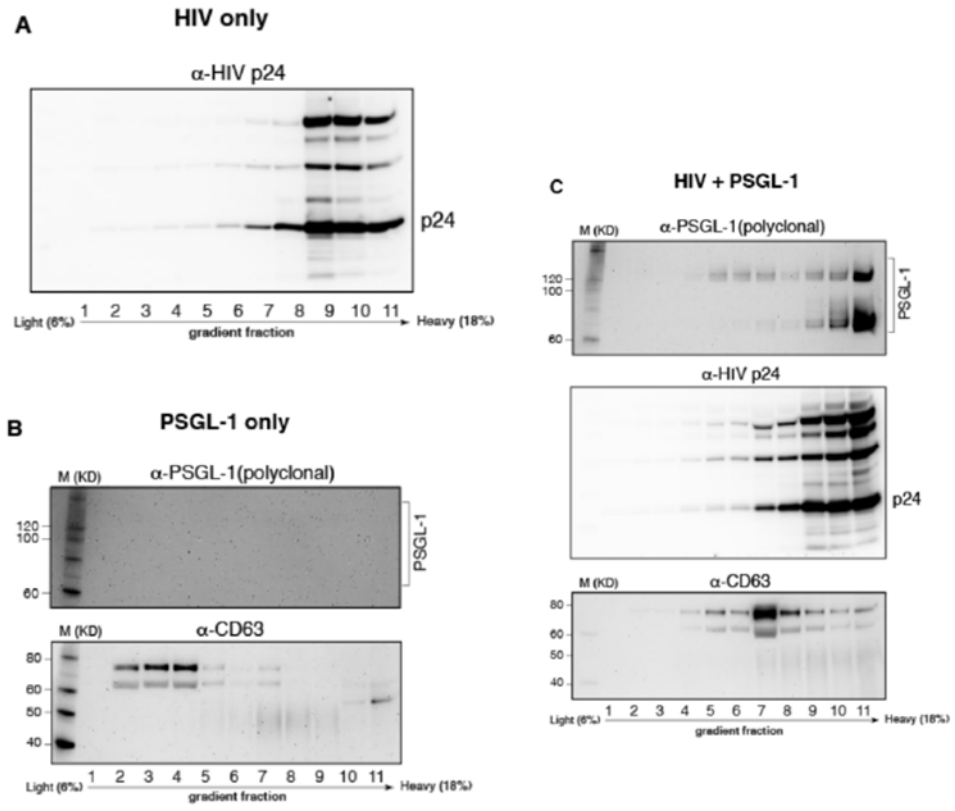

Figure 2.9 Virion incorporation of PSGL-1.
A) to C) HEK293T cells were transfected with HIV-1(NL4-3) (1 μg , HIV only), or transfected with PSGL-1 (200 ng, PSGL-1 only), or co-transfected with 1 μg HIV-1(NL4-3) plus 200 ng of PSGL-1 DNA (HIV + PSGL-1). Supernatants were harvested at 48 hours, filtered, concentrated, and purified by ultra-speed centrifugation through a 6%-18% OptiPrep gradient. PSGL-1 and viral p24 proteins in each fraction were analyzed by western blot using antibodies against PSGL-1 (polyclonal) or HIV-1 p24 (anti-p24). For comparison, an anti-CD63 antibody was used to identify the fractions also containing exosomes.

To test if PSGL-1 incorporation into virus particles inhibits virus entry, we performed a previously described Vpr-BLAM viral entry assay (61), using the HIV-1 entry inhibitor AMD3100 as a positive control for entry inhibition. As shown in figure 2.10A, PSGL-1-imprinted virus particles exhibited a marked reduction in their ability to enter target cells (Fig. 2.10A).

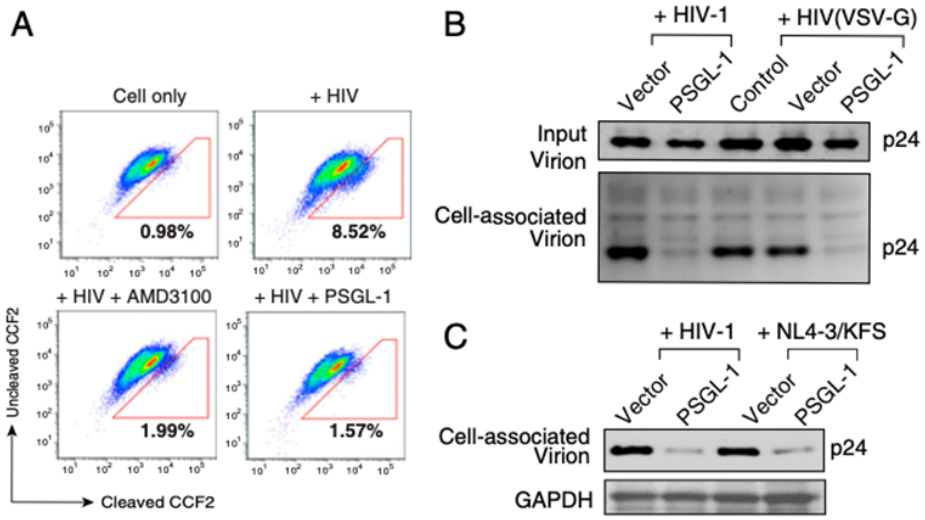

Figure 2.10 PSGL-1 blocks virion attachment and entry to target cells.
A) Virions produced from HEK293T cells co-transfected with PSGL-1 expression vector (or empty vector) plus HIV-1(NL4- 3) were used for an entry assay at equal p24 inputs of each virus. The entry inhibitor AMD3100 was used as a control to block virus entry. The percentages of cells with cleaved CCF2 are shown. B) WT or VSVG-pseudotyped HIV-1 virions produced in the presence of a PSGL-1, or an empty vector were assayed for attachment to target HeLa JC.53 cells at 4 °C for 2 h. Cells were washed and then analyzed by Western blot for bound p24. C) PSGL-1 blocks Env (−) HIV-1 particle attachment to target cells. WT HIV-1 or Env (−) HIV-1 [(NL4-3)/KFS] virions were produced in the presence of PSGL-1 or the empty vector, and viral particles were assayed for attachment to target HeLa JC.53 cells.

Next, we investigated whether the inhibition of viral entry resulted from a defect in virus binding to target cells. We performed a virion attachment assay using HeLaJC53,

a cell line that expresses both CD4 and the co-receptor CXCR4, as the target cell. PSGL-1-imprinted NL43 virions were incubated with HeLaJC53 at 4 °C, to allow for virus binding only without permitting entry. The cells were then extensively washed, lysed and assayed for cell-bound p24. Western blot analysis of the lysates showed that virions from PSGL-1–expressing cells were severely impaired in their ability to attach to target cells (Fig. 2.10C). Considering that PSGL-1 expression in virus-producing cells also inhibited the infectivity of HIV-1 particles pseudotyped with the VSV-G protein (Fig. 2.5D), we examined the effect of PSGL-1 on the incorporation of HIV-1 Env and VSV-G into virion particles. While the presence of PSGL-1 in virus-producer cells reduced the levels of HIV-1 Env on virions, the levels of the VSV-G on virions were not affected (Fig. 2.11B). Interestingly, even though virion incorporation of VSV-G was not affected by PSGL-1, we found that VSV-G-pseudotyped HIV-1 particles also became defective in binding to target cells when produced in the presence of PSGL-1 (Fig. 2.10B).

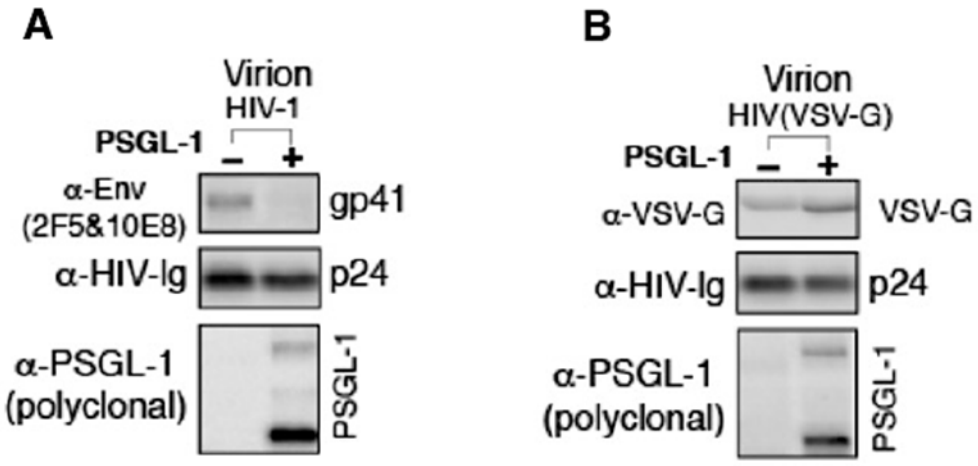

Figure 3.11 PSGL-1 disrupts HIV-1 Env but not VSV-G incorporation into virions.
A) HEK293T cells were co-transfected with HIV-1 in the presence of PSGL-1 or an empty vector. B) Cells were also co-transfected with pNL4-3/KFS plus pCMV-VSV-G in the presence of PSGL-1 or an empty vector. The produced virus particles were analyzed by western blot using antibodies against PSGL-1 (polyclonal), HIV proteins (anti-HIV serum), HIV-1 Env proteins (2F5 and 10E8), or VSV- G.

We also asked whether the PSGL-1-mediated inhibition of viral attachment depended on specific viral glycoprotein-receptor interactions. It is known that HIV-1 particles can form short-lived, non-specific interactions with the target cell membrane in the absence of Env-receptor engagement (73-75). To that end, we assembled HIV-1 particles lacking any viral envelope glycoproteins on their surface; the Env-deficient pNL4-3 (KFS) molecular clone (60) was co-transfected into HEK293T cells with either a PSGL-1-encoding- or an empty control vector. The harvested viral particles were then normalized for p24 and used to for the attachment assay as described above (Fig. 2.10B, C). Strikingly, we observed that the Env-deficient HIV-1 particles from PSGL-1-expressing producer cells were also impaired in their ability to attach to target cells. Together, these observations demonstrate that PSGL-1 inhibits virion attachment to cells independently of receptor usage.

The extracellular N-terminal domain of PSGL-1 is required for inhibiting HIV-1 infectivity

The PSGL-1 molecule constitutes a large, heavily glycosylated extracellular (N-terminal) domain (29). The N-terminal portion of PSGL-1 assumes an elongated semi-rigid, rod-like structure that extends far beyond the membrane glycocalyx (76). A study by Umeki et al. reported that PSGL-1 overexpression in HEK293T cells, as well as in other adherent cell types, caused the cells to adopt a rounded, detached, and floating phenotype (77). Mutational analysis revealed that the N-terminus of PSGL-1 was required for this detached morphology. The authors suggested that the rigid and extended nature of PSGL-1's extracellular domain was conferring these anti-adhesive properties (77). Moreover, as shown in our attachment assays, the PSGL-1-imprinted virions could not bind target cells, even in the absence of Env-receptor interaction (Fig. 2.10C). Thus, we postulated that the inhibition of virus attachment may be due to a steric hindrance effect resulting from the presence of PSGL-1 on the virus particle (Fig. 2.12A). To test this theory, we constructed PSGL-1 deletion mutants, PSGL-1 CT, and PSGL-1 NT, in which the entire extracellular N-terminal domain or most of the intracellular C-terminal domain were deleted, respectively (Fig. 2.12B).

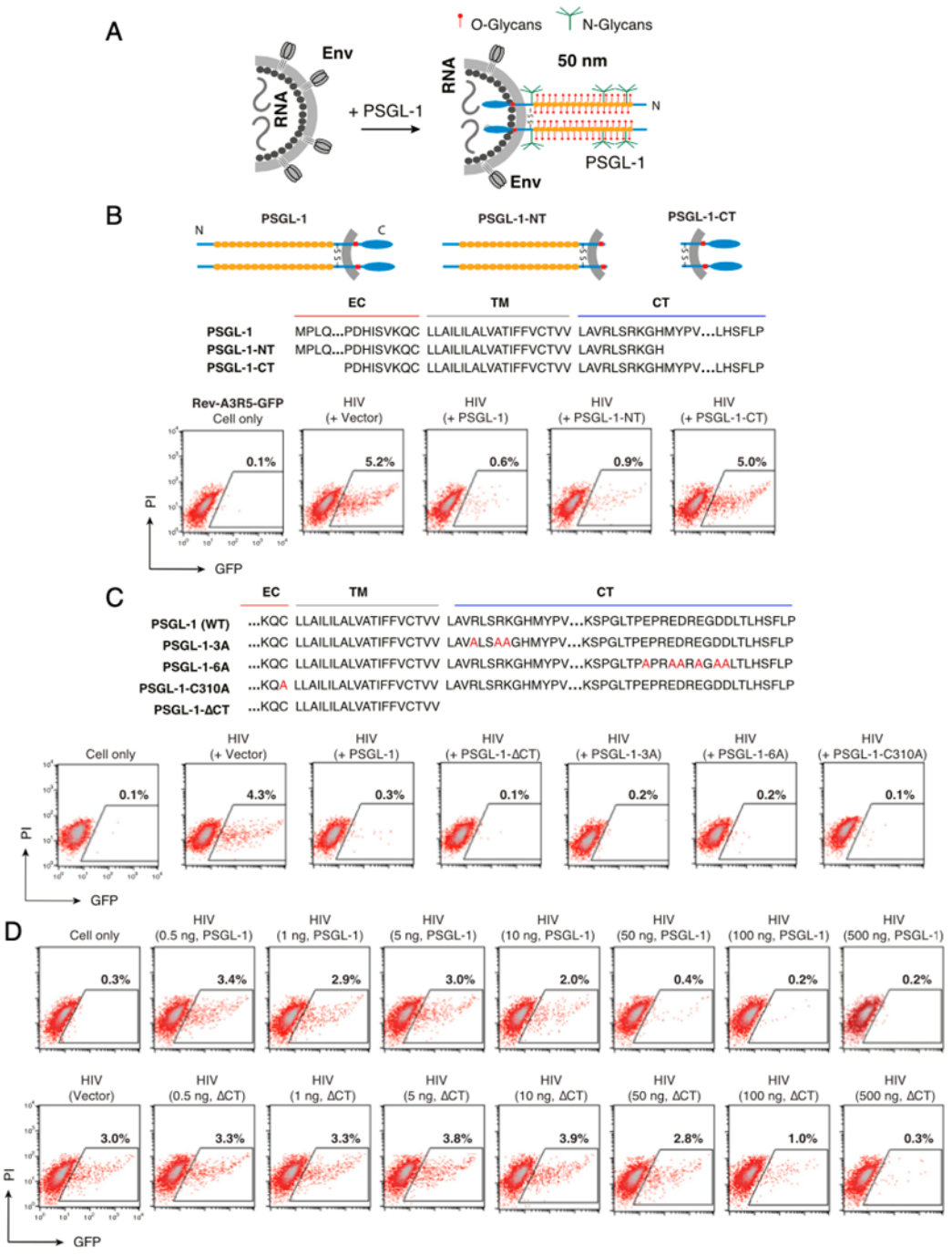

Figure 2.12 The extracellular N-terminal domain of PSGL-1 is required for its anti-HIV-1 infectivity.
A) Proposed model of incorporation of PSGL-1 into virion particles. Based on this model, incorporation of the heavily glycosylated and elongated PSGL-1 on viral particles may interfere with virion binding to target cells. B) Schematic of the tested PSGL-1 domains. HEK293T cells were co-transfected with HIV(NL4-3) DNA (1 μg) plus vectors expressing PSGL-1 or PSGL-1 truncation mutants PSGL-1-NT or PSGL-1-CT (500 ng). Virions were harvested at 48 h post-transfection and normalized for p24. Viral infectivity was quantified by infecting Rev-A3R5-GFP indicator cells. HIV-

1 replication was quantified by GFP expression. C) PSGL-1 intracellular domain mutants PSGL-1-ΔCT, PSGL-1-3A, and PSGL-1-6A and the dimerization mutant PSGL-1-C310A were similarly tested. EC, extracellular domain; TM, transmembrane domain; CT, cytoplasmic tail. (D) The PSGL-1-ΔCT mutant displays reduced antiviral activity relative to WT PSGL-1. HEK293T cells were cotransfected with HIV(NL4-3) DNA (1 μg) plus various amounts of PSGL-1 or PSGL-1-ΔCT (0.5 to 500 ng). Virions were harvested at 48 h and normalized for p24, and their infectivity was measured in Rev-A3R5-GFP indicator cells.

Next, we assembled virus particles by co-transfecting HIV-1 (NL43) DNA along with vectors expressing either full-length WT PSGL-1 (pRetroPSGL-1), PSGL-1 CT (pRetroPSGL- 1 CT), or PSGL-1 NT (pRetroPSGL-1NT). Following transfection, the expression of the mutants and their incorporation into virions were verified by surface staining and Western blot (Figs. 2.13 and 12.4). The infectivity of the virions assembled in the presence or absence of each mutant was then quantified by infecting Rev-A3R5-GFP cells. Flow cytometric analysis of the infected cells revealed that deleting most of the intracellular (C-terminal) domain did not affect the ability of PSGL-1 to restrict HIV-1. On the other hand, removal of the extracellular N-terminal domain markedly abrogated the restrictive phenotype. These findings show that the anti–HIV activity of PSGL-1 is largely dependent on its N- terminal domain.

In the study by Grover et al. (56), the authors tested a panel of PSGL-1 mutants to identify structural requirements for PSGL-1 and Gag co-clustering (56). They reported that complete deletion of the PSGL-1 cytoplasmic domain reduces PSGL-1/Gag co-clustering and virion incorporation of PSGL-1. Specifically, the authors found that a stretch of basic amino acid residues within the PSGL-1 cytoplasmic tail, termed the polybasic domain (PBD), to be an important determinant for PSGL-1 and Gag co-localization (56).

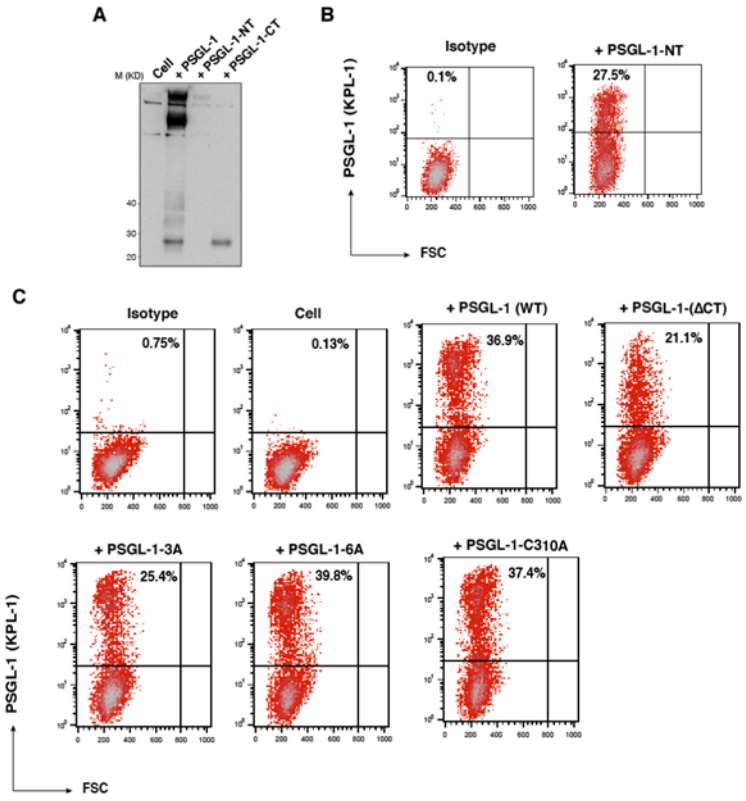

Figure 2.13 Validation of expression of the PSGL-1 mutants.
A) Detection of PSGL-1-CT in transfected cells. HEK293T cells were transfected with 500ng of WT PSGL-1, PSGL-1-NT, or PSGL-1-CT. Cell lysates were harvested at 48 hours and analyzed by western blot using an antibody against the C-terminus of PSGL-1. B-C) HEK293T cells were transfected with PSGL-1 DNA (500 ng) or each of the indicated PSGL-1 mutant DNA (500 ng). Expression of PSGL-1 was quantified by surface staining with an anti-PSGL-1 antibody (KPL-1 clone) at 48 hours.

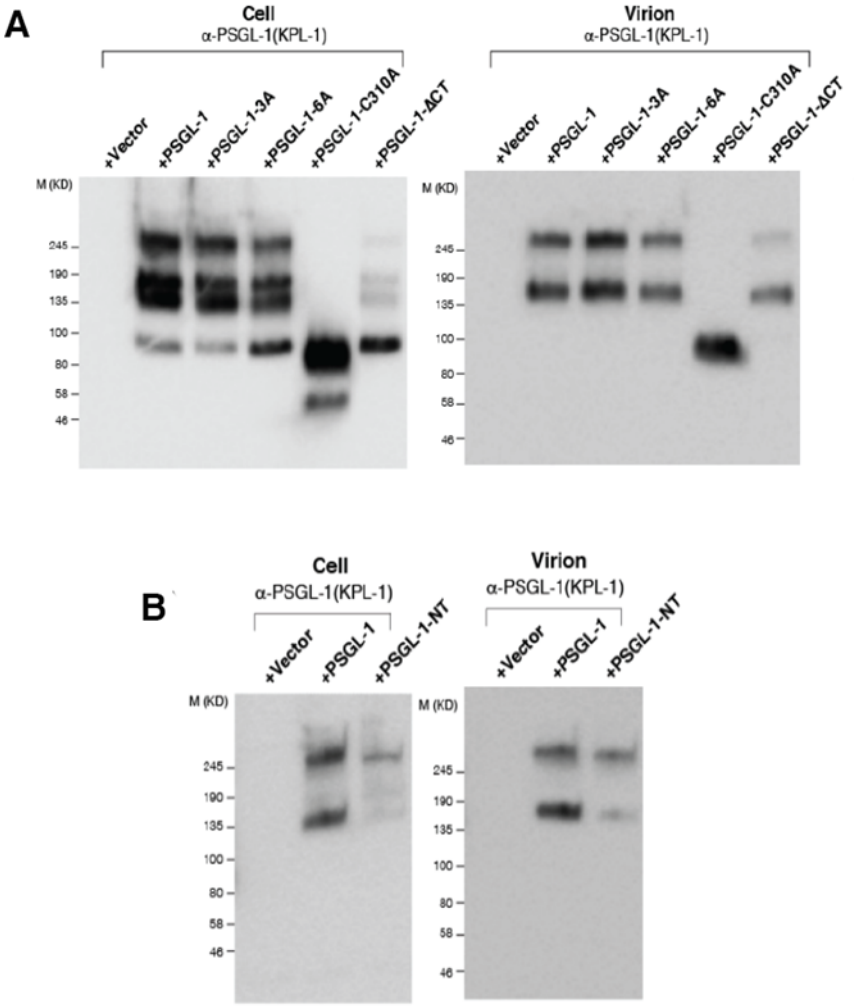

Figure 2.14 Incorporation of PSGL-1 mutants into virion particles.
A) HEK293T cells were co-transfected with HIV-1 DNA (1 μg) plus PSGL-1 DNA or each of the PSGL-1 mutant DNAs (250 ng of WT PSGL-1, PSGL-1-3A, PSGL-1-6A and PSGL-1- C310A mutants or 500 ng of PSGL-1-ΔCT. B) HEK293T cells were co-transfected with 500ng of WT pRetroPSGL-1, PSGL-1-NT, or empty vector. For A) and B), Expression of PSGL-1 or PSGL-1 mutants in co-transfected cells was detected by western blot. Viral particles were harvested from transfected cells, and virion incorporation of PSGL-1 was detected by western blotting using the anti-PSGL-1 antibody KPL-1.

To further validate our findings, we ran additional infectivity tests using the panel of PSGL-1 mutants constructed by Grover et al. (Figs. 2.12C, 2.13 and 2.14). In the PSGL-1-ΔCT mutant, the entire cytoplasmic tail is removed, while in PSGL-1-3A and

PSGL-1-6A, there are several amino acid substitutions in the cytoplasmic tail. PSGL-1-3A has the three juxtamembrane basic residues of the PDB changed to alanine, and PSGL-1-6A has the six acidic residues near the C terminus replaced by alanine (Fig. 2.12C). PSGL-1-C310A, which has an alanine in place of cysteine 310, abolishes PSGL-1 dimerization (78). Considering that mutations of the cytoplasmic tail may decrease virion incorporation of PSGL-1 (56), we used a high concentration of PSGL-1 mutant DNA (500 ng) for co-transfection with HIV-1 DNA (1 μg). This was done to ensure that even with reduced incorporation of C-terminal PSGL-1 mutants into particles, there would still be enough to confer an inhibitory phenotype. Using this high PSGL-1 mutant dose, we observed that all the C-terminal PSGL-1 mutants, and the dimerization mutant C310A, sustained the ability to restrict HIV-1 (Fig. 2.12C). These results further confirm that the anti-HIV-1 activity of PSGL-1 can be primarily attributed to its N-terminal domain, that a single subunit of the PSGL-1 dimer is sufficient to restrict HIV-1, and that the C-terminal domain is not required for HIV-1 inhibition. Nevertheless, given that the PSGL-1 C-terminus was shown to contribute to PSGL-1 incorporation into virions (56), we performed a side-by-side dose dependent comparison of the effects of WT PSGL-1 and PSGL-1- ΔCT on virion infectivity. We found that at lower doses, PSGL-1ΔCT was less potent than WT PSGL-1 at restricting HIV-1 infectivity (Fig. 2.12D), indicating that even though the C-terminus is unnecessary, it can still affect the anti-HIV activity of PSGL-1, likely by facilitating co-clustering with Gag, which in turn promotes packaging into virions.

A major portion of the PSGL-1 N-terminus consists of 14 to16 decameric (10 amino acid) repeats (DRs) (Fig. 2.15A), containing multiple O-glycosylated threonines and prolines (31, 32). These DRs are essential for adding length and durability to the PSGL-1 molecule; they allow extension of the N-terminal selectin-binding sites for effective leukocyte interaction with the activated endothelium (31). Therefore, to further confirm that the extracellular domain is important for PSGL-1's antiviral activity, we tested another N- terminal deletion mutant, PSGL-1ΔDR, described by Baïsse et al. (32), in which the decameric repeats of PSGL-1 were deleted from the N-terminal domain. As suspected, removal of the DRs also abolished PSGL-1's ability to inactivate HIV-1 infectivity (Fig. 2.15B).

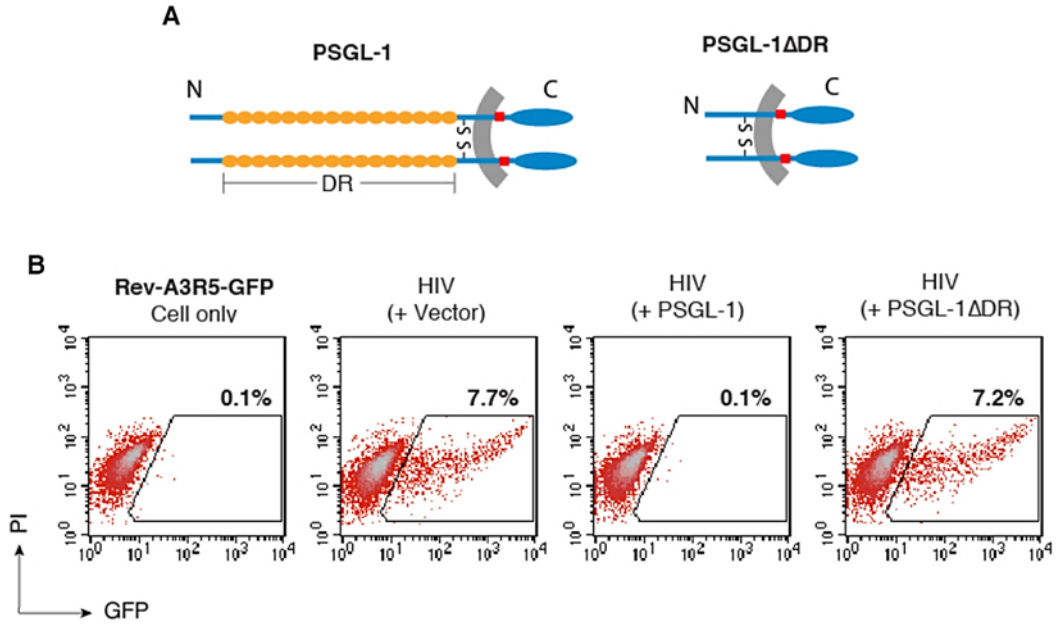

Figure 2.15 The extracellular N-terminal DR domain of PSGL-1 is required for its anti- HIV-1 infectivity. A) Schematic of the structures of WT PSGL-1 and PSGL-1ΔDR. B) HEK293T cells were co-transfected with HIV(NL4-3) DNA (1 µg) plus vectors expressing PSGL-1 or PSGL-1 decameric repeat (DR) truncation mutant PSGL-

1ΔDR (400 ng). An empty vector was used as the co-transfection control (+Vector). Virions were harvested at 48 hours post-transfection and normalized for p24, and viral infectivity was quantified by infecting Rev-A3R5-GFP indicator cells. HIV-1 replication was quantified by GFP expression.

PSGL-1's antiviral effect extends beyond HIV-1

PSGL-1 maintained its anti-HIV-1 activity even after complete removal of its intracellular domain, which was reported to be necessary for PSGL-1 co-localization with HIV-1 Gag at particle assembly sites (56). This observation suggests that PSGL-1 can block HIV-1 infectivity without directly interacting with Gag or other HIV-1 proteins intracellularly. PSGL-1 also inhibited viral attachment to target cells independently of the molecules mediating virus-cell adhesion (Fig. 2.10C). Given that the length of PSGL-1's extracellular domain (50nm) is considerably longer than the combined lengths of the extracellular domains of HIV-1 Env and CD4 (76, 79, 80) (the receptor for Env), the mere presence of PSGL-1 on the virion surface may interfere with particle binding to target cells (Fig. 2.12A). Therefore, it is reasonable to speculate that PSGL-1 may possess broad-spectrum antiviral activity against enveloped viruses. To test this possibility, we assembled a VSV-G–pseudotyped murine leukemia virus (MLV) in the presence of PSGL-1 and found that PSGL-1 also had a diminishing effect on MLV infectivity (Fig. 2.16A). We also tested the impact of PSGL-1 on the infectivity of a nonretroviral enveloped virus, the influenza A virus (Fig. 2.16B). A co-culture of HEK293T-MDCK cells was co-transfected with eight vectors encoding the segments of the influenza A/WSN/33 (H1N1) plus PSGL-1 DNA. Virus particles were harvested at 16 and 24 h post-transfection, and virion infectivity was quantified by the TCID50 assay

in MDCK cells. As seen in figure 16, a PSGL-1 dose of 1 μg caused a 100-fold reduction in the infectious titer at 16 hours, while a PSGL-1 dose of 3 μg reduced the viral titer by >8,000-fold.

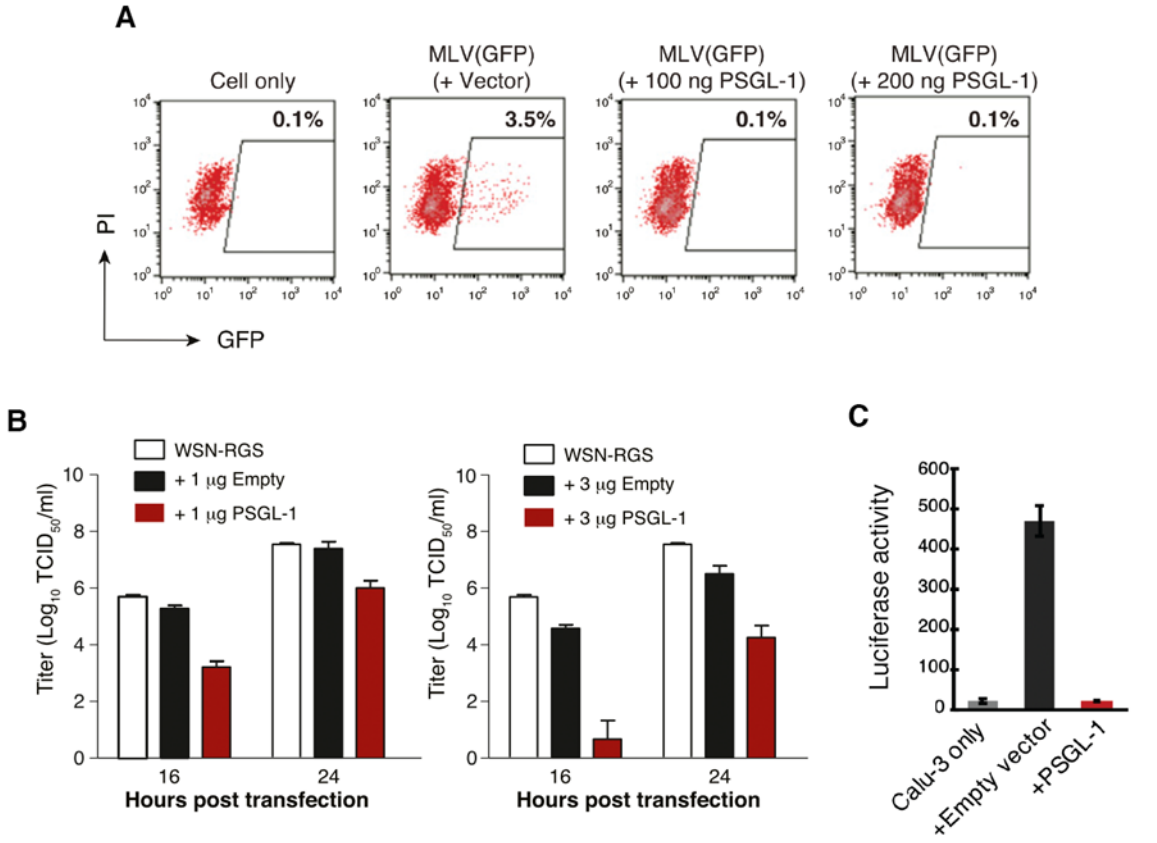

Figure 2.16 PSGL-1 possesses broad-spectrum antiviral activity.
A) PSGL-1 restricts MLV and influenza A virus infectivity. HEK293T cells were cotransfected with an MLV helper vector, pSV-ψ-MLV-env−, pRetroQ-AcGFP-N1, pHCMV-G, plus a PSGL-1 expression vector or an empty control vector. MLV virions were harvested, and viral infectivity was quantified by infecting HEK293T cells and measuring GFP expression. B) Eight vectors expressing each of the segments of the influenza A/WSN/33 (H1N1) genome were cotransfected with a PSGL-1 expression vector into HEK293T-MDCK cells. Viral particles were harvested at 16 and 24 h after co-transfection and titrated in MDCK cells to determine end-point titers (TCID50 per ml). C) SARS- CoV2-S-pseudotyped lentiviral particles were produced by HEK293T co-transfection in 10-cm dishes with pLTR-Tat-IRES-Luc (10 μg), pCMVΔR8.2 (7 μg), SARS-CoV-2 S (1 μg) and pCMV3-PSGL-1, or pCMV3-Empty DNA (2 μg). Supernatants were harvested at 48 and 72 hours and pooled for concentration through a 10% sucrose gradient. Calu-3 cells (0.5 million) were infected with equal p24 inocula of SARS-CoV-2 S-pseudotyped luciferase reporter lentiviruses. At 72 hpi, cells were lysed and luminescence was measured by using GloMax® Discover Microplate Reader (Promega).

We next examined the effect of PSGL-1 on SARS-CoV-2-S-pseudotyped lentiviral particles expressing a luciferase reporter (Fig. 2.16C). Lentiviral pseudo-virions were assembled in HEK293T in the presence of PSGL-1 or empty vector and then used to infect Calu3 cells with equal p24 inputs. We found that the expression of PSGL-1 in producer cells reduced the infectivity of the SARS-CoV-2-S-pseudotyped particles (Fig. 2.16C), further confirming that PSGL-1's anti-viral activity is not specific to a particular viral envelope glycoprotein. These results demonstrate that PSGL-1 is a broad-spectrum antiviral host factor.

CD43, a PSGL-1-related selectin ligand, also inhibits HIV-1 infectivity

As mentioned above, PSGL-1 expression in virus-producing cells diminishes HIV-1 progeny virion infectivity by blocking virus attachment to target cells. This defect in attachment was not reliant on specific interactions between PSGL-1 and HIV-1 proteins (Fig.2.10). Even in its monomeric form, PSGL-1 still effectively inactivated HIV-1 infectivity, as demonstrated by the PSGL-1 C310A mutant, which abolishes PSGL-1 dimerization (Fig. 2.12C). It is therefore possible that other molecules bearing an extracellular structure like that of PSGL-1 may also inhibit HIV-1 infectivity. CD43, or leukosialin, is a monomeric sialomucin, which also serves as an E-selectin ligand (81, 82). Like PSGL-1, CD43 is a "bulky", heavily glycosylated mucin-like protein (83), which protrudes 45 nm from the cell membrane (84). CD43 is expressed in Th1 T cells (81) and functions synergistically with PSGL-1 during E-selectin–mediated T cell rolling (85). To examine the effect of CD43 on HIV-1 infectivity, we assembled HIV-1 particles in the presence of CD43 expression by co-transfecting HEK293T cells with HIV(NL4-3)

proviral DNA (1 µg) plus varying inputs (0.5 to 400 ng) of CD43 DNA (Fig. 2.17). The infectivity of the released virions was evaluated by infecting Rev-A3R5- GFP cells.

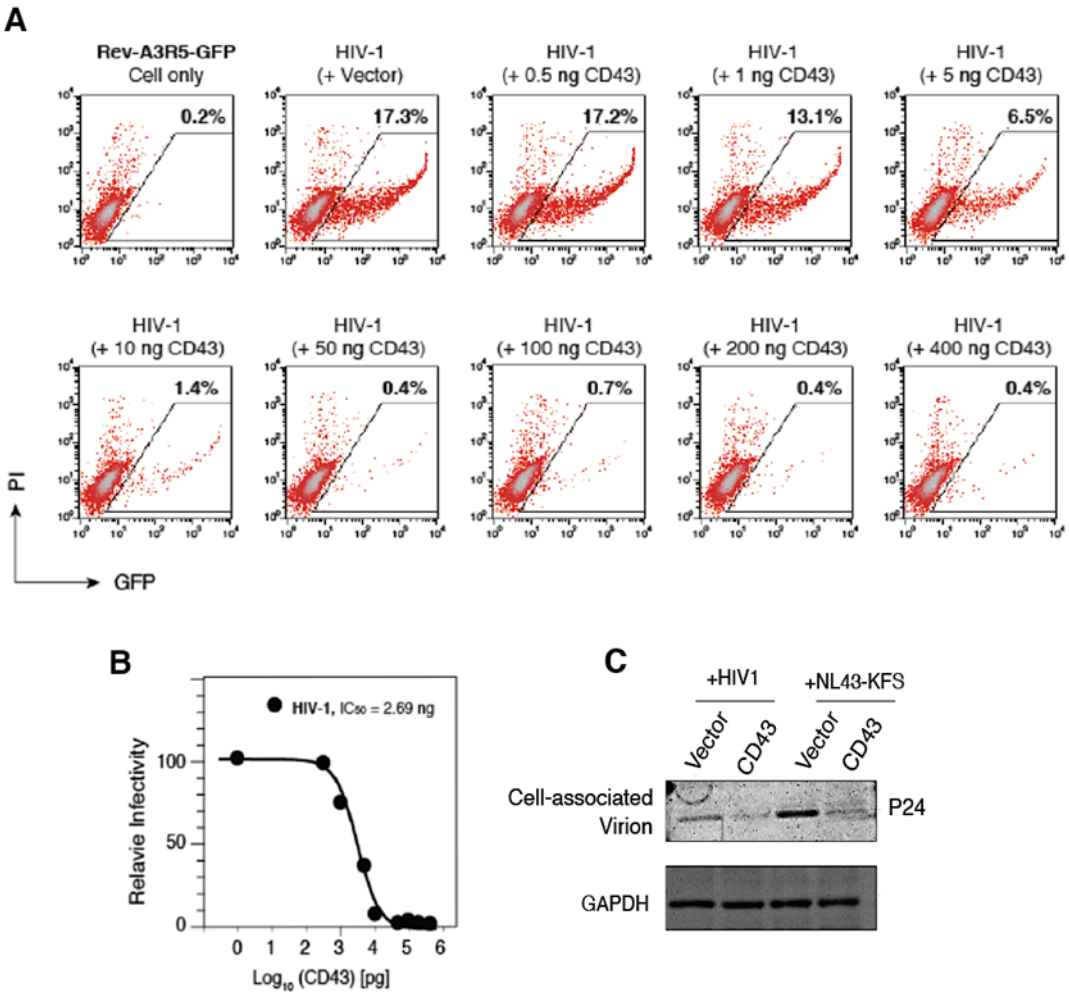

Figure 2.17 CD43 inhibits HIV-1 virions infectivity and impairs virion attachment to target cells.
A) HEK293T cells were cotransfected with various amounts of CD43 DNA (0.5 – 400 ng) plus 1 µg HIV(NL4-3) DNA. Virions were harvested at 48 hours and normalized for p24. Viral infectivity was quantified by infecting Rev-A3R5-GFP indicator cells. HIV-1 replication was quantified by GFP expression. Shown are the percentages of GFP+ cells at 48 hours post-infection. B) The CD43 dose-dependent inhibition curve was plotted. C) WT or Env-deficient HIV-1 virions produced in the presence of CD43, or empty vector were assayed for attachment to target HeLa JC.53 cells at 4 °C for 2 h. Cells were washed and then analyzed by Western blot for bound p24. GAPDH was used as a loading control for the cell lysates.

As shown in Figure 2.17A, the presence of CD43 in virus-producing cells led to a dosage-dependent reduction in HIV-1 infectivity. Doses greater than 50 ng of CD43 almost completely blocked progeny virion infectivity, while lower doses (0.5-10 ng) caused partial inhibition (Fig. 2.17A). Next, we tested whether virus attachment to target cells was also susceptible to inhibition by CD43. HIV-1 particles were assembled in the presence of CD43 and used to perform a viral attachment assay, utilizing the same method described above. We found that, just like PSGL-1, CD43 also inhibited virion binding to target cells in an Env-independent manner (Fig. 2.17C). These results suggest that molecules sharing structural properties with PSGL-1, namely having a heavily glycosylated and highly extended extracellular domain, may be detrimental to viruses if they were incorporated and displayed on the virion surface. Moreover, we asked whether, like PSGL-1, CD43 was antagonized by the HIV-1 accessory proteins, Vpu. Accordingly, we co-transfected HEK293T cells with 100 ng of CD43 DNA and different doses of a Vpu-expressing vector. Indeed, we observed downmodulation of CD43 when co-expressed with Vpu in HEK293T cells (Fig. 2.18), although the mechanism by which Vpu downregulates CD43 remains unknown.

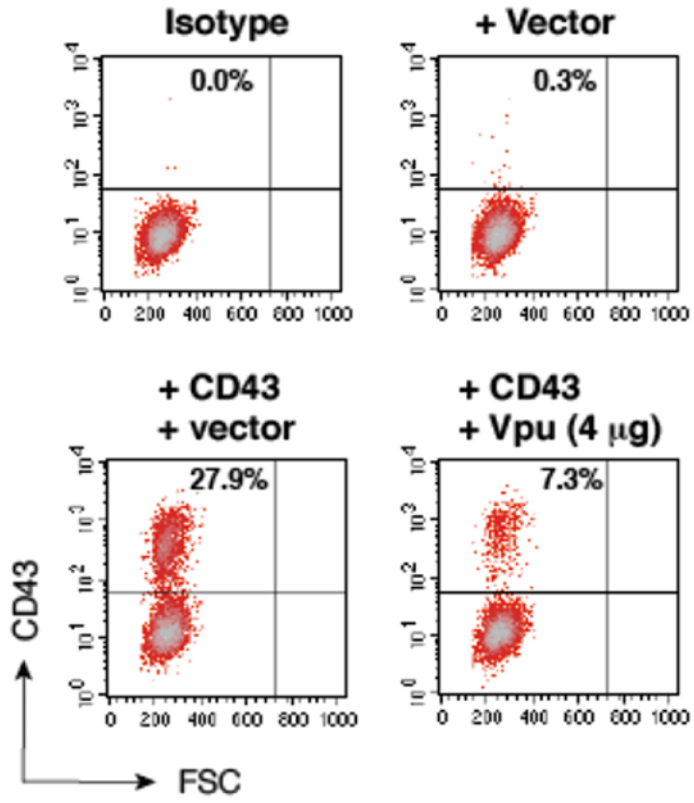

Figure 2.18 Downregulation of CD43 from the cell surface by HIV-1 Vpu.
HEK293T cells were co-transfected with CD43 (100 ng) and a Vpu expression vector (4 μg). Surface CD43 expression was quantified and shown as the percentage of cells expressing CD43. For controls, an empty vector was used (+vector). The same amount of DNA was used in the transfections.

Discussion

PSGL-1 is a mucin-like glycoprotein protein densely expressed on the surface of blood-derived CD4+ T cells and has recently been identified as an interferon-induced antiviral restriction factor. In this manuscript, we demonstrate that PSGL-1 restricts the infectivity of HIV-1 virions mainly by interfering with virus particle binding to target cells. Unlike the restriction mechanism mediated by the well-characterized tetherin,

which retains newly assembled particles at the plasma membrane (86, 87), our studies have shown that PSGL-1 does not inhibit viral release. In our dose response inhibition analysis, PSGL-1 exhibited significant potency, as there was complete abolishment of WT HIV-1 infectivity at a vector: proviral DNA ratio of approximately 0.05:1 (Fig. 2.5B).

Interestingly, HIV-1 particles expressing the VSV-G envelope glycoprotein were also susceptible to the PSGL-1-mediated restriction of particle infectivity (Fig.2.5D). We found that PSGL-1 is incorporated into progeny HIV-1 virions (Fig. 2.9), and while this led to a decrease in HIV-1 Env incorporation (Fig2.11A, it did not affect VSV-G incorporation (Fig.2.11B). During the initial interactions between HIV-1 and the cell surface, it has been reported that particles can form non-specific interactions, in the absence of HIV Env-receptor engagement, with binding factors on the target cell such as integrins and other surface molecules (75). Our attachment assay demonstrated that even when HIV-1 particles are stripped of their envelope glycoproteins, Env-deficient virions also become impaired in their ability to bind target cells if they were produced in PSGL-1-expressing cells (Fig.2.10).

Deletion of the extracellular domain of PSGL-1 rendered the molecule incapable of eliciting its inhibitory against HIV-1 (Fig. 2.12B). PSGL-1 is a bulky, relatively rigid molecule (76, 88); its heavily glycosylated, highly extended extracellular domain projects nearly 60 nm from the cell membrane (76, 89). Therefore, we hypothesize that besides inhibiting HIV-1 Env incorporation, the presence of PSGL-1 on the virion surface physically hinders the attachment of virions to target cells; the structural characteristics of

PSGL-1 may act as an obstructive barrier between the viral surface and the host cell membrane (Fig. 2.12A).

The physiological relevance of PSGL-1 in HIV-1 infection was demonstrated by our PSGL-1 knockdown experiments. Knocking down PSGL-1 from Jurkat cells, which inherently express low levels of the protein, caused a noticeable increase in HIV-1 replication (Fig.2.7B). When the PSGL-1 knockdown Jurkat cells were used as producer cells to assemble HIV-1 particles, the infectivity of the harvested virions was also enhanced (Fig.2.7C). These results were reproduced in primary CD4 T cells, which also showed increased levels of HIV-1 replication following shRNA knockdown of PSGL-1, further validating the role of PSGL-1 in HIV-1 infection.

PSGL-1 expression robustly inhibited HIV-1 infection and spread in our HeLaJC53-PSGL-1 cell line, which stably expresses PSGL-1 spreading assay (Fig. 2.3B). Some of the viral transmission in this cell line is likely to take place at the virological synapses via cell-cell contact. Considering the notion that HIV-1 Gag co-patches with PSGL-1 in virion assembly sites (55), it is possible that both proteins also co-localize at virological synapses, where PSGL-1 may exert its inhibitory effect on viral cell-cell transmission. PSGL-1 overexpression has also been found to inhibit the binding of antibodies to different cell surface receptors (77). The molecular mechanism impeding antibody-receptor interaction was suggested to be steric hindrance elicited by PSGL1's extending and heavily glycosylated extracellular domain, which was believed to be hampering antibody access to the receptors (77). Nevertheless, further investigation is

needed to determine whether PSGL-1 modulates the efficiency of virus transfer at cell-cell junctions.

Since preventing particle binding to target cells is disadvantageous to viruses, it is logical to assume that viruses have evolved mechanisms to counteract PSGL-1 restriction, by keeping it off the virion surface. A previous report showed that HIV-1 Vpu can antagonize PSGL-1 by targeting it to E3-ligase-mediated ubiquitination and proteosomal degradation. Our data corroborated these findings, as we have found the NL43delVpu mutant to be significantly more susceptible to PSGL-1 restriction than wild type NL43 (Fig.2.3B). Further, another study suggested that in addition to Vpu, HIV-1 Gag may also contribute to PSGL-1 downregulation from the cell surface by promoting PSGL-1 incorporation into virions (91).

Besides disrupting the binding of HIV-1 virions to target cells, we observed that PSGL-1 expression in the virus-producer cells can also interfere with the infectivity of another retrovirus, MLV, as well as the influenza A virus and a SARS-CoV-2-S lenti-pseudovirus (Fig.2.16), confirming that the antiviral effect of PSGL-1 is independent of specific viral glycoprotein-receptor interactions. As mentioned above, we and others have illustrated that HIV-1 can antagonize PSGL-1 through the activity of Vpu. Further work is needed to determine whether the other viruses used in this study have also acquired protective strategies to overcome the blockade inflicted by PSGL-1.

HIV-1 is known to incorporate various host transmembrane proteins during assembly (90); however, only a few of these have been investigated for their roles on the surface of HIV-1 particles (90). Our work describes a unique anti-HIV-1 mechanism, by

which virion incorporation of the host transmembrane protein PSGL-1, sterically obstructs virus interaction with the target cell membrane. We also found that CD43, a sialomucin structurally similar to PSGL-1, blocks HIV-1 infectivity by preventing virion attachment to target cells (Fig. 2.17). The inhibitory effects of PSGL-1 and CD43 on HIV-1 have been further confirmed in a separate study conducted by Murakami et al. (91), indicating that an extended and heavily glycosylated mucin-like domain is a molecular feature that may confer anti-viral properties to a protein. These findings broaden our understanding of the means employed by host cells to restrict infection by HIV-1 and other enveloped viruses and may be useful for developing novel antiviral therapeutic approaches.

References

1. Sako D, Chang XJ, Barone KM, Vachino G, White HM, Shaw G, et al. Expression cloning of a functional glycoprotein ligand for P-selectin. Cell. 1993;75(6):1179-86.
2. Guyer DA, Moore KL, Lynam EB, Schammel CM, Rogelj S, McEver RP, et al. P-selectin glycoprotein ligand-1 (PSGL-1) is a ligand for L-selectin in neutrophil aggregation. Blood. 1996;88(7):2415-21.
3. Goetz DJ, Greif DM, Ding H, Camphausen RT, Howes S, Comess KM, et al. Isolated P-selectin glycoprotein ligand-1 dynamic adhesion to P- and E-selectin. J Cell Biol. 1997;137(2):509-19.
4. Frenette PS, Denis CV, Weiss L, Jurk K, Subbarao S, Kehrel B, et al. P-Selectin glycoprotein ligand 1 (PSGL-1) is expressed on platelets and can mediate platelet-endothelial interactions in vivo. J Exp Med. 2000;191(8):1413-22.
5. Fujimoto TT, Noda M, Takafuta T, Shimomura T, Fujimura K, Kuramoto A. Expression and functional characterization of the P-selectin glycoprotein ligand-1 in various cells. Int J Hematol. 1996;64(3-4):231-9.
6. Laszik Z, Jansen PJ, Cummings RD, Tedder TF, McEver RP, Moore KL. P-selectin glycoprotein ligand-1 is broadly expressed in cells of myeloid, lymphoid, and dendritic lineage and in some nonhematopoietic cells. Blood. 1996;88(8):3010-21.
7. Somers WS, Tang J, Shaw GD, Camphausen RT. Insights into the molecular basis of leukocyte tethering and rolling revealed by structures of P- and E-selectin bound to SLe(X) and PSGL-1. Cell. 2000;103(3):467-79.
8. Almulki L, Noda K, Amini R, Schering A, Garland RC, Nakao S, et al. Surprising up-regulation of P-selectin glycoprotein ligand-1 (PSGL-1) in endotoxin-induced uveitis. FASEB J. 2009;23(3):929-39.
9. Schumacher A, Liebers U, John M, Gerl V, Meyer M, Witt C, et al. P-selectin glycoprotein ligand-1 (PSGL-1) is up-regulated on leucocytes from patients with chronic obstructive pulmonary disease. Clin Exp Immunol. 2005;142(2):370-6.
10. Borges E, Eytner R, Moll T, Steegmaier M, Campbell MA, Ley K, et al. The P-selectin glycoprotein ligand-1 is important for recruitment of neutrophils into inflamed mouse peritoneum. Blood. 1997;90(5):1934-42.
11. Asaduzzaman M, Mihaescu A, Wang Y, Sato T, Thorlacius H. P-selectin and P-selectin glycoprotein ligand 1 mediate rolling of activated CD8+ T cells in inflamed colonic venules. J Investig Med. 2009;57(7):765-8.
12. Haddad W, Cooper CJ, Zhang Z, Brown JB, Zhu Y, Issekutz A, et al. P-selectin and P-selectin glycoprotein ligand 1 are major determinants for Th1 cell recruitment to nonlymphoid effector sites in the intestinal lamina propria. J Exp Med. 2003;198(3):369-77.
13. Martin-Fontecha A, Baumjohann D, Guarda G, Reboldi A, Hons M, Lanzavecchia A, et al. CD40L+ CD4+ memory T cells migrate in a CD62P-dependent fashion into reactive lymph nodes and license dendritic cells for T cell priming. J Exp Med. 2008;205(11):2561-74.

14. Zimmerman GA, McIntyre TM, Prescott SM. Adhesion and signaling in vascular cell-cell interactions. J Clin Invest. 1997;100(11 Suppl):S3-5.
15. Konstantopoulos K, McIntire LV. Effects of fluid dynamic forces on vascular cell adhesion. J Clin Invest. 1997;100(11 Suppl):S19-23.
16. Springer TA. Traffic signals for lymphocyte recirculation and leukocyte emigration: the multistep paradigm. Cell. 1994;76(2):301-14.
17. Ley K, Laudanna C, Cybulsky MI, Nourshargh S. Getting to the site of inflammation: the leukocyte adhesion cascade updated. Nat Rev Immunol. 2007;7(9):678-89.
18. Langer HF, Chavakis T. Leukocyte-endothelial interactions in inflammation. J Cell Mol Med. 2009;13(7):1211-20.
19. Chavakis E, Choi EY, Chavakis T. Novel aspects in the regulation of the leukocyte adhesion cascade. Thromb Haemost. 2009;102(2):191-7.
20. Zarbock A, Muller H, Kuwano Y, Ley K. PSGL-1-dependent myeloid leukocyte activation. J Leukoc Biol. 2009;86(5):1119-24.
21. Muller WA. Getting leukocytes to the site of inflammation. Vet Pathol. 2013;50(1):7-22.
22. Nourshargh S, Alon R. Leukocyte migration into inflamed tissues. Immunity. 2014;41(5):694-707.
23. McEver RP. Selectins: initiators of leucocyte adhesion and signalling at the vascular wall. Cardiovasc Res. 2015;107(3):331-9.
24. Green CE, Schaff UY, Sarantos MR, Lum AF, Staunton DE, Simon SI. Dynamic shifts in LFA-1 affinity regulate neutrophil rolling, arrest, and transmigration on inflamed endothelium. Blood. 2006;107(5):2101-11.
25. Chesnutt BC, Smith DF, Raffler NA, Smith ML, White EJ, Ley K. Induction of LFA-1-dependent neutrophil rolling on ICAM-1 by engagement of E-selectin. Microcirculation. 2006;13(2):99-109.
26. Kuwano Y, Spelten O, Zhang H, Ley K, Zarbock A. Rolling on E- or P-selectin induces the extended but not high-affinity conformation of LFA-1 in neutrophils. Blood. 2010;116(4):617-24.
27. McEver RP, Cummings RD. Perspectives series: cell adhesion in vascular biology. Role of PSGL-1 binding to selectins in leukocyte recruitment. J Clin Invest. 1997;100(3):485-91.
28. Lam FW, Burns AR, Smith CW, Rumbaut RE. Platelets enhance neutrophil transendothelial migration via P-selectin glycoprotein ligand-1. Am J Physiol Heart Circ Physiol. 2011;300(2):H468-75.
29. Cummings RD. Structure and function of the selectin ligand PSGL-1. Braz J Med Biol Res. 1999;32(5):519-28.
30. Moore KL. Structure and function of P-selectin glycoprotein ligand-1. Leuk Lymphoma. 1998;29(1-2):1-15.
31. Tauxe C, Xie X, Joffraud M, Martinez M, Schapira M, Spertini O. P-selectin glycoprotein ligand-1 decameric repeats regulate selectin-dependent rolling under flow conditions. J Biol Chem. 2008;283(42):28536-45.

32. Baisse B, Galisson F, Giraud S, Schapira M, Spertini O. Evolutionary conservation of P-selectin glycoprotein ligand-1 primary structure and function. BMC Evol Biol. 2007;7:166.
33. Snapp KR, Craig R, Herron M, Nelson RD, Stoolman LM, Kansas GS. Dimerization of P-selectin glycoprotein ligand-1 (PSGL-1) required for optimal recognition of P-selectin. J Cell Biol. 1998;142(1):263-70.
34. Alonso-Lebrero JL, Serrador JM, Dominguez-Jimenez C, Barreiro O, Luque A, del Pozo MA, et al. Polarization and interaction of adhesion molecules P-selectin glycoprotein ligand 1 and intercellular adhesion molecule 3 with moesin and ezrin in myeloid cells. Blood. 2000;95(7):2413-9.
35. Schaff UY, Shih HH, Lorenz M, Sako D, Kriz R, Milarski K, et al. SLIC-1/sorting nexin 20: a novel sorting nexin that directs subcellular distribution of PSGL-1. Eur J Immunol. 2008;38(2):550-64.
36. Spertini C, Baisse B, Spertini O. Ezrin-radixin-moesin-binding sequence of PSGL-1 glycoprotein regulates leukocyte rolling on selectins and activation of extracellular signal-regulated kinases. J Biol Chem. 2012;287(13):10693-702.
37. Serrador JM, Urzainqui A, Alonso-Lebrero JL, Cabrero JR, Montoya MC, Vicente-Manzanares M, et al. A juxta-membrane amino acid sequence of P-selectin glycoprotein ligand-1 is involved in moesin binding and ezrin/radixin/moesin-directed targeting at the trailing edge of migrating lymphocytes. Eur J Immunol. 2002;32(6):1560-6.
38. Takai Y, Kitano K, Terawaki S, Maesaki R, Hakoshima T. Structural basis of PSGL-1 binding to ERM proteins. Genes Cells. 2007;12(12):1329-38.
39. Snapp KR, Heitzig CE, Kansas GS. Attachment of the PSGL-1 cytoplasmic domain to the actin cytoskeleton is essential for leukocyte rolling on P-selectin. Blood. 2002;99(12):4494-502.
40. Zarbock A, Abram CL, Hundt M, Altman A, Lowell CA, Ley K. PSGL-1 engagement by E-selectin signals through Src kinase Fgr and ITAM adapters DAP12 and FcR gamma to induce slow leukocyte rolling. J Exp Med. 2008;205(10):2339-47.
41. Stadtmann A, Germena G, Block H, Boras M, Rossaint J, Sundd P, et al. The PSGL-1-L-selectin signaling complex regulates neutrophil adhesion under flow. J Exp Med. 2013;210(11):2171-80.
42. Zarbock A, Lowell CA, Ley K. Spleen tyrosine kinase Syk is necessary for E-selectin-induced alpha(L)beta(2) integrin-mediated rolling on intercellular adhesion molecule-1. Immunity. 2007;26(6):773-83.
43. Yago T, Shao B, Miner JJ, Yao L, Klopocki AG, Maeda K, et al. E-selectin engages PSGL-1 and CD44 through a common signaling pathway to induce integrin alphaLbeta2-mediated slow leukocyte rolling. Blood. 2010;116(3):485-94.
44. Mueller H, Stadtmann A, Van Aken H, Hirsch E, Wang D, Ley K, et al. Tyrosine kinase Btk regulates E-selectin-mediated integrin activation and neutrophil recruitment by controlling phospholipase C (PLC) gamma2 and PI3Kgamma pathways. Blood. 2010;115(15):3118-27.

45. Block H, Herter JM, Rossaint J, Stadtmann A, Kliche S, Lowell CA, et al. Crucial role of SLP-76 and ADAP for neutrophil recruitment in mouse kidney ischemia-reperfusion injury. J Exp Med. 2012;209(2):407-21.
46. Urzainqui A, Serrador JM, Viedma F, Yanez-Mo M, Rodriguez A, Corbi AL, et al. ITAM-based interaction of ERM proteins with Syk mediates signaling by the leukocyte adhesion receptor PSGL-1. Immunity. 2002;17(4):401-12.
47. Sanchez-Madrid F, del Pozo MA. Leukocyte polarization in cell migration and immune interactions. EMBO J. 1999;18(3):501-11.
48. Xu H, Manivannan A, Jiang HR, Liversidge J, Sharp PF, Forrester JV, et al. Recruitment of IFN-gamma-producing (Th1-like) cells into the inflamed retina in vivo is preferentially regulated by P-selectin glycoprotein ligand 1:P/E-selectin interactions. J Immunol. 2004;172(5):3215-24.
49. Tinoco R, Otero DC, Takahashi AA, Bradley LM. PSGL-1: A New Player in the Immune Checkpoint Landscape. Trends Immunol. 2017;38(5):323-35.
50. Tinoco R, Carrette F, Barraza ML, Otero DC, Magana J, Bosenberg MW, et al. PSGL-1 Is an Immune Checkpoint Regulator that Promotes T Cell Exhaustion. Immunity. 2016;44(6):1470.
51. Nishimura Y, Shimizu H. [Identification of P-selectin glycoprotein ligand-1 as one of the cellular receptors for enterovirus 71]. Uirusu. 2009;59(2):195-203.
52. Nishimura Y, Lee H, Hafenstein S, Kataoka C, Wakita T, Bergelson JM, et al. Enterovirus 71 binding to PSGL-1 on leukocytes: VP1-145 acts as a molecular switch to control receptor interaction. PLoS Pathog. 2013;9(7):e1003511.
53. Nishimura Y, Wakita T, Shimizu H. Tyrosine sulfation of the amino terminus of PSGL-1 is critical for enterovirus 71 infection. PLoS Pathog. 2010;6(11):e1001174.
54. Connor R, Jones LD, Qiu X, Thakar J, Maggirwar SB. Frontline Science: c-Myc regulates P-selectin glycoprotein ligand-1 expression in monocytes during HIV-1 infection. J Leukoc Biol. 2017;102(4):953-64.
55. Llewellyn GN, Grover JR, Olety B, Ono A. HIV-1 Gag associates with specific uropod-directed microdomains in a manner dependent on its MA highly basic region. J Virol. 2013;87(11):6441-54.
56. Grover JR, Veatch SL, Ono A. Basic motifs target PSGL-1, CD43, and CD44 to plasma membrane sites where HIV-1 assembles. J Virol. 2015;89(1):454-67.
57. Liu Y, Fu Y, Wang Q, Li M, Zhou Z, Dabbagh D, et al. Proteomic profiling of HIV-1 infection of human CD4(+) T cells identifies PSGL-1 as an HIV restriction factor. Nat Microbiol. 2019;4(5):813-25.
58. Yoder A, Yu D, Dong L, Iyer SR, Xu X, Kelly J, et al. HIV envelope-CXCR4 signaling activates cofilin to overcome cortical actin restriction in resting CD4 T cells. Cell. 2008;134(5):782-92.
59. Yee JK, Miyanohara A, LaPorte P, Bouic K, Burns JC, Friedmann T. A general method for the generation of high-titer, pantropic retroviral vectors: highly efficient infection of primary hepatocytes. Proc Natl Acad Sci U S A. 1994;91(20):9564-8.
60. Freed EO, Delwart EL, Buchschacher GL, Jr., Panganiban AT. A mutation in the human immunodeficiency virus type 1 transmembrane glycoprotein gp41 dominantly interferes with fusion and infectivity. Proc Natl Acad Sci U S A. 1992;89(1):70-4.

61. Cavrois M, De Noronha C, Greene WC. A sensitive and specific enzyme-based assay detecting HIV-1 virion fusion in primary T lymphocytes. Nat Biotechnol. 2002;20(11):1151-4.
62. Pan X, Baldauf HM, Keppler OT, Fackler OT. Restrictions to HIV-1 replication in resting CD4+ T lymphocytes. Cell Res. 2013;23(7):876-85.
63. Unutmaz D, KewalRamani VN, Marmon S, Littman DR. Cytokine signals are sufficient for HIV-1 infection of resting human T lymphocytes. J Exp Med. 1999;189(11):1735-46.
64. Trinite B, Chan CN, Lee CS, Levy DN. HIV-1 Vpr- and Reverse Transcription-Induced Apoptosis in Resting Peripheral Blood CD4 T Cells and Protection by Common Gamma-Chain Cytokines. J Virol. 2016;90(2):904-16.
65. Matheson NJ, Sumner J, Wals K, Rapiteanu R, Weekes MP, Vigan R, et al. Cell Surface Proteomic Map of HIV Infection Reveals Antagonism of Amino Acid Metabolism by Vpu and Nef. Cell Host Microbe. 2015;18(4):409-23.
66. Yu D, Wang W, Yoder A, Spear M, Wu Y. The HIV envelope but not VSV glycoprotein is capable of mediating HIV latent infection of resting CD4 T cells. PLoS Pathog. 2009;5(10):e1000633.
67. Kane M, Zang TM, Rihn SJ, Zhang F, Kueck T, Alim M, et al. Identification of Interferon-Stimulated Genes with Antiretroviral Activity. Cell Host Microbe. 2016;20(3):392-405.
68. Wilson SJ, Schoggins JW, Zang T, Kutluay SB, Jouvenet N, Alim MA, et al. Inhibition of HIV-1 particle assembly by 2',3'-cyclic-nucleotide 3'-phosphodiesterase. Cell Host Microbe. 2012;12(4):585-97.
69. Lee WJ, Fu RM, Liang C, Sloan RD. IFITM proteins inhibit HIV-1 protein synthesis. Sci Rep. 2018;8(1):14551.
70. Kluge SF, Sauter D, Kirchhoff F. SnapShot: antiviral restriction factors. Cell. 2015;163(3):774- e1.
71. Wu Y, Beddall MH, Marsh JW. Rev-dependent lentiviral expression vector. Retrovirology. 2007;4:12.
72. Wu Y, Beddall MH, Marsh JW. Rev-dependent indicator T cell line. Curr HIV Res. 2007;5(4):394-402.
73. Marechal V, Clavel F, Heard JM, Schwartz O. Cytosolic Gag p24 as an index of productive entry of human immunodeficiency virus type 1. J Virol. 1998;72(3):2208-12.
74. Olinger GG, Saifuddin M, Spear GT. CD4-Negative cells bind human immunodeficiency virus type 1 and efficiently transfer virus to T cells. J Virol. 2000;74(18):8550-7.
75. Wilen CB, Tilton JC, Doms RW. HIV: cell binding and entry. Cold Spring Harb Perspect Med. 2012;2(8).
76. Li F, Erickson HP, James JA, Moore KL, Cummings RD, McEver RP. Visualization of P-selectin glycoprotein ligand-1 as a highly extended molecule and mapping of protein epitopes for monoclonal antibodies. J Biol Chem. 1996;271(11):6342-8.

77. Umeki S, Suzuki R, Ema Y, Shimojima M, Nishimura Y, Okuda M, et al. Anti-adhesive property of P-selectin glycoprotein ligand-1 (PSGL-1) due to steric hindrance effect. J Cell Biochem. 2013;114(6):1271-85.
78. Epperson TK, Patel KD, McEver RP, Cummings RD. Noncovalent association of P-selectin glycoprotein ligand-1 and minimal determinants for binding to P-selectin. J Biol Chem. 2000;275(11):7839-53.
79. Cicala C, Arthos J, Fauci AS. HIV-1 envelope, integrins and co-receptor use in mucosal transmission of HIV. J Transl Med. 2011;9 Suppl 1:S2.
80. Gelderblom HR, Hausmann EH, Ozel M, Pauli G, Koch MA. Fine structure of human immunodeficiency virus (HIV) and immunolocalization of structural proteins. Virology. 1987;156(1):171-6.
81. Alcaide P, King SL, Dimitroff CJ, Lim YC, Fuhlbrigge RC, Luscinskas FW. The 130-kDa glycoform of CD43 functions as an E-selectin ligand for activated Th1 cells in vitro and in delayed-type hypersensitivity reactions in vivo. J Invest Dermatol. 2007;127(8):1964-72.
82. Matsumoto M, Atarashi K, Umemoto E, Furukawa Y, Shigeta A, Miyasaka M, et al. CD43 functions as a ligand for E-Selectin on activated T cells. J Immunol. 2005;175(12):8042-50.
83. Clark MC, Baum LG. T cells modulate glycans on CD43 and CD45 during development and activation, signal regulation, and survival. Ann N Y Acad Sci. 2012;1253:58-67.
84. Cyster JG, Shotton DM, Williams AF. The dimensions of the T lymphocyte glycoprotein leukosialin and identification of linear protein epitopes that can be modified by glycosylation. EMBO J. 1991;10(4):893-902.
85. Matsumoto M, Shigeta A, Furukawa Y, Tanaka T, Miyasaka M, Hirata T. CD43 collaborates with P-selectin glycoprotein ligand-1 to mediate E-selectin-dependent T cell migration into inflamed skin. J Immunol. 2007;178(4):2499-506.
86. Neil SJ, Zang T, Bieniasz PD. Tetherin inhibits retrovirus release and is antagonized by HIV-1 Vpu. Nature. 2008;451(7177):425-30.
87. Van Damme N, Goff D, Katsura C, Jorgenson RL, Mitchell R, Johnson MC, et al. The interferon-induced protein BST-2 restricts HIV-1 release and is downregulated from the cell surface by the viral Vpu protein. Cell Host Microbe. 2008;3(4):245-52.
88. McEver RP, Moore KL, Cummings RD. Leukocyte trafficking mediated by selectin-carbohydrate interactions. J Biol Chem. 1995;270(19):11025-8.
89. Patel KD, Nollert MU, McEver RP. P-selectin must extend a sufficient length from the plasma membrane to mediate rolling of neutrophils. J Cell Biol. 1995;131(6 Pt 2):1893-902.
90. Burnie J, Guzzo C. The Incorporation of Host Proteins into the External HIV-1 Envelope. Viruses. 2019;11(1):85.
91. Murakami T, Carmona N, Ono A. Virion-incorporated PSGL-1 and CD43 inhibit both cell-free infection and transinfection of HIV-1 by preventing virus-cell binding. Proc Natl Acad Sci U S A. 2020;117(14):8055-63.

CHAPTER THREE: IDENTIFICATION OF THE SHREK FAMILY OF PROTEINS AS BROAD-SPECTRUM ANTIVIRAL HOST FACTORS

Abstract

Mucins and mucin-like molecules are heavily glycosylated, high-molecular-weight cell surface proteins that possess a semi-rigid and highly extended extracellular domain. In our previous work, we identified P-selectin glycoprotein ligand-1 (PSGL-1), a mucin-like glycoprotein, as a host factor that restricts HIV-1 infectivity. Mechanistically, virion-incorporated PSGL-1 was found to sterically hinder virus particle interaction with target cells. Here, we report the identification of a family of antiviral cellular proteins, named the Surface-Hinged, Rigidly-Extended Killer (SHREK) family of virion inactivators (PSGL-1, CD43, TIM-1, CD34, PODXL1, PODXL2, CD164, MUC1, MUC4, and TMEM123) that possess similar structural features to PSGL-1. We demonstrate that these SHREK proteins block HIV-1 infectivity by inhibiting virus particle attachment to target cells. In addition, we demonstrate that SHREK proteins are broad-spectrum host antiviral factors that block the infection of diverse viruses such as influenza A. Furthermore, we demonstrate that a subset of SHREKs also blocks the infectivity of a hybrid alphavirus-SARS-CoV-2 (Ha-CoV-2) pseudovirus. These results suggest that SHREK proteins may be a part of host innate immunity against enveloped viruses.

Introduction

Mucins and mucin-like molecules are heavily glycosylated, high-molecular-weight cell surface proteins that possess a rigid and highly extended extracellular domain (1). P-selectin glycoprotein ligand-1 (PSGL-1), a mucin-like glycoprotein (2-4), has recently been identified as an interferon-induced restriction factor that abolishes HIV-1 infectivity (5), through steric hindrance (6, 7). The block in infectivity was shown to result from the incorporation of PSGL-1 into virion particles, which inhibits virion attachment to target cells in the next round of infection. This was attributed to the long and "bulky" shape of the PSGL-1 molecule, which acts as a barrier between the viral and cell membranes (6, 7). Mutational mapping revealed that the extracellular domain of PSGL-1 is necessary for its antiviral activity (6).

PSGL-1 contains a structural characteristic common among mucins and mucin-like proteins. It has a heavily glycosylated and elongated extracellular domain that extends nearly 50 nm from the plasma membrane (8-11), which is farther than the protruding distance of most proteins expressed on the cell surface. To test whether molecules with a similar structure also possess the ability to block virus infectivity, we selected a group of cellular proteins encompassing CD43, TIM-1, CD34, PODXL1, PODXL2, CD164, MUC1, MUC4, and TMEM123. These proteins have diverse coding sequences, tissue expression patterns, and functionalities, but share a common hallmark, a highly extended and heavily glycosylated extracellular mucin domain.

CD43, also known as leukosialin or sialophorin, is a pass transmembrane glycoprotein belonging to the sialomucin family (12). It is expressed by most leukocytes

except for resting B cells (13, 14). The CD43 extracellular domain has a rodlike structure predicted to extend 45 nm from the cell surface (15), and contains numerous serine or threonine residues modified with heavily sialylated O-linked glycans (16, 17). Like PSGL-1, CD43 mediates the rolling of lymphocytes on E-selectin expressed on vascular endothelium for recruitment of activated T cells to sites of inflammation (18, 19). CD43 has also been described as a negative regulator of T-cell activation (20); CD43 depletion in T cells was found to be associated with a hyper-proliferative phenotype (20). Interestingly, CD43 is reported to be excluded from the immunological synapse away from the antigen-presenting cell (APC) contact site (21) to promote efficient contact at T-cell-APC junctions (22). It was hypothesized that the negative function of CD43 arises from a repulsive effect on cell-cell contact owing to its large, extensively sialylated and negatively charged extracellular domain (20, 23). Contrariwise, CD43 has also been found to have a co-stimulatory role during T-cell activation at the immunological synapse (24). In HIV infection, CD43 ligation was found to enhance the transcriptional activity of HIV-1 (25). CD43 was also found to co-cluster, along with PSGL-1 and CD44, with HIV-1 at lipid raft microdomains where HIV-1 assembles (26, 27). Additionally, we and others have recently found that CD43 blocks HIV-1 infection by reducing virion infectivity (6).

T cell immunoglobulin and mucin domain 1 (TIM-1) is a type I membrane protein with an extracellular domain containing an IgV domain followed and a heavily glycosylated mucin domain with a variable number of threonine, serine and proline hexametric repeats (28). TIM-1 is expressed by all activated CD4+ T cells and its

expression remains high on TH2 cells but is reduced on TH1and TH17 cells following differentiation (29). Functionally, TIM-1 has been shown to play an important role in regulating TH2-cell responses (29). Overexpression of TIM-1 in vitro was shown to increase IL-4 transcription and induce spontaneous activation of nuclear factor of activated T cells (NFAT) and activator protein 1 (AP1) elements (29). TIM-1 can also function as a co-stimulatory molecule for T-cell activation in the presence of T cell receptor ligation (30). In viral infections, TIM-1 was identified as a host cellular receptor for Hepatitis A virus (31, 32), and has been also shown to function as a receptor or entry cofactor for Ebola virus (EBOV) (33) and Dengue virus (DV) (33, 34). Additional studies later revealed that TIM-family proteins are involved in the entry of a variety of viruses, presumably via interactions with virion-associated phosphatidylserine (PS) (35, 36), pointing to a broader role of TIMs in viral infections (35). In HIV-1 infection, TIM-1 was shown to be a potent inhibitor of virion release, resulting in decreased virus production. It was demonstrated that TIM-1 retains viral particles at the cell surface, similar to the phenotype observed with tetherin (37, 38). Virion-incorporated TIM-1 was found to link virus particles to the plasma membrane through interactions with phosphatidylserine (PS) on both the cell and viral membranes (37).

CD34, podocalyxin (PODXL1), and endoglycan (PODXL2) are closely related proteins belonging to the CD34 family of cell surface sialomucins (39). All three CD34-family proteins contain a serine-, threonine- and proline-rich extracellular mucin domain that is extensively O-glycosylated and sialylated, resulting in large molecular masses ranging from 90-170 kDa (39). The expression patterns of the CD34-family proteins are

overlapping, but the individual proteins are also distinctly expressed in specific tissues (40). CD34 is widely used as a marker of hematopoietic stem cells and progenitor cells and vascular endothelial cells and (41-43), and PODXL1 is also extensively expressed on vascular endothelial cells and hematopoietic stem and progenitor cells (44). However, PODXL1 was initially identified as a marker of kidney glomerular epithelial cells (podocytes) (45) and was found to be essential for kidney development as PODXL1-deficient mice exhibit perinatal lethality (46). The third CD34 family member, PODXL2 was discovered through its sequence similarity to CD34 and PODXL1 and is also expressed by a subset of hematopoietic cells (47). Besides being surface cell markers of hematopoietic progenitor cells, several other functions have been proposed for this family of proteins. One such function is enhancing the proliferation and blocking the differentiation of progenitor stem cells (48, 49). Another function of CD34, PODXL1, and PODXL2 is their involvement in lymphocyte adhesion to the vascular endothelium through interactions mediated by CD34 family members (on endothelial cells) and L-selectin (on lymphocytes) (40). Additionally, CD34 on hematopoietic stem/progenitor cells has been reported to facilitate cell migration to specialized microvascular beds in the bone marrow that express E- or P-selectins (50). In viral diseases, CD34 has been studied only as a cell marker of infected cells, whereas other members of the CD34 family have not been implicated in viral infection. Several studies have detected viral products of different viruses including, Cytomegalovirus, hepatitis C virus (HCV), hepatitis B virus (HBV), and HIV-1, in CD34+ stem cells (51-56). Nevertheless, unlike PSGL-1, CD43,

and TIM-1, it remains unclear whether the CD34 family molecules themselves pose any direct effects on viral infection.

CD164, or endolyn, is a homodimeric 80- to 90-kD mucin-like molecule that is co-expressed with CD34 on the surface of human hematopoietic cells (57, 58). Like the other mucins, CD164 has a high content of proline, threonine, and/or serine residues densely modified with O-linked carbohydrates (59). It has been implicated in regulating the proliferation, adhesion, differentiation, and migration of hematopoietic stem cells (57, 60-62). Additionally, many studies on CD164 have indicated a role for this molecule in a variety of cancers including prostate- and colon cancers and glioblastoma, suggestive of its potential as a marker of tumorigenesis (63-65). With relevance to viral infections, CD164 has been identified as a potential HIV restriction factor in a genome-wide scan for genes having molecular and evolutionary characteristics of known restriction factors (66). CD164 was found to suppress the production of infectious HIV particles (66), although the mechanism of the CD164-mediated HIV inhibition was not investigated. TMEM123 (Porimin) is a CD164-related sialomucin with a high density of glycosylated threonine and serine residues in its extracellular domain (67). The exact functions of TMEM123 are unclear; however, it was found to induce oncotic cell death upon crosslinking with an anti-porimin antibody (67, 68). TMEM123 was also suggested to have anti-adhesive properties as TMEM123 transfectants were shown to detach from supporting cell culture dishes (67). Regarding HIV-1 or other viral infections, no roles for TMEM123 have been previously described.

We also selected MUC1 and MUC4, which are large transmembrane mucins with dense arrays of O-linked oligosaccharides attached to threonine and serine residues in the extracellular domains (69). Both MUC1 and MUC4 were reported to modulate cell-cell and cell-extracellular matrix (ECM) interactions by steric hindrance and have been reported to protect against pathogens (70). MUC1 and MUC4 are expressed in the airways (71), and on a variety of secretory epithelia (72, 73). The expression patterns of MUC1 and MUC4 in the lung have been suggested to form a filtering mesh that decreases the size of particles allowed to enter the intraciliary space (71). MUC1 was found to regulate gastric inflammation in repones to Helicobacter pylori infection (74, 75), and to downregulate inflammation during acute lung infection by Pseudomonas aeruginosa (76). Regarding viral infections, MUC1 has been found to protect against infection with influenza A virus (IAV). It was shown that the sialylated form of MUC1 binds to IAV virions, capturing them and reducing their ability to infect host cells (77). A more recent study also demonstrated, using a viral dynamics model, that MUC1 has an anti-inflammatory role in the immune response against influenza virus (78). MUC1 and MUC4 from mucosal secretions have also been reported to have anti-HIV properties (79-82).

In this study, we sought to determine whether these mucins and mucin-like proteins (TIM-1, CD34, PODXL1, PODXL2, CD164, MUC1, MUC4, and TMEM123) possess PSGL-1- and CD43-like capacities to inactivate HIV-1 infectivity. We found that all these proteins can block the infectivity of HIV-1 by inhibiting virus particle attachment to target cells. We also demonstrated that SHREK proteins are broad-

spectrum host antiviral factors that block the infection of diverse viruses such as influenza A. These results suggest that SHREK proteins may be a part of host defense mechanisms against enveloped viruses. The results presented in this chapter were published in the journal Viruses in May 2021.

Materials and Methods

Cells and cell culture

HEK293T (ATCC), MDCK (ATCC), and HeLaJC.53 (kindly provided by Dr. David Kabat) cells were maintained in Dulbecco's modified Eagle's medium (DMEM) (Invitrogen, Carlsbad, CA, USA) containing 10% heat inactivated FBS and 50 units/mL of penicillin and 50 μg/mL of streptomycin (Invitrogen). HEK293T(ACE2/TMPRSS2) cells (kindly provided by Virongy) were maintained in DMEM (Invitrogen) supplemented with 10% FBS and puromycin (1 μg/mL) and hygromycin B (200 μg/mL) as instructed by the manufacturer. HIV Rev-dependent GFP indicator Rev-A3R5-GFP cells (kindly provided by Virongy) were cultured in RPMI-1640 plus 10% FBS supplemented with 1 mg/mL geneticin (G418) (Sigma-Aldrich, Saint Louis, MO, USA), 1 μg/mL puromycin (Sigma-Aldrich), and 50 units/mL of penicillin and 50 μg/mL of streptomycin (Invitrogen).

Plasmids, transfection, and virus production

The infectious HIV-1 molecular clone pHIV-1(NL4-3) was obtained from the NIH AIDS Reagent Program. pCMV3-PSGL-1, pCMV3-CD43, pCMV3-CD164, pCMV3-TMEM123, pCMV3-CD34, pCMV3-PODXL1, pCMV3-PODXL2, pCMV3-TIM1, pCMV3-MUC1, pCMV3-MUC4, pCMV3-Empty, pMUC1-HA, pTMEM123-HA

and SARS-CoV-2 S, M, E, or N expression vectors were purchased from Sinobiological. The Ha-CoV-2(Luc) vector was described previously (83). pCMV6-XL5-ICAM1, pCMV6-XL5-CD2, pCMV6-AC-ITGB2, pCMV6-XL5-CD62L were purchased from Origene. The pHW-NA-GFP(ΔAT6) reporter plasmid and the A/WSN/1933 H1N1-derived plasmids pHW2000-PB2, pHW2000-PB1, pHW2000-PA, pHW2000-HA, pHW2000-NP, pHW2000-NA, pHW2000-M, and pHW2000-NS were kindly provided by Dr. Feng Li.

For HIV-1 virus production, HEK293T cells were cotransfected in a 6-well plate with 1 μg of pHIV-1(NL4-3) plus the indicated doses of pCMV3-CD164, pCMV3-TMEM123, pCMV3-CD34, pCMV3-PODXL1, pCMV3-PODXL2, pCMV3-TIM1, pCMV3-MUC1, pCMV3-MUC4 or pCMV3-Empty. Supernatants were collected at 48 h post cotransfection. For influenza A-GFP reporter particle assembly, HEK293T cells were cotransfected with pHW2000-PB2, pHW2000-PB1, pHW2000-PA, pHW2000-HA, pHW2000-NP, pHW2000-NA, pHW2000-M, and pHW2000-NS (0.25 μg each); pHW-NA-GFP(ΔAT6) (1.5 μg); and pCMV3-PSGL-1, pCMV3-CD43, pCMV3-CD164, pCMV3-TMEM123, pCMV3-CD34, pCMV3-PODXL1, pCMV3-PODXL2, pCMV3-TIM1, pCMV3-MUC1, pCMV3-MUC4, or pCMV3-Empty DNA (0.5 μg each) in a 6-well plate. Viral supernatants were harvested at 48 h. Hybrid alphavirus-SARS-CoV-2 (Ha-CoV-2) particles were produced by cotransfection of HEK293T cells in 6-well plates with SARS-CoV-2 S, M, N, and E expression vectors (0.3 μg each), Ha-CoV-2(Luc) (1.2 μg), and each individual SHREK-expressing vector or a control empty vector (1.6 μg). Ha-CoV-2 particles were harvested at 48 h post-transfection.

Viral infectivity assays

For the HIV-1 infectivity assay, p24-normalized HIV-1 particles produced in the presence of PSGL-1, CD43, CD164, TMEM123, CD34, PODXL1, PODXL2, TIM-1, MUC1, MUC4, or empty vector were used to infect Rev-A3R5-GFP cells (0.2 to 0.5 million cells per infection). The percentage of GFP+ cells was quantified by flow cytometry at 48 or 72 h post-infection. The IC50 inhibition curves were generated using GraphPad Software. For the influenza A virion infectivity assay, influenza A-GFP reporter viruses were assembled in the presence of PSGL-1, CD43, CD164, TMEM123, CD34, PODXL1, PODXL2, TIM-1, MUC1, MUC4, or empty vectors. Virions were harvested at 48 h and used to infect MDCK cells (3 × 104 cells per infection). GFP expression was quantified at 24 h post-infection by flow cytometry. For Ha-CoV-2 infectivity assay, HEK293T(ACE2/TMPRSS2) cells were infected for 2 h with Ha-CoV-2 particles assembled in the presence of each SHREK-expressing vector or an empty vector. Infected cells were washed and cultured for 18 h. Cells were lysed with Luciferase Assay Lysis Buffer (Promega, Madison, WI, USA). Luminescence was measured on GloMax® Discover Microplate Reader (Promega).

HIV-1 Env incorporation assay

HIV-1 particles were produced by cotransfection of HEK293T cells with pHIV-1(NL4-3) DNA (1 μg) plus 100 ng of a vector expressing CD43, CD164, TMEM123, CD34, PODXL1, or PODXL2, or 200 ng of a vector expressing MUC1 or MUC4. Empty vector was used to keep the amount of DNA equal in each cotransfection. Virus particles were harvested at 48 h and purified through a 10% sucrose gradient by ultracentrifugation

(10,000× g for 4 h at 4 °C). Particles were resuspended in LDS lysis buffer (Invitrogen) and subjected to Western blot analysis.

Detection of SHREK proteins in HIV-1 particles

HIV-1 particles were assembled in 6-well plates by co-transfection of HEK293T cells with pHIV-1(NL4-3) DNA (1 μg) plus an empty vector or the vector expressing each individual SHREK protein (400 ng). For MUC1 and TMEM123, vectors expressing hemagglutinin tagged MUC1 or TMEM123 were used. Particles were harvested at 48 h, normalized for HIV-1 p24, and subjected to immuno-magnetic capture as previously described (84). Briefly, magnetic Dynabeads Pan Mouse IgG (Invitrogen) (1 × 108 beads/0.25 mL) were conjugated with one of these antibodies: mouse anti-PSGL-1 antibody (KPL-1) (BD Pharmingen), mouse anti-CD43 antibody (1G10) (BD Biosciences, San Jose, CA, USA), mouse anti-CD164 antibody (67D2) (Biolegend, San Diego, CA, USA), mouse anti-PODXL1 antibody (222328) (R & D Systems, Minneapolis, MN, USA), mouse anti-PODXL2 antibody (R & D Systems), mouse anti-CD34 antibody (563) (BD Biosciences) or mouse anti-HA tag (HA.C5) antibody (Abcam, Cambridge, UK) for 30 min at room temperature. After conjugation, antibody-conjugated beads were incubated with SHREK-bearing viral particles for 1 h at 37 °C. The complex was pulled down with a magnet and washed with cold PBS 5 times. Captured viral particles were eluted in 10% Triton x-100 PBS, diluted, and quantified by p24 ELISA.

Viral attachment assay

HIV-1 virus particles produced in the presence of PSGL-1, CD43, CD164, TMEM123, CD34, PODXL1, PODXL2, TIM-1, MUC1, MUC4, or empty vector were incubated with HelaJC.53 cells (prechilled at 4 °C for 1 h) at 4 °C for 2 h. The cells were then washed extensively (5 times) with cold PBS buffer and then lysed with LDS lysis buffer (Invitrogen) for analysis by Western blot. The attachment of HIV-1 virus produced in the presence of TMEM123 was also separately tested by pre-incubating the virus with the mouse monoclonal anti-TMEM123 antibody (297617) (ThermoFisher, Waltham, MA, USA) (25 μg/mL) at 37 °C for 1 h, followed by incubation of the virus with HeLaJC.53 cells at 4 °C for 2 h and lysis of the cells with LDS buffer.

Western blots

Cells were lysed in LDS lysis buffer (Invitrogen). Proteins were denatured by boiling in sample buffer and subjected to SDS-PAGE, transferred to a nitrocellulose membrane, and incubated overnight at 4 °C with one of these primary antibodies: mouse anti-HIV-1 p24 monoclonal antibody (183-H12-5C) (NIH AIDS Reagent Program) (1:1000 dilution), human anti-HIV-1 gp41 antibody (2F5) (1:1000 dilution) (NIH AIDS Reagent Program), mouse anti-MUC1 antibody (HMPV) (BD Biosciences) (1:1000 dilution), mouse monoclonal anti-MUC4 antibody (1G8) (ThermoFisher) (1:1000 dilution), mouse monoclonal anti-TMEM123 antibody (297617) (ThermoFisher) (1:1000 dilution), or anti-GAPDH goat polyclonal antibody (Abcam) (1:1000 dilution). Membranes were incubated with HRP-labeled goat anti-mouse IgG (KPL) (1:2500 dilution) for 60 min at room temperature, or goat anti-human 800cw-labeled antibodies

(Li-Cor Biosciences) (1:2500 dilution) for 30 min at room temperature. Chemiluminescence signal was detected by using West Femto chemiluminescence substrate (Thermo Fisher Scientific), and images were captured with a CCD camera (FluorChem 9900 Imaging Systems) (Alpha Innotech, San Leandro, CA, USA). Blots stained with infrared antibodies were scanned with the Odyssey infrared imager (Li-Cor Biosciences).

P24 ELISA

Detection of extracellular HIV-1 p24 was performed using an in-house p24 ELISA kit. Briefly, microtiter plates (Sigma-Aldrich) were coated with anti-HIV-1 p24 monoclonal antibody (183-H12-5C) (NIH AIDS Reagent Program). Samples were incubated for 2 h at 37 °C, followed by washing and incubating with biotinylated anti-HIV immune globulin (HIVIG) (NIH AIDS Reagent Program) for 1 h at 37 °C. Plates were then washed and incubated with avidin-peroxidase conjugate (R &D Systems) for 1 h at 37 °C, followed by washing and incubating with tetramethylbenzidine (TMB) substrate. Plates were kinetically read using an ELx808 automatic microplate reader (Bio-Tek Instruments, Winooski, VT, USA) at 630 nm.

Surface staining

HEK293T cells were transfected with 400 ng of pCMV3-PSGL-1, pCMV3-CD43, pCMV3-CD164, pCMV3-CD34, pCMV3-PODXL1, pCMV3-PODXL2, pCMV3-TIM-1, or pCMV3-Empty DNA. At 48 h post transfection, 0.5–1 million cells were stained with one of the following primary antibodies: mouse anti-PSGL1 antibody (KPL-1) (BD Pharmingen), mouse anti-CD43 antibody (1G10) (BD Biosciences), mouse anti-

CD164 antibody (67D2) (Biolegend), mouse anti-CD34 antibody (563) (BD Biosciences), mouse anti-TIM-1 antibody (219211) (R & D Systems), mouse monoclonal anti-PODXL1 antibody (222328) (R & D systems), or mouse monoclonal anti-PODXL2 antibody (211816) (R & D Systems), followed by staining with Alexa Fluor 488 conjugated goat anti-mouse secondary antibody (Invitrogen).

Results

Inactivation of HIV-1 infectivity by mucin and mucin-like proteins

Our previous studies have demonstrated that the mucin-like adhesion molecule, PSGL-1, blocks HIV-1 virion infectivity through particle incorporation of PSGL-1 which hinders virion attachment to target cells. Deletion of the extended and highly glycosylated extracellular domain of PSGL-1 was found to abolish its antiviral activity (6). The bulk of the extracellular domain of PSGL-1 comprises 14-16 decameric repeats (DRs) with multiple O-glycosylated threonine and proline residues (85, 86). These repeats are essential for PSGL-1's selectin binding function as they elongate and strengthen the extracellular domain of PSGL-1 (86). As shown in the previous chapter, removal of the DR portion from the PSGL-1 N-terminus abrogates the molecule's capacity to restrict HIV-1 (6) (Figure 3.1A and 3.1C). This finding demonstrates that the heavily glycosylated, large extracellular mucin domain of PSGL-1 is required for blocking virion infectivity (6, 7). To that end, we sought to determine whether the anti-HIV-1 activity of PSGL-1 extends to other mucins and mucin-like proteins with similar extracellular domains. We selected a group of mucins and mucin-like proteins including CD43, TIM-1, CD34, PODXL1, PODXL2, CD164, MUC1, MUC4, and TMEM123

(Figs. 3.1 and 3.2), all of which contain extended mucin domains that are heavily glycosylated (Fig. 3.1A).

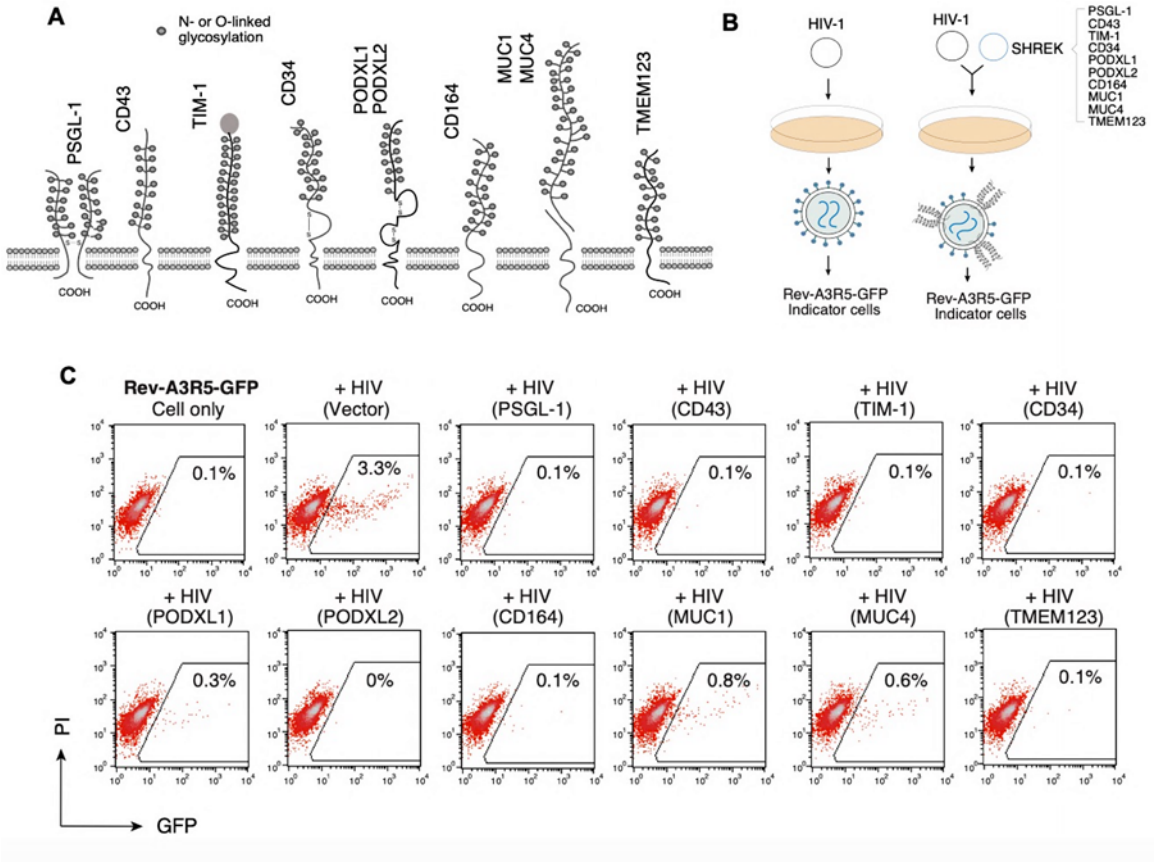

Figure 3.1 Inactivation of HIV-1 infectivity by SHREK proteins.
A) Schematic of PSGL-1 and SHREK proteins used in this study. B) Schematic of HIV-1 virion production in the presence of SHREK proteins. C) SHREK proteins inactivate HIV-1 virion infectivity. HEK293T cells were cotransfected with HIV(NL4-3) DNA (1 μg) plus each individual SHREK-expressing vector (100 ng for TIM-1, 500 ng for other SHREKs). Virions were harvested at 48 hours and normalized for p24, and viral infectivity was quantified by infecting Rev-A3R5-GFP indicator cells with equal p24 input of each virus. Shown are the percentages of GFP+ cells at 72 hours post-infection. Shown are representative results from 3 independent experiments.

Each mucin or mucin-like protein was co-transfected separately with HIV-1(NL4-3) DNA into HEK293T cells to assemble viral particles. The expression of these proteins

was verified post transfection (Fig. 3.2) and the infectivity of the released virions was quantified by infecting the HIV-1 Rev-dependent indicator cell line, Rev-A3R5-GFP (87), using equal inputs of p24 for each virus. We found that the expression of each protein individually in virus producer cells blocked the infectivity of the progeny HIV-1 virions (Figure 3.1C).

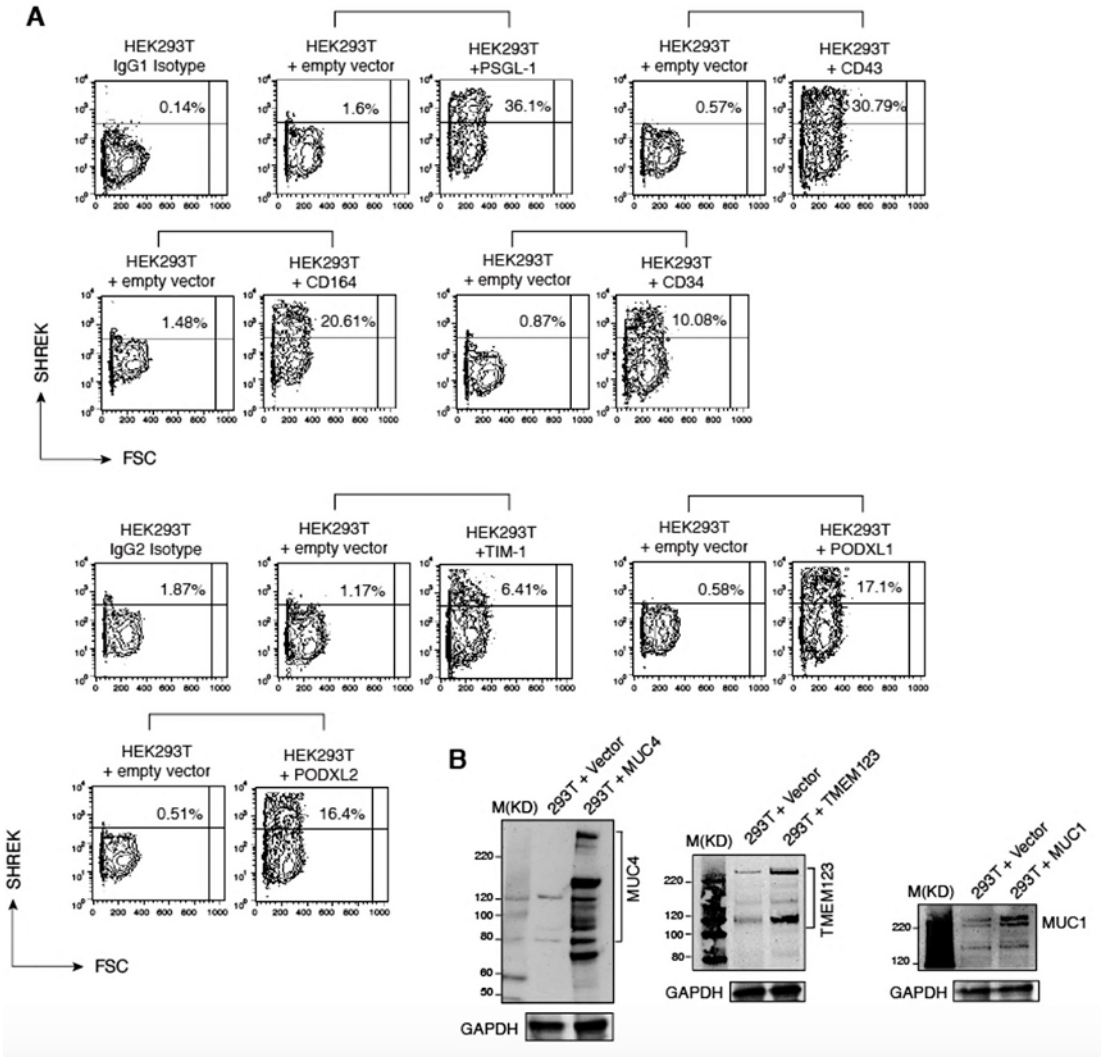

Figure 3.2 Expression of SHREK proteins in HEK293T cells following transfection.
A) HEK293T cells were transfected with 400 ng of either PSGL-1, CD43, CD164, CD34, TIM-1, PODXL1, or PODXL2. Expression of each protein was quantified at 48 hours by surface staining using antibodies against each of the indicated proteins. B) HEK293T cells were transfected with 400 ng of MUC1, MUC4, TMEM123, or an empty vector. Expression of each protein was measured by Western blot using antibodies against MUC1, MUC4 or TMEM123.

Anti-HIV-1 activity is not a shared attribute among transmembrane proteins

Next, we asked whether this antiviral capacity is a general characteristic found in any transmembrane protein with a large extracellular domain. We randomly selected

several non-mucin adhesion molecules containing varying numbers of extracellular repeat domains; CD2, ICAM-1, E-selectin, L-selectin and ITGB2 (Fig. 3.3). CD2 and ICAM-1 are members of the immunoglobulin (Ig) superfamily of proteins that contain heavily glycosylated extracellular Ig repeat domains (2 and 5 Ig domain repeats for CD2 and ICAM-1, respectively) (88). L-selectin and E-selectin belong to the selectin family of adhesion molecules that share a similar extracellular structure with a variable number of consensus repeats (2 and 6 repeats for L- and E-, respectively) (89). We also selected integrin beta chain-2 (ITGB2), which has a large extracellular domain with integrin epidermal growth factor-like repeat domains (I-EGF repeats) (90). Using the similar experimental conditions described above, each non-mucin protein was similarly co-transfected with HIV-1(NL4-3) DNA into HEK293T cells to assemble viral particles, which were then harvested and tested for their infectivity on Rev-A3R5-GFP cells. In contrast to the mucin and mucin-like proteins, which all elicited anti-HIV activity, the non-mucin adhesion molecules had minimal effects on the infectivity of released particles (Figure. 3.3B). Only one of the non-mucin proteins tested, E-selectin, was found to inhibit virion infectivity (Fig. 3.4). Taken together, these results demonstrate that the anti-HIV effect exerted by mucin and mucin-like proteins is not a common feature of transmembrane proteins expressed in virus-producing cells.

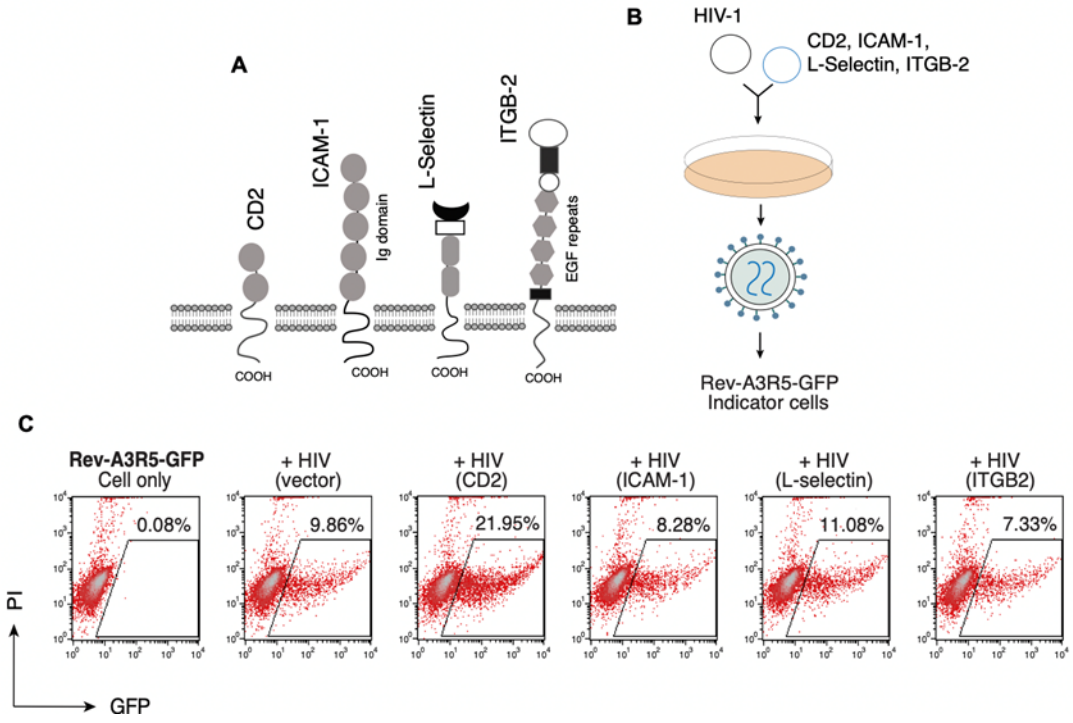

Figure 3.3 Not all transmembrane proteins can inhibit HIV-1 infectivity.
A) Schematic of HIV-1 virion production in the presence of non-mucin proteins. B) Schematic of non-mucin cell surface proteins used in this study. C) HEK293T cells were co-transfected with HIV(NL4-3) DNA (1 µg) plus an empty vector of a vector expressing each of CD2, ICAM-1, L-selectin, or ITGB2. Virions were harvested and normalized for p24. Viral infectivity was quantified by infecting Rev-A3R5-GFP indicator cells with equal p24 inputs of each virus. Representative results from 3 independent experiments are shown.

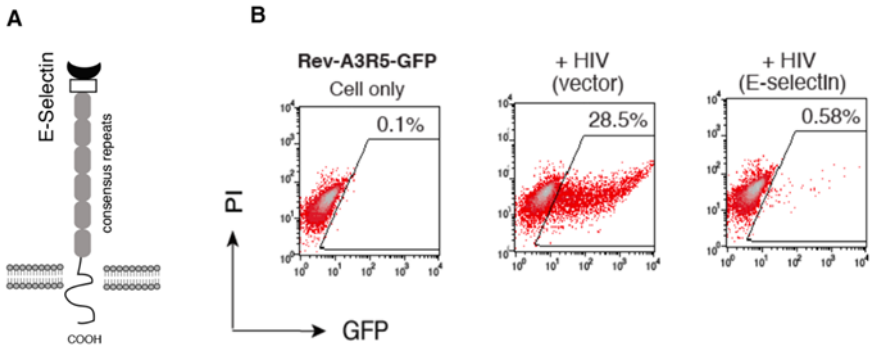

Figure 3.4 E-selectin inhibits HIV-1 infectivity.
A) Schematic of the E-selectin structure. B) HEK293T cells were co-transfected with HIV(NL4-3) DNA (1 µg) plus the vector expressing E-selectin or an empty vector (400 ng). Virions were harvested at 48 hours and normalized for p24, and viral infectivity was quantified by infecting Rev-A3R5-GFP indicator cells. Shown are the percentages of GFP+ cells at 72 hours post-infection.

Mucins and mucin-like proteins inhibit HIV-1 in a dose-dependent manner

We next performed a dose-response assay by assembling HIV-1 particles in the presence of increasing doses (0.5 ng – 400 ng) of each protein in our panel. Using equal p24 equivalents of each virus for infection, we observed a dosage-dependent inhibition of HIV-1 by all the proteins tested (Figs. 3.5-3.13). The 50% inhibition dosage for each protein was also calculated (Figure 3.5B). Among these proteins, CD34, the well-known stem cell maker, was highly potent against HIV- 1 (Fig. 3.5 and 3.8); while MUC1 showed the least potency, requiring high doses (200ng) for complete virion inactivated (Figs. 3.5 and 3.11). Based on the antiviral activity and shared structural features of these proteins, we named them the Surface-Hinged, Rigidly Extended Killer (SHREK) family of virion inactivators.

A

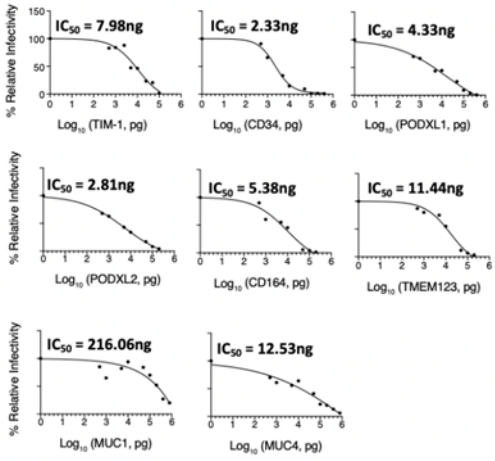

B

SHREK Proteins	M.W. (KD)	Half Maximal Inhibition Dosage (IC_{50}) (ng)
CD34	90 - 120	2.33
CD43	115 - 130	2.69
PSGL-1	120	2.70
PODXL2	120 - 160	2.81
PODXL1	160 - 170	4.33
CD164	80 - 100	5.38
TIM-1	70 - 80	7.98
TMEM123	110	11.44
MUC4	550 - 930	12.53
MUC1	> 200	216.06

Figure 3.5 Dose-dependent inhibition of HIV-1 infectivity by SHREK proteins.
A) HEK293T cells were co-transfected with HIV(NL4-3) DNA (1 μg) plus each individual SHREK-expressing expression vector (0.5 to 400 ng of DNA). Virions were harvested at 48 hours and normalized for p24, and viral infectivity was quantified by infecting Rev-A3R5-GFP indicator cells. The dose-dependent inhibition curve by each

individual SHREK protein was plotted from two independent experiments. B) The 50% inhibition dosage (IC50) for each SHREK protein was calculated.

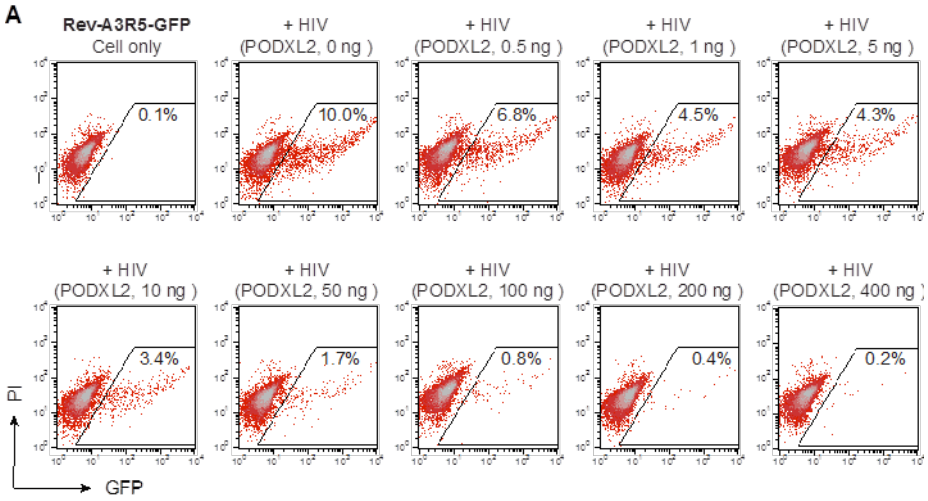

Figure 3.6 Dose-dependent inhibition of HIV-1 by PODXL2.
HIV-1 particles were produced in HEK293T cells by co-transfection of HIV-1(NL4-3) DNA (1 μg) plus an empty vector or the indicated doses of PODXL2. P24-normalized virions were used to infect Rev-A3R5-GFP cells. The percentage of GFP+ cells was quantified by flow cytometry at 72 hours post-infection.

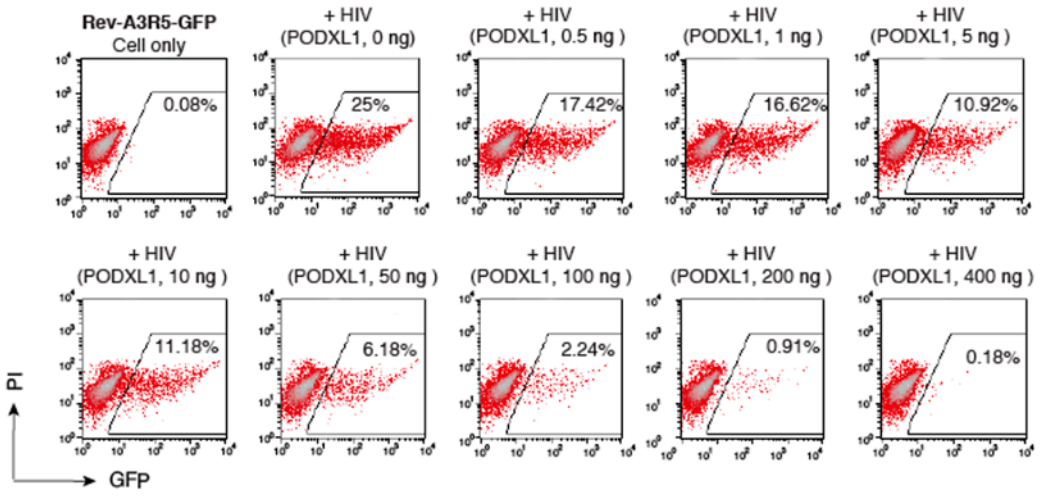

Figure 3.7 Dose-dependent inhibition of HIV-1 by PODXL1.
HIV-1 particles were produced in HEK293T cells by co-transfection of HIV-1(NL4-3) DNA (1 μg) plus an empty vector or the indicated doses of PODXL1. P24-normalized virions were used to infect Rev-A3R5-GFP cells. The percentage of GFP+ cells was quantified by flow cytometry at 72 hours post-infection.

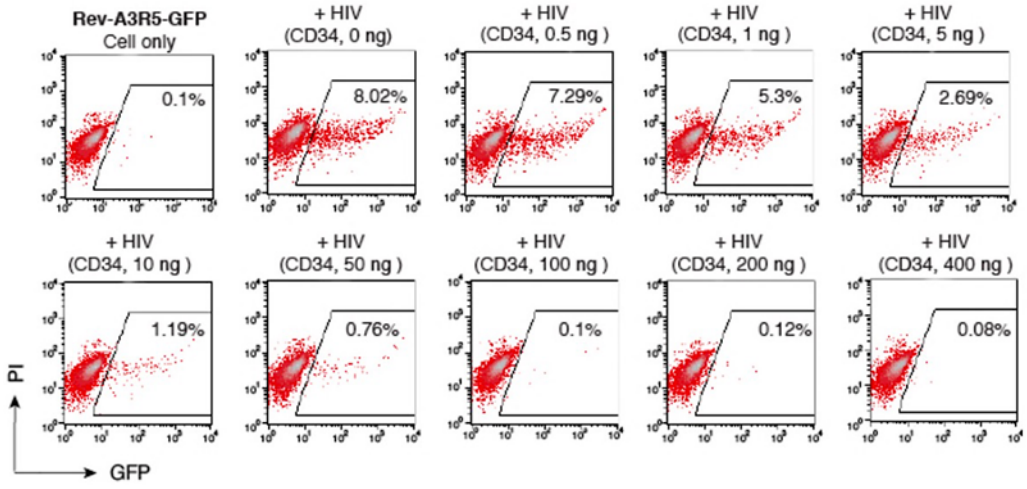

Figure 3.8 Dose-dependent inhibition of HIV-1 by CD34.
HIV-1 particles were produced in HEK293T cells by co-transfection of HIV-1(NL4-3) DNA (1 μg) plus an empty vector or the indicated doses of CD34. P24-normalized virions were used to infect Rev-A3R5-GFP cells. The percentage of GFP+ cells was quantified by flow cytometry at 72 hours post-infection.

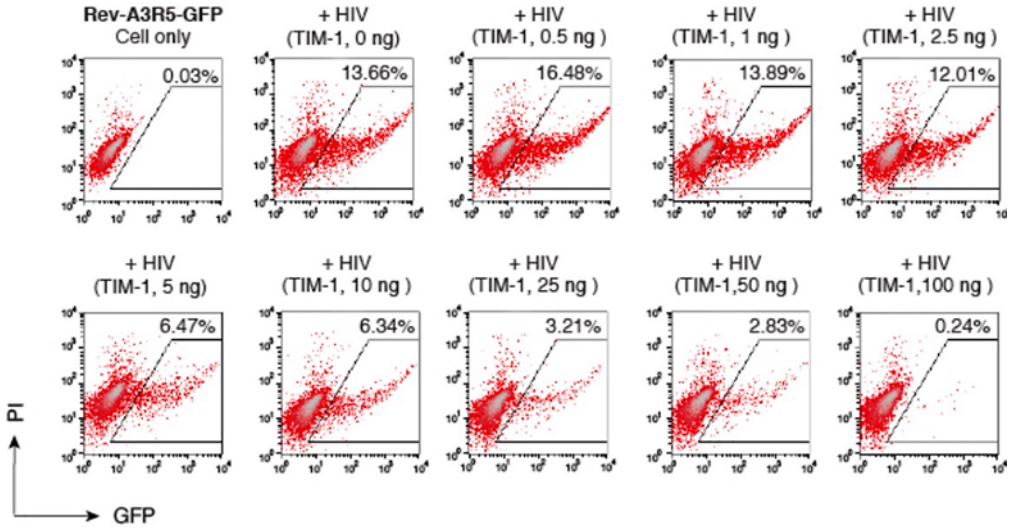

Figure 3.9 Dose-dependent inhibition of HIV-1 by TIM-1.
HIV-1 particles were produced in HEK293T cells by co-transfection of HIV-1(NL4-3) DNA (1 μg) plus an empty vector or the indicated doses of TIM-1. P24-normalized virions were used to infect Rev-A3R5-GFP cells. The percentage of GFP+ cells was quantified by flow cytometry at 72 hours post-infection.

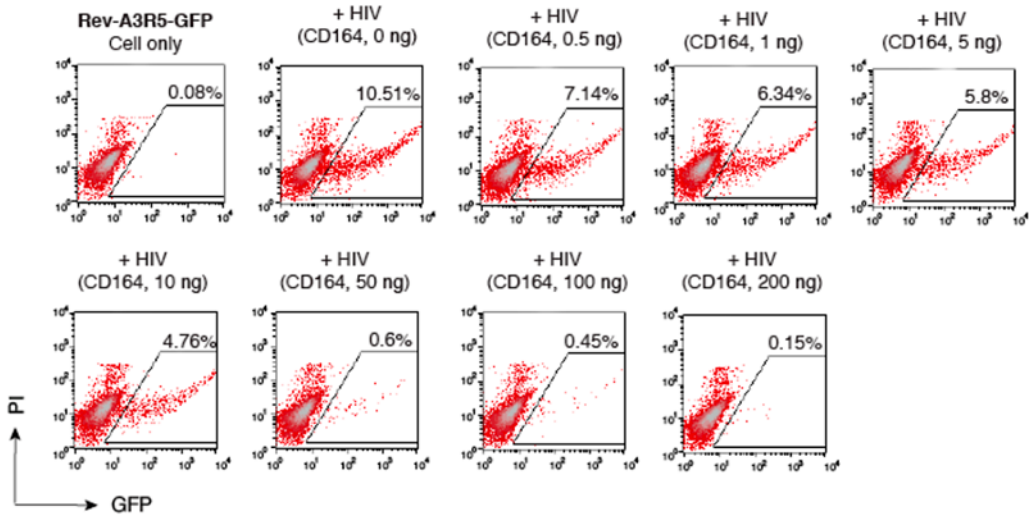

Figure 3.10 Dose-dependent inhibition of HIV-1 by CD164.
HIV-1 particles were produced in HEK293T cells by co-transfection of HIV-1(NL4-3) DNA (1 μg) plus an empty vector or the indicated doses of CD164. P24-normalized virions were used to infect Rev-A3R5-GFP cells. The percentage of GFP+ cells was quantified by flow cytometry at 72 hours post-infection.

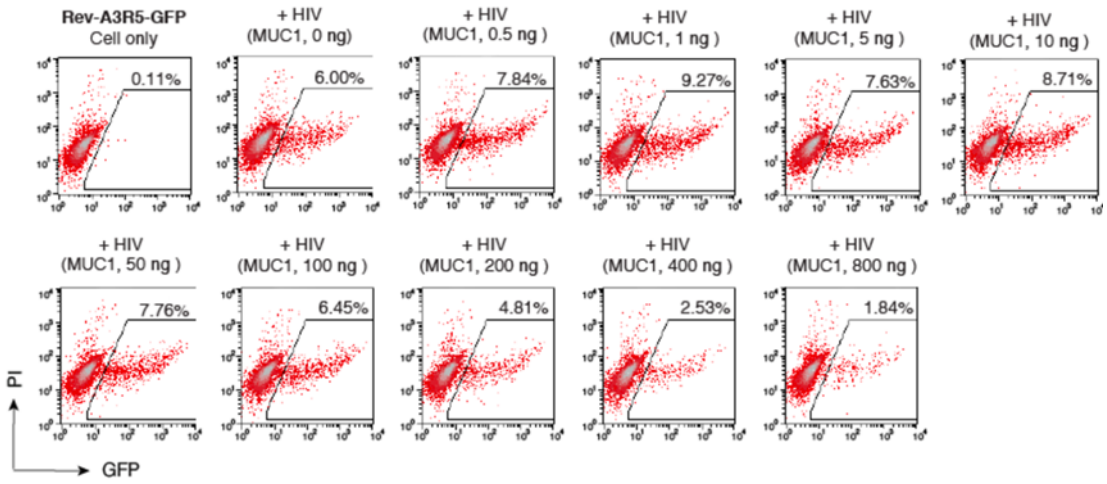

Figure 3.11 Dose-dependent inhibition of HIV-1 by MUC1.
HIV-1 particles were produced in HEK293T cells by co-transfection of HIV-1(NL4-3) DNA (1 µg) plus an empty vector or the indicated doses of MUC1. P24-normalized virions were used to infect Rev-A3R5-GFP cells. The percentage of GFP+ cells was quantified by flow cytometry at 72 hours post-infection.

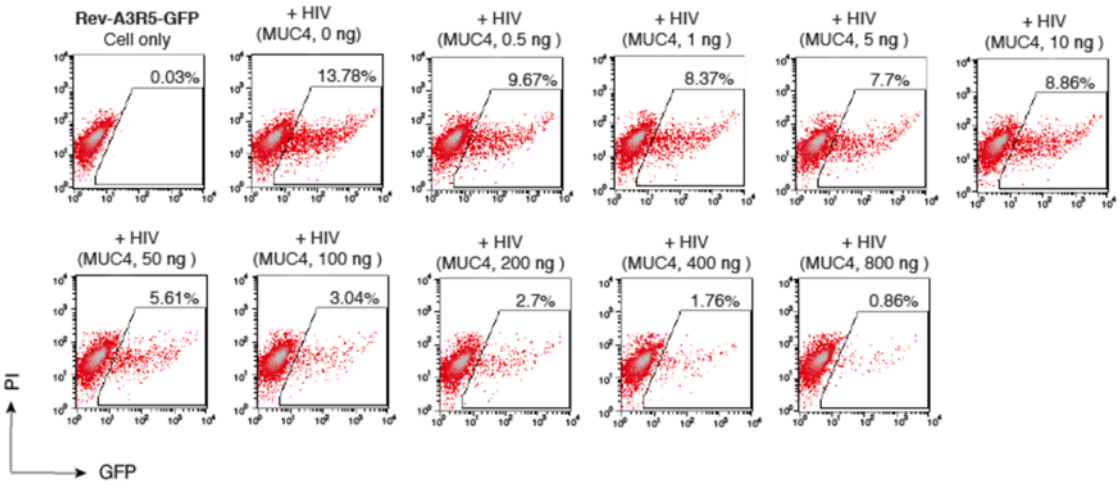

Figure 42 Dose-dependent inhibition of HIV-1 by MUC4.
HIV-1 particles were produced in HEK293T cells by co-transfection of HIV-1(NL4-3) DNA (1 µg) plus an empty vector or the indicated doses of MUC4. P24-normalized virions were used to infect Rev-A3R5-GFP cells. The percentage of GFP+ cells was quantified by flow cytometry at 72 hours post-infection.

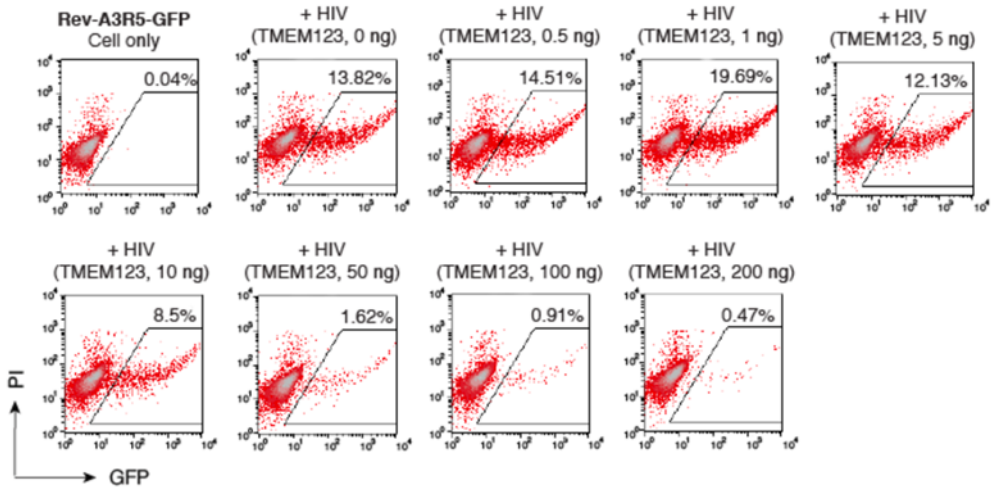

Figure 3.13 Dose-dependent inhibition of HIV-1 by TMEM123.
HIV-1 particles were produced in HEK293T cells by co-transfection of HIV-1(NL4-3) DNA (1 µg) plus an empty vector or the indicated doses of TMEM123. P24-normalized virions were used to infect Rev-A3R5-GFP cells. The percentage of GFP+ cells was quantified by flow cytometry at 72 hours post-infection.

The effects of SHREK proteins on virion release

We previously showed that the expression of the mucin-like protein PSGL-1 had minimal effects on HIV-1 particle release when expressed in virus-producing cells (6). To determine the effects of SHREK proteins on virion particle production, we co-transfected HEK293T cells with HIV-1 (NL4-3) proviral DNA (1 µg) and varying inputs (0.5 ng- 400 ng) of each of the SHREK-protein-expressing vectors (Fig. 3.14). Viral production in the presence of each SHREK protein was evaluated by quantifying p24 levels in the transfection supernatant. At doses below 100 ng, all the proteins except TIM-1 showed minor effects on virion release (Fig. 3.14), while CD34, PODXL1, and CD164 (66) inhibited HIV-1 virion release at higher dosages (100 ng and above). TIM-1 potently inhibited virion release in a dose-dependent fashion, consistent with previous reports (37, 38). While the proteins did not have a substantial effect on virion release, all

the tested proteins, except for MUC1, showed effective blockage of virion infectivity at doses below 50 ng (Figs. 3.5-3.13). These results demonstrate that like PSGL-1 (6), abolishing the infectivity of virions rather than affecting their release is a predominant mechanism enacted by the SHREK proteins.

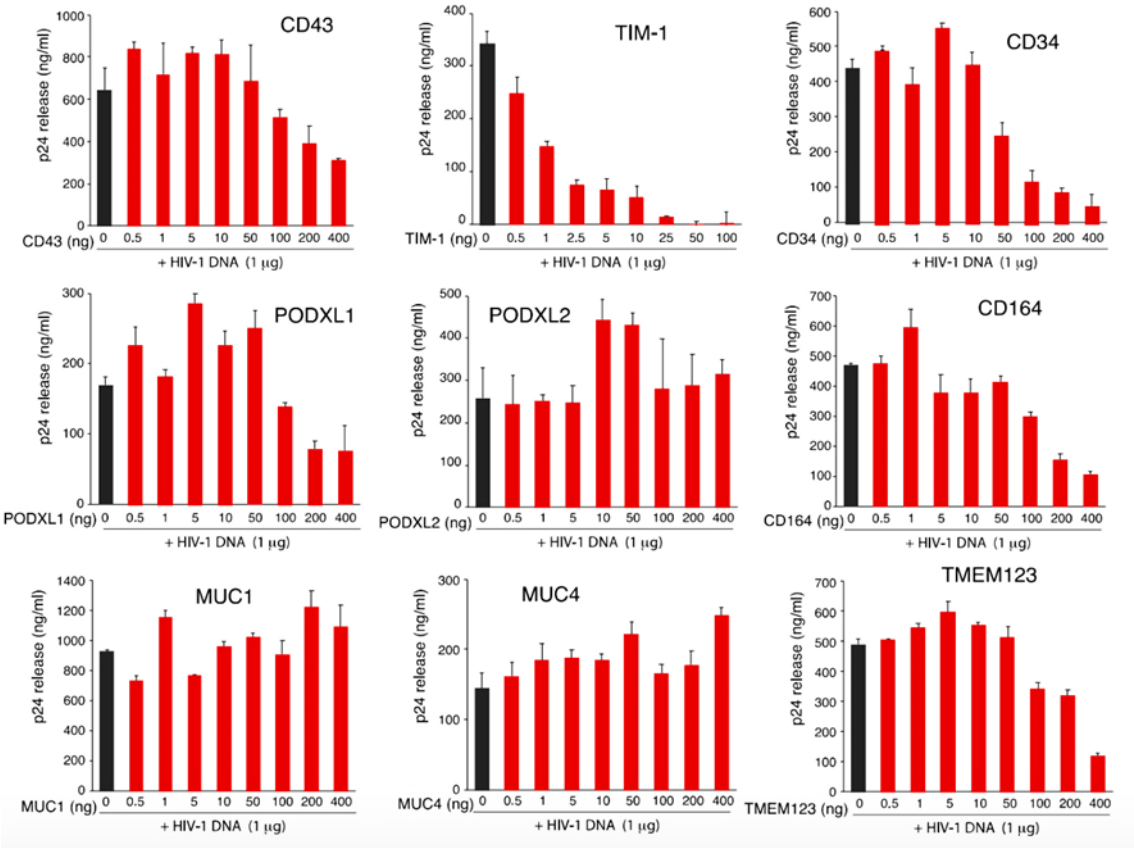

Figure 3.14 Effects of SHREK proteins on HIV-1 viral release.
HEK293T cells were co-transfected with HIV(NL4-3) DNA (1 μg) plus each individual SHREK expression vector (0.5 to 400 ng of DNA). Virion release was quantified at 48 h post co-transfection by HIV-1 p24 ELISA. Data are represented as mean ± SD from ELISA triplicate. Experiments on the effects of TIM-1 were independently repeated 3 times, and experiments on effects of other SHREKs on release were independently repeated twice.

Virion incorporation of SHREK proteins and their effect on HIV-1 Env incorporation

Previous work on PSGL-1-mediated HIV-1 restriction supports a model in which PSGL-1 blocks the virus attachment step; PSGL-1 is incorporated into assembling virion particles in producer cells, which sterically hinders progeny virion binding to target cells (6, 7). Virion incorporation of PSGL-1 was also shown to reduce HIV-1 Env protein incorporation into the virus particle (6, 7). Thus, we asked whether SHREK proteins are similarly incorporated into HIV-1 during particle assembly. We employed a previously described immunomagnetic particle pull-down assay (84), in which SHREK antibody-coupled beads were used to pull down virion particles bearing SHREK proteins on their surface (Fig. 3.15A). The quantities of particles pulled down by each antibody were determined by p24 ELISA. As a positive control, we also used an anti-PSGL-1 antibody to pull down particles derived from PSGL-1-expressing cells. The PSGL-1 antibody specifically pulled down virion particles produced from cells expressing PSGL-1 but not from cells co-transfected with an empty vector, confirming recent findings that PSGL-1 is incorporated into HIV-1 particles (6, 7). We thus proceeded with this magnetic capture assay to detect virion incorporation of the SHREK proteins. The anti- CD43, -CD164, -PODXL1, -PODXL2, and -CD34 antibodies selectively captured virions produced from cells expressing these SHREK proteins (Fig. 3.15A, B), demonstrating their incorporation into HIV-1 particles. However, the commercially available anti-TMEM123, -MUC1, and -MUC4 antibodies were ineffective at pulling down virus particles.

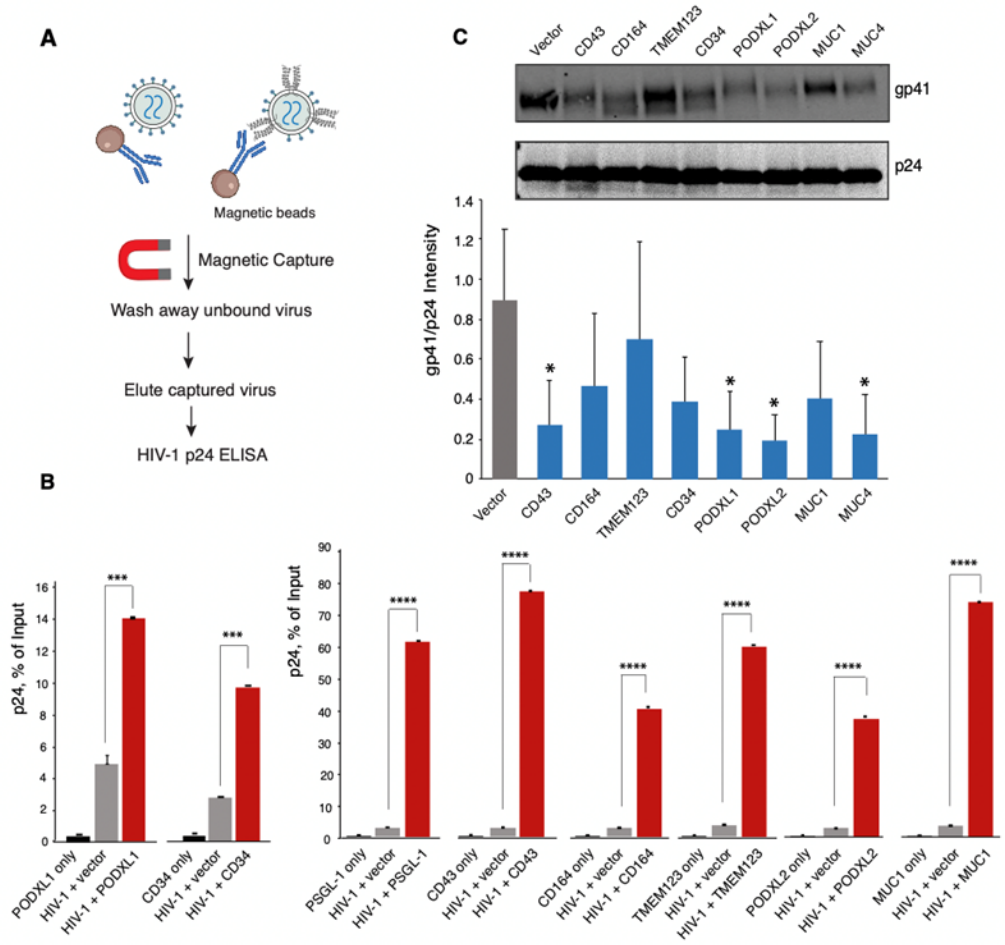

Figure 3.15 Virion incorporation of SHREK proteins and its effects on HIV-1 Env incorporation.
A) Schematic of the immune-magnetic capture assay used to detect SHREK proteins on HIV-1 particles. B) HEK293T cells were cotransfected with pHIV-1(NL4-3) DNA (1 µg) plus each individual SHREK protein expression vector or empty vector (400 ng of DNA). As a control, cells were also transfected with only a SHREK-expressing vector (400 ng). Empty vector was used to maintain an equal DNA concentration. For MUC1 and TMEM123, vectors expressing hemagglutinin tagged TMEM123 or MUC1 were used. Supernatants were harvested at 48 h, normalized for p24, and incubated with magnetic beads coated with antibodies for each individual SHREK or hemagglutinin. Captured particles were washed, eluted, and quantified for the p24 levels with HIV-1 p24 ELISA. Data are presented as the percentage of input particles captured by the beads. The experiment was independently repeated 3 times, and the means ± SD from ELISA triplicates are shown. C) Effect of SHREK proteins on HIV-1 Env incorporation. HEK293T cells were co-transfected with HIV(NL4-3) DNA plus each SHREK protein expression vector or an empty vector. Particles were harvested at 48 h and purified through a sucrose gradient. Virions were lysed and analyzed with Western blot using antibodies against HIV-1 gp41 and p24. Representative blots from 3 independent experiment repeats are shown. The band intensities were quantified from the three blots and normalized for p24. p-values were calculated using the two-tailed T-test. Significance values are indicated using asterisks as follows; * = $p < 0.05$, *** = $p < 0.001$, **** = $p < 0.0001$.

Therefore, we replaced TMEM123 and MUC1 with hemagglutinin-tagged TMEM123 or MUC1 to assemble HIV-1 virions and used anti-hemagglutinin magnetic beads to pull down these particles. Using this method, we observed that TMEM123 and MUC1 were also incorporated into HIV-1 particles (Figure 3.15A, B). Next, we sought to determine whether virion incorporation of SHREK proteins affected HIV-1 Env incorporation. Virion particles were assembled in the presence or absence of each SHREK protein, purified through a sucrose gradient, and then analyzed by western blot for HIV-1 Env gp41 and p24. As shown in Figure 3.15C, the tested SHREK proteins, except TMEM123, had varying levels of inhibitory effects on HIV-1 Env incorporation.

SHREK proteins inhibit virus particle attachment to target cells

We and others have reported that PSGL-1 sterically hinders HIV-1 particle attachment to target cells (6, 7). To determine whether the SHREK proteins in this study also inhibited virion binding, we performed an attachment assay using virus particles derived from cells expressing each SHREK protein individually (Fig. 3.16). HeLaJC53 cells were incubated with HIV-1 particles (assembled in the presence of each SHREK protein) for 2 h at 4 °C. Virus attachment was then detected by western blot analysis as the amount of cell-associated p24 after extensive washing. As shown in Figure 3.16A, particles produced from the PSGL-1-expressing cells were highly impaired in their ability to attach to target cells. A similar strong impairment was observed for virions produced from the CD34- and the PODXL2-expressing cells. The other proteins (CD43, CD164, PODXL1, MUC1, and MUC4) also inhibited virion attachment with various degrees (Fig. 3.16). Interestingly, TMEM123 slightly enhanced HIV-1 virion attachment to target

cells (Fig. 3.16), although it inhibited viral infection (Fig. 3.3 and 3.14). We speculated that TMEM123 may be interacting with surface proteins on the target cells, resulting in non-productive binding of virus particles to target cells. When the attachment assay was done in the presence of an anti-TMEM123 antibody to block possible TMEM123 interaction with cell surface proteins, virion attachment was decreased (Figure 3.16B).

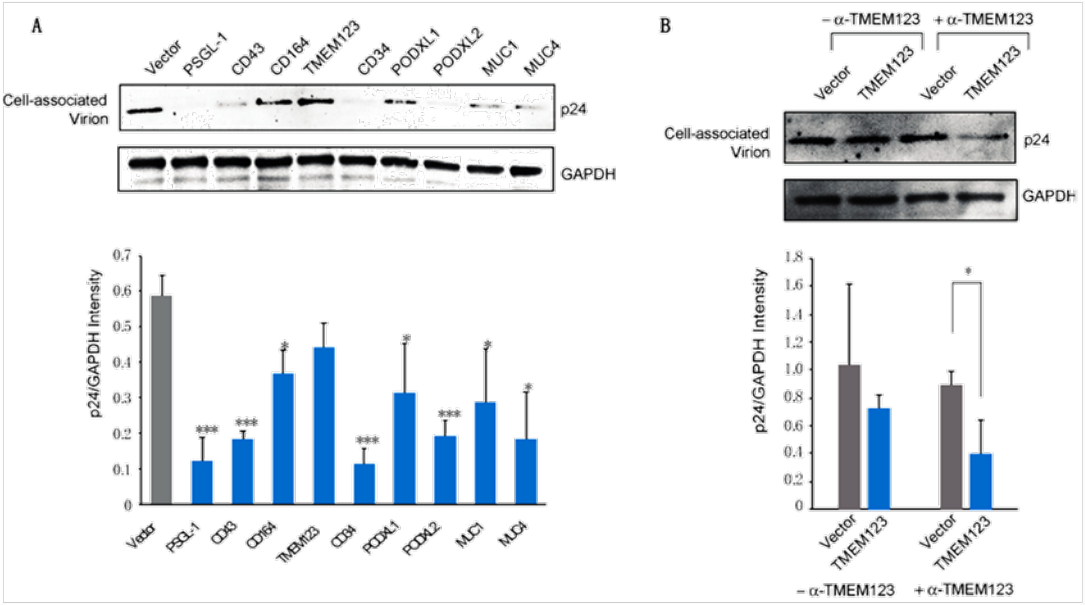

Figure 3.16 SHREK proteins block HIV-1 virion attachment to target cells.
A) Viral particles were produced by co-transfection of HEK293T cells with pHIV-1(NL4-3) DNA (1 µg) and each SHREK protein expression vector individually, or an empty vector (500 ng). HIV-1 p24-normalized viral particles were then assayed for attachment to target HeLaJC.53 cells by Western blot for cell-bound p24. B) Virions produced in the presence of the TMEM123 expression vector, or the empty vector were assayed for attachment in the presence or absence of an anti-TMEM123 antibody. Representative blots from 3 experiment repeats are shown. The band intensities were quantified (for A and B) from the three blots and normalized with GAPDH. p-values were calculated using the two-tailed T-test. Significance values are indicated using asterisks as follows; * = $p < 0.05$, *** = $p < 0.001$.

SHREK proteins inhibit infection by influenza A and SARS-CoV-2 pseudoparticles

PSGL-1 has been reported to be a broad-spectrum antiviral host factor (6). To determine whether SHREK proteins also have broad-spectrum capacities, we examined their effect on influenza A virus and SARS-CoV-2 virus-like particles (VLPs). For assembling influenza A virus, eight vectors encoding the influenza A/WSN/33 (H1N1) genome segments and a GFP-reporter vector were co-transfected with the individual SHREK proteins into HEK293T cells (Fig. 3.17A). Virus particles harvested from the co-transfection were used to infect MDCK cells. We found that the presence of each of the SHREK proteins in virus-producer cells inhibited infection by the released virions in the target cells to varying degrees (Figure 3.17B). MUC1, PODXL1, and MUC4 elicited the strongest inhibition of influenza A virus, although MUC1 and MUC4 had a weaker effect on HIV-1. Whereas CD164 and TMEM123 were the least effective at inhibiting influenza A.

Next, we inspected the potential effects of SHREK proteins on SARS-CoV-2, using a recently developed SARS-CoV-2 VLP system comprising hybrid alphavirus-SARS-CoV-2 particles (Ha-CoV-2) (83). Ha-CoV-2 is a non-replicating SARS-CoV-2 virus-like particle, composed only of the SARS-CoV-2 structural proteins S, M, N, and E, and an alphavirus-based vector expressing luciferase (83). Recently, a study from our lab showed that PSGL-1 blocks SARS-CoV-2 S protein virion incorporation, virus attachment, and Ha-CoV-2 infection of target cells (91). Thus, we assembled Ha-CoV-2 virus-like particles in the presence of each SHREK protein in HEK293T cells. The harvested VLPs were then used to infect target HEK293T ACE2/TMPRSS2 cells.

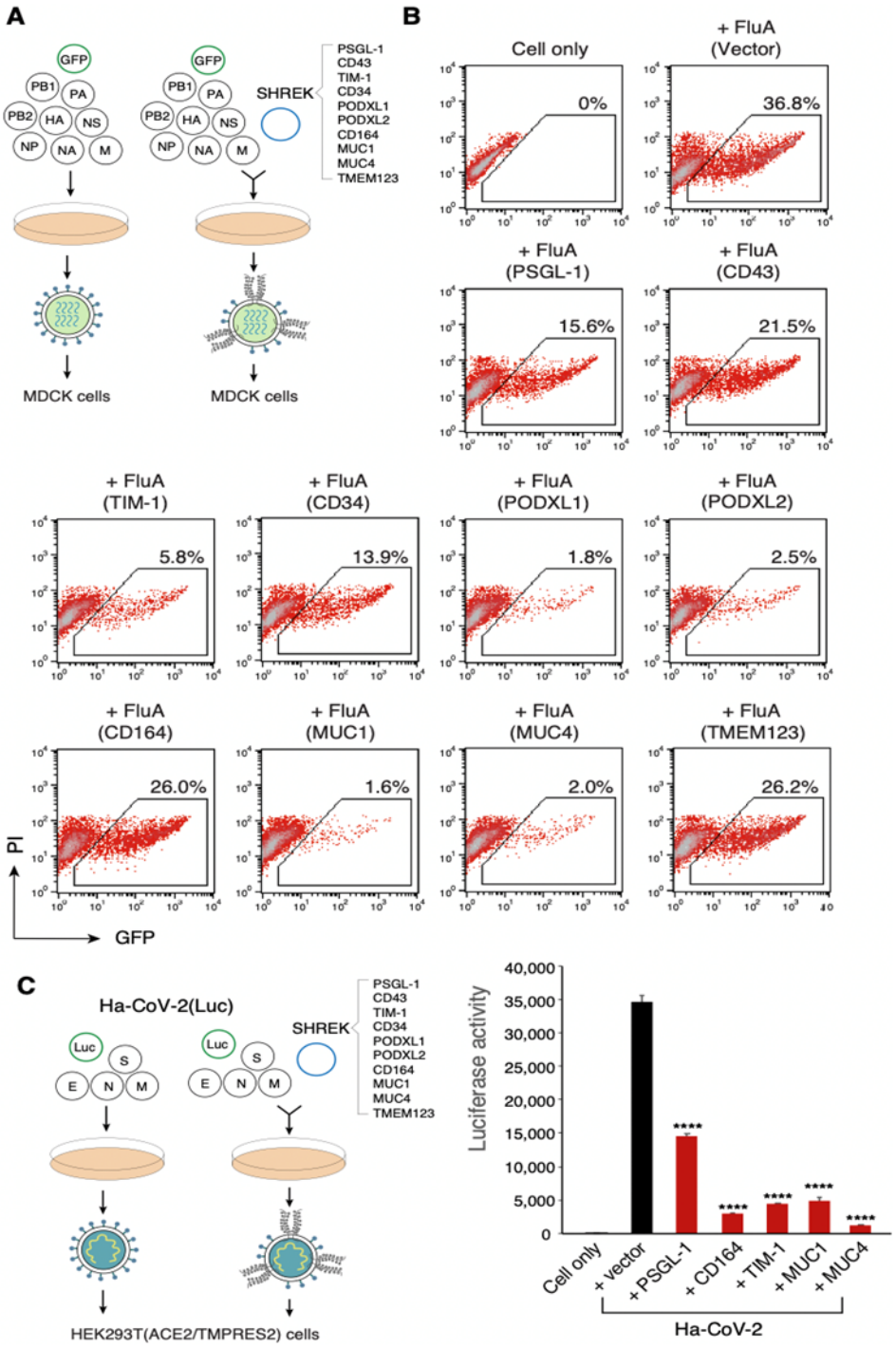

Figure 3.17 SHREK proteins are broad-spectrum host antiviral factors.
A) SHREK proteins inactivate influenza A virion infectivity. Influenza A-GFP reporter viruses were assembled by cotransfection of HEK293T cells with eight vectors expressing each of the segments of influenza A/WSN/33 (H1N1) (0.25 μg each), pHW-NA-GFP (ΔAT6) (1.5 μg), and each individual SHREK-expressing vector or an empty vector (0.5 μg). Viral particles were harvested at 48 h and used to infect target MDCK cells. This experiment was repeated 3 times. B) Representative results from A), showing GFP+ cells being quantified by flow cytometry following infection

for 24 h. C) SHREK proteins inhibit Ha-CoV-2 infection. Ha-CoV-2(Luc) particles were assembled in HEK293T cells by cotransfection of SARS-CoV-2 S-, M-, N- and E- expressing vectors (0.3 μg each), Ha-CoV-2(Luc) vector (1.2 μg), and each individual SHREK-expressing vector or an empty vector (1.6 μg). Virions were harvested and used to infect HEK293T(ACE2/TMPRSS2) target cells. Luciferase activity was quantified at 18 h post infection. The experiment was repeated four times. Data are presented as means ± SD from experiment triplicate. p-values were calculated using the two-tailed T-test. Significance values are indicated using asterisks as follows; **** = $p < 0.0001$.

We found that besides PSGL-1, CD164, TIM-1, MUC1, and MUC4 also inhibited Ha-CoV-2 virus infection (Fig. 3.17C), with MUC4 exhibiting the strongest inhibition. However, we detect no inhibition of Ha-CoV-2 by CD43, CD34, PODXL1, PODXL2, and TMEM123 (Fig. 3.18), although they were effective inhibitors of HIV-1 (Figs. 3.5-3.13). Collectively, these observations indicate that SHREK proteins possess broad-spectrum capabilities and can block the infectivity of multiple viruses. Nonetheless, as shown in our infectivity assays, the antiviral potency of each SHREK can vary depending on the targeted virus. These differences could have arisen from possible viral antagonisms, cellular localization of SHREK proteins, sites of viral budding or other unknown factors.

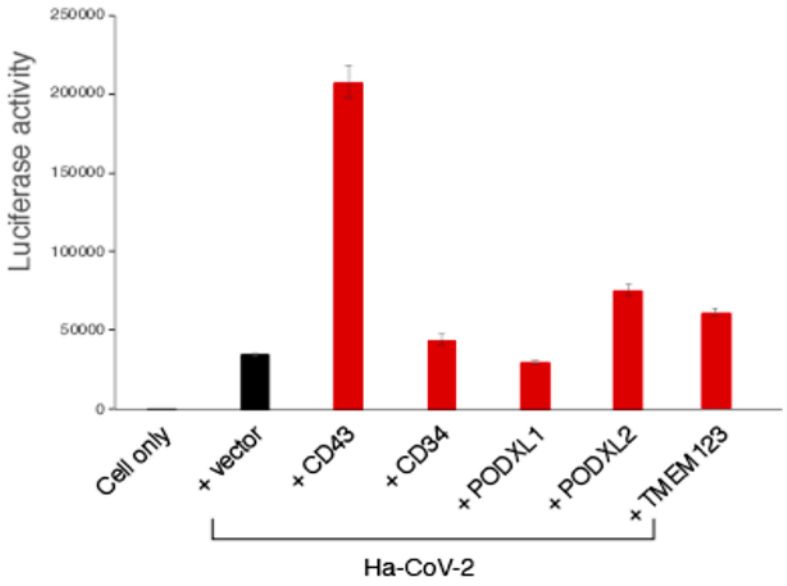

Figure 3.18 Lack of inhibition of Ha-CoV-2 virion infectivity by CD43, CD43, PODXL1, PODXL2, and TMEM123.
Ha-CoV-2(Luc) particles were assembled in HEK293T cells by cotransfection of SARS-CoV-2 S-, M-, N- and E-expressing vectors (0.3 µg each), Ha-CoV-2(Luc) vector (1.2 µg), and each individual SHREK-expressing vector (CD43, CD34, PODXL1, PODXL2, or TMEM123) or an empty vector (1.6 µg). Virions were harvested and used to infect HEK293T (ACE2/TMPRSS2) target cells. Luciferase activity was quantified at 18 hours post infection. Data are presented as means ± SD from experiment triplicate.

Discussion

Using HIV-1 as a model, we identified a group of host proteins, which we have named SHREK, possessing the ability to broadly inactivate virion infectivity (Fig. 3.1). These proteins share structural characteristics with PSGL-1 and are expressed in a wide variety of cells and tissues. We observed a dosage-dependent inhibition of HIV-1 virion infectivity by SHREKs using a range of doses of each protein (from 0.5 ng to 400 ng of SHREK expression vector) (Figs. 3.5-3.13).

Our primary focus in the current study was on proteins with mucin and mucin-like domains; however, it is possible that the SHREK family may encompass other proteins

with different molecular structures, such as E-selectin (Fig. 3.4). Several proteins in this report have been previously implicated in HIV-1 infection; PSGL-1 and CD43 were shown by us and others to inactivate HIV-1 infectivity (5-7, 92); CD164 was identified in a genome-wide screening analysis as a potential anti-HIV-1 restriction factor (66); TIM-1 has been shown to inhibit particle release by retaining virions at the plasma membrane (37, 38); and MUC1 and MUC4 purified from human breast milk were reported to have a neutralizing effect against HIV-1 (79-82). So far, it has been demonstrated that SHREK proteins may exert their antiviral activities through various mechanisms including blocking virion release (e.g., inhibition of HIV-1 release by TIM-1 (37, 38); inhibition of virion incorporation of viral surface glycoproteins (e.g., PSGL-1 inhibiting HIV-1 gp160 incorporation (6); or virion incorporation of a SHREK that sterically hinders progeny virus attachment to target cells (e.g., PSGL-1 inhibition of HIV-1 virus attachment to target cells (6, 7).

The physiological relevance of SHREK family members, PSGL-1 and CD43, in restricting HIV-1 virion infectivity has been previously demonstrated (6, 7). PSGL-1 knockdown from human CD4 T cells showed that even slight reductions of endogenous PSGL-1 in primary CD4 T cells can lead to an enhancement of virion infectivity (6, 7). Murakami el. al showed that knocking out CD43, from CD4 T cells also enhances HIV-1 infectivity (7). Nevertheless, the effects of depleting other SHREK family members on viral infectivity are yet to be determined.

Although several SHREK proteins, such as PSGL-1 (5), CD43 (93), CD164 (66, 94), TMEM123 (95), MUC1 (96), and MUC4 (97), are reported to be inducible by

interferons, we do not define the SHREK proteins as typical restriction factors; further work is needed to classify them as such. Rather, we postulate that they may act as natural barriers of innate immunity against infection, analogous to the skin (98) or the mucous membranes (99, 100). The SHREK family likely includes a wide variety of proteins that could either be interferon-inducible or constitutively expressed in specific cell types (e.g., CD34) to protect critical cell populations against invading pathogens.

Curiously, some of the SHREK proteins identified in our study (CD34, PODXL1, PODXL2, and CD164) are abundantly expressed on the surface of stem and progenitor cells (40, 57). CD34, the well-known stem and progenitor cell marker (43), was potent against HIV-1 in our dose-dependent inhibition assay (Figs. 3.5 and 3.8). It is therefore possible these SHREKs serve as a type of natural defense that limits retroviral replication in critical cell populations, such as progenitor cells. Several studies have reported that HIV-1 can enter and express viral genes in CD34+ hematopoietic progenitor cells, albeit with low levels of replication (56, 101). Viral replication was shown to become more admissible in HPCs with GM-CSF and TNF-α treatment, which induces myeloid differentiation. This cytokine-induced viral permissiveness is concurrent with cytokine-mediated CD34 downmodulation from the cell surface (101).

Given the antiviral effects of the SHREKs, it can be expected that viruses have evolved mechanisms to counteract these proteins. Previous studies have shown that viruses such as HIV-1 can antagonize the blockade imposed by some of the SHREK proteins. For example, HIV-1 uses the accessory proteins Vpu and Nef to degrade and downregulate PSGL-1 on CD4 T cells (5, 6). Other studies also reported that cell surface

CD43 is reduced in the presence of HIV-1 infection (102), and upon CD43 and Vpu ectopic co-transfection (6). It remains to be determined whether there are any similar mechanisms, by which different viruses could antagonize individual SHREK proteins.

Several SHREK proteins (PSGL-1, CD164, TIM-1, MUC1, and MUC4) inhibited HaCoV-2 infection. MUC4 displayed the strongest inhibition among these SHREKs in our VLP infection assay. Reportedly, cell-free mucins purified from human breast milk possess neutralizing effects against HIV-1 (81). A recent study has also reported that MUC4 expression plays a protective role in female mice in SARS-CoV infection (103). In chikungunya virus (CHIKV) infection, loss of MUC4 was shown to result in augmented disease during early infection, indicating that MUC4 may a play a broad role in viral infection and pathogenesis (103).

We detected no inhibition of Ha-CoV-2 by CD43, CD34, PODXL1, PODXL2, and TMEM123 (Fig. 3.18), although these proteins were efficient inhibitors of HIV-1 (Fig.3.5). The observed variation in the viruses targeted by SHREK proteins could be stemming from differences in sites of viral assembly and budding. While the SARS-CoV-2 budding site is mainly at the membranes of the ER-Golgi compartments (104), HIV-1 buds from the plasma membrane (105). Because of these differences, distinct cellular SHREK proteins may be incorporated into different viruses.

In summary, we have demonstrated that members of the SHREK protein family can inhibit the infectivity of a broad range of enveloped viruses. The identification of these proteins as antiviral factors may be useful for developing potential new antiviral therapeutics that induce or modulate SHREK activities in virus-infected cells.

References

1. Hattrup CL, Gendler SJ. Structure and function of the cell surface (tethered) mucins. Annu Rev Physiol. 2008;70:431-57.
2. Sako D, Chang XJ, Barone KM, Vachino G, White HM, Shaw G, et al. Expression cloning of a functional glycoprotein ligand for P-selectin. Cell. 1993;75(6):1179-86.
3. Goetz DJ, Greif DM, Ding H, Camphausen RT, Howes S, Comess KM, et al. Isolated P-selectin glycoprotein ligand-1 dynamic adhesion to P- and E-selectin. J Cell Biol. 1997;137(2):509-19.
4. Guyer DA, Moore KL, Lynam EB, Schammel CM, Rogelj S, McEver RP, et al. P-selectin glycoprotein ligand-1 (PSGL-1) is a ligand for L-selectin in neutrophil aggregation. Blood. 1996;88(7):2415-21.
5. Liu Y, Fu Y, Wang Q, Li M, Zhou Z, Dabbagh D, et al. Proteomic profiling of HIV-1 infection of human CD4(+) T cells identifies PSGL-1 as an HIV restriction factor. Nat Microbiol. 2019;4(5):813-25.
6. Fu Y, He S, Waheed AA, Dabbagh D, Zhou Z, Trinite B, et al. PSGL-1 restricts HIV-1 infectivity by blocking virus particle attachment to target cells. Proc Natl Acad Sci U S A. 2020;117(17):9537-45.
7. Murakami T, Carmona N, Ono A. Virion-incorporated PSGL-1 and CD43 inhibit both cell-free infection and transinfection of HIV-1 by preventing virus-cell binding. Proc Natl Acad Sci U S A. 2020;117(14):8055-63.
8. Li F, Erickson HP, James JA, Moore KL, Cummings RD, McEver RP. Visualization of P-selectin glycoprotein ligand-1 as a highly extended molecule and mapping of protein epitopes for monoclonal antibodies. J Biol Chem. 1996;271(11):6342-8.
9. McEver RP, Moore KL, Cummings RD. Leukocyte trafficking mediated by selectin-carbohydrate interactions. J Biol Chem. 1995;270(19):11025-8.
10. Patel KD, Nollert MU, McEver RP. P-selectin must extend a sufficient length from the plasma membrane to mediate rolling of neutrophils. J Cell Biol. 1995;131(6 Pt 2):1893-902.
11. Li F, Wilkins PP, Crawley S, Weinstein J, Cummings RD, McEver RP. Post-translational modifications of recombinant P-selectin glycoprotein ligand-1 required for binding to P- and E-selectin. J Biol Chem. 1996;271(6):3255-64.
12. Shelley CS, Remold-O'Donnell E, Rosen FS, Whitehead AS. Structure of the human sialophorin (CD43) gene. Identification of features atypical of genes encoding integral membrane proteins. Biochem J. 1990;270(3):569-76.
13. Pallant A, Eskenazi A, Mattei MG, Fournier RE, Carlsson SR, Fukuda M, et al. Characterization of cDNAs encoding human leukosialin and localization of the leukosialin gene to chromosome 16. Proc Natl Acad Sci U S A. 1989;86(4):1328-32.
14. Naeim F, Nagesh Rao P, Song SX, Phan RT. Chapter 2 - Principles of Immunophenotyping. In: Naeim F, Nagesh Rao P, Song SX, Phan RT, editors. Atlas of Hematopathology (Second Edition): Academic Press; 2018. p. 29-56.

15. Cyster JG, Shotton DM, Williams AF. The dimensions of the T lymphocyte glycoprotein leukosialin and identification of linear protein epitopes that can be modified by glycosylation. EMBO J. 1991;10(4):893-902.
16. Maemura K, Fukuda M. Poly-N-acetyllactosaminyl O-glycans attached to leukosialin. The presence of sialyl Le(x) structures in O-glycans. J Biol Chem. 1992;267(34):24379-86.
17. Piller F, Piller V, Fox RI, Fukuda M. Human T-lymphocyte activation is associated with changes in O-glycan biosynthesis. J Biol Chem. 1988;263(29):15146-50.
18. Velázquez F, Grodecki-Pena A, Knapp A, Salvador AM, Nevers T, Croce K, et al. CD43 Functions as an E-Selectin Ligand for Th17 Cells In Vitro and Is Required for Rolling on the Vascular Endothelium and Th17 Cell Recruitment during Inflammation In Vivo. J Immunol. 2016;196(3):1305-16.
19. Matsumoto M, Atarashi K, Umemoto E, Furukawa Y, Shigeta A, Miyasaka M, et al. CD43 functions as a ligand for E-Selectin on activated T cells. J Immunol. 2005;175(12):8042-50.
20. Manjunath N, Correa M, Ardman M, Ardman B. Negative regulation of T-cell adhesion and activation by CD43. Nature. 1995;377(6549):535-8.
21. Allenspach EJ, Cullinan P, Tong J, Tang Q, Tesciuba AG, Cannon JL, et al. ERM-dependent movement of CD43 defines a novel protein complex distal to the immunological synapse. Immunity. 2001;15(5):739-50.
22. Delon J, Kaibuchi K, Germain RN. Exclusion of CD43 from the immunological synapse is mediated by phosphorylation-regulated relocation of the cytoskeletal adaptor moesin. Immunity. 2001;15(5):691-701.
23. Ardman B, Sikorski MA, Staunton DE. CD43 interferes with T-lymphocyte adhesion. Proc Natl Acad Sci U S A. 1992;89(11):5001-5.
24. Sperling AI, Green JM, Mosley RL, Smith PL, DiPaolo RJ, Klein JR, et al. CD43 is a murine T cell costimulatory receptor that functions independently of CD28. J Exp Med. 1995;182(1):139-46.
25. Barat C, Tremblay MJ. Engagement of CD43 enhances human immunodeficiency virus type 1 transcriptional activity and virus production that is induced upon TCR/CD3 stimulation. J Biol Chem. 2002;277(32):28714-24.
26. Llewellyn GN, Grover JR, Olety B, Ono A. HIV-1 Gag associates with specific uropod-directed microdomains in a manner dependent on its MA highly basic region. J Virol. 2013;87(11):6441-54.
27. Grover JR, Veatch SL, Ono A. Basic motifs target PSGL-1, CD43, and CD44 to plasma membrane sites where HIV-1 assembles. J Virol. 2015;89(1):454-67.
28. Kuchroo VK, Umetsu DT, DeKruyff RH, Freeman GJ. The TIM gene family: emerging roles in immunity and disease. Nat Rev Immunol. 2003;3(6):454-62.
29. Kuchroo VK, Dardalhon V, Xiao S, Anderson AC. New roles for TIM family members in immune regulation. Nat Rev Immunol. 2008;8(8):577-80.
30. Umetsu SE, Lee WL, McIntire JJ, Downey L, Sanjanwala B, Akbari O, et al. TIM-1 induces T cell activation and inhibits the development of peripheral tolerance. Nat Immunol. 2005;6(5):447-54.

31. Kaplan G, Totsuka A, Thompson P, Akatsuka T, Moritsugu Y, Feinstone SM. Identification of a surface glycoprotein on African green monkey kidney cells as a receptor for hepatitis A virus. EMBO J. 1996;15(16):4282-96.
32. McIntire JJ, Umetsu SE, Macaubas C, Hoyte EG, Cinnioglu C, Cavalli-Sforza LL, et al. Immunology: hepatitis A virus link to atopic disease. Nature. 2003;425(6958):576.
33. Kondratowicz AS, Lennemann NJ, Sinn PL, Davey RA, Hunt CL, Moller-Tank S, et al. T-cell immunoglobulin and mucin domain 1 (TIM-1) is a receptor for Zaire Ebolavirus and Lake Victoria Marburgvirus. Proc Natl Acad Sci U S A. 2011;108(20):8426-31.
34. Meertens L, Carnec X, Lecoin MP, Ramdasi R, Guivel-Benhassine F, Lew E, et al. The TIM and TAM families of phosphatidylserine receptors mediate dengue virus entry. Cell Host Microbe. 2012;12(4):544-57.
35. Moller-Tank S, Kondratowicz AS, Davey RA, Rennert PD, Maury W. Role of the phosphatidylserine receptor TIM-1 in enveloped-virus entry. J Virol. 2013;87(15):8327-41.
36. Jemielity S, Wang JJ, Chan YK, Ahmed AA, Li W, Monahan S, et al. TIM-family proteins promote infection of multiple enveloped viruses through virion-associated phosphatidylserine. PLoS Pathog. 2013;9(3):e1003232.
37. Li M, Ablan SD, Miao C, Zheng YM, Fuller MS, Rennert PD, et al. TIM-family proteins inhibit HIV-1 release. Proc Natl Acad Sci U S A. 2014;111(35):E3699-707.
38. Li M, Waheed AA, Yu J, Zeng C, Chen HY, Zheng YM, et al. TIM-mediated inhibition of HIV-1 release is antagonized by Nef but potentiated by SERINC proteins. Proc Natl Acad Sci U S A. 2019;116(12):5705-14.
39. Furness SG, McNagny K. Beyond mere markers: functions for CD34 family of sialomucins in hematopoiesis. Immunol Res. 2006;34(1):13-32.
40. Nielsen JS, McNagny KM. Novel functions of the CD34 family. J Cell Sci. 2008;121(Pt 22):3683-92.
41. Krause DS, Ito T, Fackler MJ, Smith OM, Collector MI, Sharkis SJ, et al. Characterization of murine CD34, a marker for hematopoietic progenitor and stem cells. Blood. 1994;84(3):691-701.
42. Ando K. Human CD34- hematopoietic stem cells: basic features and clinical relevance. Int J Hematol. 2002;75(4):370-5.
43. Sidney LE, Branch MJ, Dunphy SE, Dua HS, Hopkinson A. Concise review: evidence for CD34 as a common marker for diverse progenitors. Stem Cells. 2014;32(6):1380-9.
44. Doyonnas R, Nielsen JS, Chelliah S, Drew E, Hara T, Miyajima A, et al. Podocalyxin is a CD34-related marker of murine hematopoietic stem cells and embryonic erythroid cells. Blood. 2005;105(11):4170-8.
45. Kerjaschki D, Sharkey DJ, Farquhar MG. Identification and characterization of podocalyxin--the major sialoprotein of the renal glomerular epithelial cell. J Cell Biol. 1984;98(4):1591-6.

46. Doyonnas R, Kershaw DB, Duhme C, Merkens H, Chelliah S, Graf T, et al. Anuria, omphalocele, and perinatal lethality in mice lacking the CD34-related protein podocalyxin. J Exp Med. 2001;194(1):13-27.
47. Sassetti C, Van Zante A, Rosen SD. Identification of endoglycan, a member of the CD34/podocalyxin family of sialomucins. J Biol Chem. 2000;275(12):9001-10.
48. Krause DS, Fackler MJ, Civin CI, May WS. CD34: structure, biology, and clinical utility. Blood. 1996;87(1):1-13.
49. Fackler MJ, Krause DS, Smith OM, Civin CI, May WS. Full-length but not truncated CD34 inhibits hematopoietic cell differentiation of M1 cells. Blood. 1995;85(11):3040-7.
50. AbuSamra DB, Aleisa FA, Al-Amoodi AS, Jalal Ahmed HM, Chin CJ, Abuelela AF, et al. Not just a marker: CD34 on human hematopoietic stem/progenitor cells dominates vascular selectin binding along with CD44. Blood Adv. 2017;1(27):2799-816.
51. Lee JH, Kalejta RF. Human Cytomegalovirus Enters the Primary CD34(+) Hematopoietic Progenitor Cells Where It Establishes Latency by Macropinocytosis. J Virol. 2019;93(15):e00452-19.
52. Sansonno D, Lotesoriere C, Cornacchiulo V, Fanelli M, Gatti P, Iodice G, et al. Hepatitis C virus infection involves CD34(+) hematopoietic progenitor cells in hepatitis C virus chronic carriers. Blood. 1998;92(9):3328-37.
53. Stanley SK, Kessler SW, Justement JS, Schnittman SM, Greenhouse JJ, Brown CC, et al. CD34+ bone marrow cells are infected with HIV in a subset of seropositive individuals. J Immunol. 1992;149(2):689-97.
54. Redd AD, Avalos A, Essex M. Infection of hematopoietic progenitor cells by HIV-1 subtype C, and its association with anemia in southern Africa. Blood. 2007;110(9):3143-9.
55. Bordoni V, Bibas M, Abbate I, Viola D, Rozera G, Agrati C, et al. Bone marrow CD34+ progenitor cells may harbour HIV-DNA even in successfully treated patients. Clin Microbiol Infect. 2015;21(3):290 e5-8.
56. McNamara LA, Collins KL. Hematopoietic stem/precursor cells as HIV reservoirs. Curr Opin HIV AIDS. 2011;6(1):43-8.
57. Watt SM, Chan JY. CD164--a novel sialomucin on CD34+ cells. Leuk Lymphoma. 2000;37(1-2):1-25.
58. Watt SM, Bühring HJ, Simmons PJ, Zannettino AWC. The stem cell revolution: on the role of CD164 as a human stem cell marker. NPJ Regen Med. 2021;6(1):33.
59. Watt SM, Bühring HJ, Rappold I, Chan JY, Lee-Prudhoe J, Jones T, et al. CD164, a novel sialomucin on CD34(+) and erythroid subsets, is located on human chromosome 6q21. Blood. 1998;92(3):849-66.
60. Zannettino AC, Bühring HJ, Niutta S, Watt SM, Benton MA, Simmons PJ. The sialomucin CD164 (MGC-24v) is an adhesive glycoprotein expressed by human hematopoietic progenitors and bone marrow stromal cells that serves as a potent negative regulator of hematopoiesis. Blood. 1998;92(8):2613-28.
61. Lee YN, Kang JS, Krauss RS. Identification of a role for the sialomucin CD164 in myogenic differentiation by signal sequence trapping in yeast. Mol Cell Biol. 2001;21(22):7696-706.

62. Forde S, Tye BJ, Newey SE, Roubelakis M, Smythe J, McGuckin CP, et al. Endolyn (CD164) modulates the CXCL12-mediated migration of umbilical cord blood CD133+ cells. Blood. 2007;109(5):1825-33.
63. Havens AM, Jung Y, Sun YX, Wang J, Shah RB, Buhring HJ, et al. The role of sialomucin CD164 (MGC-24v or endolyn) in prostate cancer metastasis. BMC Cancer. 2006;6:195.
64. Tang J, Zhang L, She X, Zhou G, Yu F, Xiang J, et al. Inhibiting CD164 expression in colon cancer cell line HCT116 leads to reduced cancer cell proliferation, mobility, and metastasis in vitro and in vivo. Cancer Invest. 2012;30(5):380-9.
65. Wang CC, Hueng DY, Huang AF, Chen WL, Huang SM, Yi-Hsin Chan J. CD164 regulates proliferation, progression, and invasion of human glioblastoma cells. Oncotarget. 2019;10(21):2041-54.
66. McLaren PJ, Gawanbacht A, Pyndiah N, Krapp C, Hotter D, Kluge SF, et al. Identification of potential HIV restriction factors by combining evolutionary genomic signatures with functional analyses. Retrovirology. 2015;12:41.
67. Ma F, Zhang C, Prasad KV, Freeman GJ, Schlossman SF. Molecular cloning of Porimin, a novel cell surface receptor mediating oncotic cell death. Proc Natl Acad Sci U S A. 2001;98(17):9778-83.
68. Zhang C, Xu Y, Gu J, Schlossman SF. A cell surface receptor defined by a mAb mediates a unique type of cell death similar to oncosis. Proc Natl Acad Sci U S A. 1998;95(11):6290-5.
69. Albrecht H, Carraway KL, 3rd. MUC1 and MUC4: switching the emphasis from large to small. Cancer Biother Radiopharm. 2011;26(3):261-71.
70. Gendler SJ, Spicer AP. Epithelial mucin genes. Annu Rev Physiol. 1995;57:607-34.
71. Sheehan JK, Kesimer M, Pickles R. Innate immunity and mucus structure and function. Novartis Found Symp. 2006;279:155-66; discussion 67-9, 216-9.
72. Brayman M, Thathiah A, Carson DD. MUC1: a multifunctional cell surface component of reproductive tissue epithelia. Reprod Biol Endocrinol. 2004;2:4.
73. Carraway KL, Perez A, Idris N, Jepson S, Arango M, Komatsu M, et al. Muc4/sialomucin complex, the intramembrane ErbB2 ligand, in cancer and epithelia: to protect and to survive. Prog Nucleic Acid Res Mol Biol. 2002;71:149-85.
74. Guang W, Ding H, Czinn SJ, Kim KC, Blanchard TG, Lillehoj EP. Muc1 cell surface mucin attenuates epithelial inflammation in response to a common mucosal pathogen. J Biol Chem. 2010;285(27):20547-57.
75. Ng GZ, Menheniott TR, Every AL, Stent A, Judd LM, Chionh YT, et al. The MUC1 mucin protects against Helicobacter pylori pathogenesis in mice by regulation of the NLRP3 inflammasome. Gut. 2016;65(7):1087-99.
76. Lu W, Hisatsune A, Koga T, Kato K, Kuwahara I, Lillehoj EP, et al. Cutting edge: enhanced pulmonary clearance of Pseudomonas aeruginosa by Muc1 knockout mice. J Immunol. 2006;176(7):3890-4.
77. McAuley JL, Corcilius L, Tan HX, Payne RJ, McGuckin MA, Brown LE. The cell surface mucin MUC1 limits the severity of influenza A virus infection. Mucosal Immunol. 2017;10(6):1581-93.

78. Li K, Cao P, McCaw JM. Modelling the Effect of MUC1 on Influenza Virus Infection Kinetics and Macrophage Dynamics. Viruses. 2021;13(5):850.
79. Mall AS, Habte H, Mthembu Y, Peacocke J, de Beer C. Mucus and Mucins: do they have a role in the inhibition of the human immunodeficiency virus? Virol J. 2017;14(1):192.
80. Khan S. The epithelial mucin (MUC1) and virus-specific antibodies target cell-free human immunodeficiency virus in human breast milk. Pediatr Infect Dis J. 2009;28(10):932; author reply
81. Habte HH, de Beer C, Lotz ZE, Tyler MG, Kahn D, Mall AS. Inhibition of human immunodeficiency virus type 1 activity by purified human breast milk mucin (MUC1) in an inhibition assay. Neonatology. 2008;93(3):162-70.
82. Mthembu Y, Lotz Z, Tyler M, de Beer C, Rodrigues J, Schoeman L, et al. Purified human breast milk MUC1 and MUC4 inhibit human immunodeficiency virus. Neonatology. 2014;105(3):211-7.
83. Hetrick B, He S, Chilin LD, Dabbagh D, Alem F, Narayanan A, et al. Development of a novel hybrid alphavirus-SARS-CoV-2 particle for rapid in vitro screening and quantification of neutralization antibodies, antiviral drugs, and viral mutations. bioRxiv. 2020:2020.12.22.423965.
84. Thibault S, Tardif MR, Gilbert C, Tremblay MJ. Virus-associated host CD62L increases attachment of human immunodeficiency virus type 1 to endothelial cells and enhances trans infection of CD4+ T lymphocytes. J Gen Virol. 2007;88(Pt 9):2568-73.
85. Baïsse B, Galisson F, Giraud S, Schapira M, Spertini O. Evolutionary conservation of P-selectin glycoprotein ligand-1 primary structure and function. BMC Evol Biol. 2007;7:166.
86. Tauxe C, Xie X, Joffraud M, Martinez M, Schapira M, Spertini O. P-selectin glycoprotein ligand-1 decameric repeats regulate selectin-dependent rolling under flow conditions. J Biol Chem. 2008;283(42):28536-45.
87. Wu Y, Beddall MH, Marsh JW. Rev-dependent indicator T cell line. Curr HIV Res. 2007;5(4):394-402.
88. Barclay AN. Membrane proteins with immunoglobulin-like domains--a master superfamily of interaction molecules. Semin Immunol. 2003;15(4):215-23.
89. Ley K. The role of selectins in inflammation and disease. Trends Mol Med. 2003;9(6):263-8.
90. Hynes RO. Integrins: bidirectional, allosteric signaling machines. Cell. 2002;110(6):673-87.
91. He S, Waheed AA, Hetrick B, Dabbagh D, Akhrymuk IV, Kehn-Hall K, et al. PSGL-1 Inhibits the Incorporation of SARS-CoV and SARS-CoV-2 Spike Glycoproteins into Pseudovirions and Impairs Pseudovirus Attachment and Infectivity. Viruses. 2020;13(1):46.
92. Liu Y, Song Y, Zhang S, Diao M, Huang S, Li S, et al. PSGL-1 inhibits HIV-1 infection by restricting actin dynamics and sequestering HIV envelope proteins. Cell Discov. 2020;6:53.

93. Zhou HF, Yan H, Cannon JL, Springer LE, Green JM, Pham CT. CD43-mediated IFN-γ production by CD8+ T cells promotes abdominal aortic aneurysm in mice. J Immunol. 2013;190(10):5078-85.
94. Khunger A, Piazza E, Warren S, Smith TH, Ren X, White A, et al. CTLA-4 blockade and interferon-alpha induce proinflammatory transcriptional changes in the tumor immune landscape that correlate with pathologic response in melanoma. PLoS One. 2021;16(1):e0245287.
95. Rosengren AT, Nyman TA, Syyrakki S, Matikainen S, Lahesmaa R. Proteomic and transcriptomic characterization of interferon-alpha-induced human primary T helper cells. Proteomics. 2005;5(2):371-9.
96. Reddy PK, Gold DV, Cardillo TM, Goldenberg DM, Li H, Burton JD. Interferon-gamma upregulates MUC1 expression in haematopoietic and epithelial cancer cell lines, an effect associated with MUC1 mRNA induction. Eur J Cancer. 2003;39(3):397-404.
97. Andrianifahanana M, Singh AP, Nemos C, Ponnusamy MP, Moniaux N, Mehta PP, et al. IFN-gamma-induced expression of MUC4 in pancreatic cancer cells is mediated by STAT-1 upregulation: a novel mechanism for IFN-gamma response. Oncogene. 2007;26(51):7251-61.
98. Coates M, Blanchard S, MacLeod AS. Innate antimicrobial immunity in the skin: A protective barrier against bacteria, viruses, and fungi. PLoS Pathog. 2018;14(12):e1007353.
99. McAuley JL, Linden SK, Png CW, King RM, Pennington HL, Gendler SJ, et al. MUC1 cell surface mucin is a critical element of the mucosal barrier to infection. J Clin Invest. 2007;117(8):2313-24.
100. Linden SK, Sutton P, Karlsson NG, Korolik V, McGuckin MA. Mucins in the mucosal barrier to infection. Mucosal Immunol. 2008;1(3):183-97.
101. Carter CC, Onafuwa-Nuga A, McNamara LA, Riddell Jt, Bixby D, Savona MR, et al. HIV-1 infects multipotent progenitor cells causing cell death and establishing latent cellular reservoirs. Nat Med. 2010;16(4):446-51.
102. Matheson NJ, Sumner J, Wals K, Rapiteanu R, Weekes MP, Vigan R, et al. Cell Surface Proteomic Map of HIV Infection Reveals Antagonism of Amino Acid Metabolism by Vpu and Nef. Cell Host Microbe. 2015;18(4):409-23.
103. Plante JA, Plante KS, Gralinski LE, Beall A, Ferris MT, Bottomly D, et al. Mucin 4 Protects Female Mice from Coronavirus Pathogenesis. bioRxiv. 2020:2020.02.19.957118.
104. V'Kovski P, Kratzel A, Steiner S, Stalder H, Thiel V. Coronavirus biology and replication: implications for SARS-CoV-2. Nat Rev Microbiol. 2021;19(3):155-70.
105. Freed EO. HIV-1 assembly, release and maturation. Nat Rev Microbiol. 2015;13(8):484-96.

BIOGRAPHY

Deemah M. Dabbagh graduated from graduated from Altarbiya School, Riyadh, Saudi Arabia, in 2004. She received her Bachelor of Science from King Saud University in 2009. She was employed as a lab technologist at King Faisal Specialist Hospital and Research Center for a year and a half, and as a lab instructor and lecturer at King Saud University for two years. She later received her Master of Science in Microbiology and Immunology from Georgetown University in 2014.